ABSTRACT

DILLON, WHALEN WILLIAM. Spatial Scale, Pathogen Spillover and Coexistence in an Emerging Forest Disease System. (Under the direction of Ross K. Meentemeyer).

Emerging infectious diseases (EIDs), exacerbated by rapidly increasing global connectivity, growing human population, and climate change, threaten human well-being. Effectively managing EIDs requires understanding pathogen-host-environment interactions across complex and changing landscapes. In my dissertation I investigate disease-environment interactions of the plant pathogen *Phytophthora ramorum* in naïve forest ecosystems. This exotic, generalist pathogen causes sudden oak death, which is responsible for inducing mortality of millions of susceptible trees in coastal forests of California and Oregon. Knowledge gained by monitoring complex plant disease systems such as this in uncontrolled environments can inform data collection and analysis efforts in other plant and animal disease systems.

For my first chapter, I explored how the spatial scale of disease intensity, and direct or indirect host density measurements, affected model inference. This demonstrated that direct measurements outperformed indirect measurements of host density in predicting disease intensity; and that the relationship between host density and disease intensity weakened when observations were made at broader spatial extents. In my second chapter, I used path analysis to simultaneously assess direct and indirect effects from the biotic and abiotic environment on pathogen spillover. Biotic factors had a relatively stronger influence on spillover, but abiotic factors still had significant effects that could inform disease management and future monitoring efforts. In my third chapter, I examined the impacts of sudden oak death on coexistence of common tree species in these forest communities. Results from this analysis showed that pathogen-related oak tree mortality is leading to

increasing dominance of the reservoir host, California bay laurel. In summary, I found that direct measurements across multiple spatial scales can provide information on which spatial scales disease dynamics are operating; simultaneously examining biotic and abiotic factors could enhance disease management and control efforts; and that coexistence of species can be destabilized by an exotic, generalist pathogen. In the face of rapid global change, understanding how diseases are responding to biotic and abiotic environmental variation is essential to prevent severe negative impacts to ecosystems and human health.

Spatial Scale, Pathogen Spillover, and Coexistence in an Emerging Forest Disease System

by
Whalen William Dillon

A dissertation submitted to the Graduate Faculty of
North Carolina State University
in partial fulfillment of the
requirements for the degree of
Doctor of Philosophy

Forestry and Environmental Resources

Raleigh, North Carolina

2017

APPROVED BY:

_____	_____
Ross Meentemeyer Committee Chair	Ryan Emanuel
_____	_____
Beth Gardner	Jamian Pacifici

_____
David Rizzo (External Member)

DEDICATION

To my parents, sisters, family, and friends for believing I could do this, even when they didn't understand what "this" is. The members of the Landscape Dynamics Lab for offering feedback, assistance, and beer; especially Devon Gaydos and Sarah Haas for commiserating as members of the SOD Squad. And to Monica Dorning, my chosen partner for every adventure who has helped with everything, from cups of tea to developing and interpreting necessary analytical methods. You're the best!

BIOGRAPHY

I was born in 1983, the middle of three children, in a remote area on the Oregon Coast. Roaming the forests, fields, and beaches, I have been steeped in ecology from a young age. When I was eight, my parents (William and Deborah) purchased 20-acres of forested property two miles from the nearest power-pole and erected a 17-foot diameter wooden yurt. The area cleared was just large enough for the yurt, so that the door opened only about three-quarters of the way before hitting a tree. Nature was quite literally at our doorstep. Along with my two sisters, Islande (older) and Aurora (younger), we started homesteading with our small herd of dairy goats. I was homeschooled until the 5th grade, and upon my return found out I was a little behind in some conventional areas of education. But, I was a quick learner and excellent problem solver, and became the valedictorian of my high school class. After graduation, I pursued a Bachelor's of Science in Biology at The Evergreen State College in Olympia, Washington. Upon completing my degree, I moved to Sonoma County, California and found work in construction until the Great Recession in 2008. I was able to find part time work as a field technician collecting data for sudden oak death research. This catapulted me back into ecology, providing the opportunity to make my case to pursue graduate level research. I re-entered academic research at the University of North Carolina – Charlotte, and then transferred to North Carolina State University to complete by dissertation with my advisor.

ACKNOWLEDGMENTS

Brian Anacker and Deanne DiPietro, who were responsible for getting the original data collection project off the ground, including establishing plots and developing the database. Many people assisted in data collection/management/coordination throughout the past decade: J. Anderson, T.E. Condesso, C. DeLong, J. DiRenzo, S. Flynn, K. Frangioso, D. Gaydos, A. Gauthier, S. Gordon, R. Hunter, A. Johnson, S. Johnston, M. Kennedy, A. Klevtcova, M. Kozanitas, S. Lamsal, S. Leung, A. Oguchi, M. Potter, C. Ross, L. Smart, J. Stone, M. Vaclavikova, T. Vaclavik, D. van Berkel, R. Whitkus, and S. Wolf. I apologize for the many names I forgot, but know that you are appreciated for helping make this possible. I also wish to acknowledge Sonoma State University's Fairfield Osborn Preserve, the Sonoma Mountain Ranch Preservation Foundation, the Sonoma Agriculture and Open Space District, the Sonoma Land Trust, California State Parks, Sonoma County Regional Parks, and many private landowners for granting us access to their properties for long-term ecological measurements. This research was supported by grants from the National Science Foundation (DEB-EF-0622677 and EF-0622770) as part of the joint NSF- NIH Ecology of Infectious Disease pro- gram, along with key financial support from the USDA Forest Service-Pacific Southwest Research Station.

TABLE OF CONTENTS

LIST OF TABLES vii

LIST OF FIGURES viii

CHAPTER 1. INTRODUCTION 1

CHAPTER 2. PERSPECTIVES OF SPATIAL SCALE IN A WILDLAND FOREST EPIDEMIC 4

- **ABSTRACT** 4
- **INTRODUCTION** 5
- **METHODS** 9
  - Data Collection 9
  - Analysis 11
- **RESULTS** 14
  - Individual-level Models 15
  - Extent-level Models: Focal and Aggregate Views 16
- **DISCUSSION** 17

CHAPTER 3. RELATIVE INFLUENCES OF THE BIOTIC AND ABIOTIC ENVIRONMENT ON PATHOGEN SPILLOVER 22

- **ABSTRACT** 22
- **INTRODUCTION** 22
- **METHODS** 26
  - Study Area 26
  - Data Collection 27
  - Landscape Context 28
  - Community 29
  - Local Climate 30
  - Pathogen Spillover 31
  - Modeling Framework 31
  - Path Analysis 32
- **RESULTS** 36
- **DISCUSSION** 37

CHAPTER 4. SPILLOVER OF AN EXOTIC FOREST PATHOGEN PROMOTES ITS NATIVE RESERVOIR HOST 43

- **ABSTRACT** 43
- **INTRODUCTION** 44
- **METHODS** 47
  - Study Area 47
  - Study System 48
  - Data Collection 48
  - Analyses 49
- **RESULTS** 55
  - Changes in Species Diversity 56
  - Change in importance value, basal area, and density 56

Path Models 58
DISCUSSION 60
Douglas-fir Importance Value 62
White Oak Importance Value 63
Species Diversity 64
Comparing Mortality Rates 65
CHAPTER 5. CONCLUSION 68
REFERENCES 70
APPENDICES 112
Appendix A. Chapter 3 Detailed Model Results 113
Appendix B. Chapter 2 Additional Model Results 120
Appendix C. Steps to Performing the d-sep Test 130

LIST OF TABLES

Table 2.1 Standardized coefficients and model fit for disease intensity on individual bay laurel stems....83

Table 2.2 Results from focal and aggregate-level models....84

Table 3.1 Results from the d-sep test of the path model in Fig. 3.3 using unstandardized variables....85

Table 3.2 Standardized coefficients from the fitted path model....86

Table 3.3 Unstandardized coefficients from the fitted path model....87

Table 4.1 Paired t-tests comparing diversity metrics in 2005 to 2016....88

Table A1 Results from the d-sep test of conditional independence claims for the path model in Fig. 4.7....112

Table A2 Standardized and unstandardized coefficient estimates for the path model in Fig. 4.7....113

Table A3 Results from the d-sep test of conditional independence claims for the path model in Fig. 4.8....114

Table A4 Results from the d-sep test of conditional independence claims for the path model in Fig. 4.9....115

Table A5 Results from the d-sep test of conditional independence claims for the path model in Fig. 4.10....116

Table A6 Standardized coefficients for the path model structure in Fig. 4.7....117

Table A7 Standardized coefficients for the path model structure in Fig. 4.8....118

Table B1 Unstandardized path coefficients for the path model in Fig. B1....121

Table B2 Unstandardized path coefficients for the path model in Fig. B2....123

LIST OF FIGURES

Figure 2.1 The selection of spatial extent for a given study may influence the model results and conclusions....89

Figure 2.2 Study area and multiscale site locations in Sonoma County, California....90

Figure 2.3 Point-quarter sampling diagram: (a) transects (b) point quarter sampling method....91

Figure 2.4 Stem-level model coefficients and AIC scores....92

Figure 2.5 Focal-view model coefficients and R^2 values....93

Figure 2.6 Aggregate-view model coefficients and R^2 values....94

Figure 2.7 Bay laurel density, host habitat, and disease intensity....95

Figure 2.8 Correlation matrix for bay laurel density and proportion of host habitat across spatial extents....96

Figure 3.1 Conceptual path model of influences on pathogen spillover....97

Figure 3.2 Study area in Sonoma County, California with plot (yellow) and rain gauge (blue triangles) locations....98

Figure 3.3 Results from path analysis with standardized and unstandardized coefficients....99

Figure 3.4 Total rainfall with 10-year average estimated at plot locations for the 2005-2014 rainy seasons....100

Figure 4.1 Structural path model of apparent competition....101

Figure 4.2 Study area in Sonoma County, California....102

Figure 4.3 Species occurrence across the plot network....103

Figure 4.4 Relationship between pathogen load and species diversity....104

Figure 4.5 Total stem abundance and basal area across the plot network....105

Figure 4.6 Change in importance value, basal area, and stem density....106

Figure 4.7 Apparent competition between coast live oak and bay laurel....107

Figure 4.8 Apparent competition between California black oak and bay laurel.....108

Figure 4.9 Effects on changes in Douglas-fir importance value.....109

Figure 4.10 Apparent competition between susceptible oaks and white oak species.....110

Figure B1 Path analysis results using the change in basal area of species from 161 plots with bay laurel.....120

Figure B2 Path analysis results using the change in basal area of species from 114 plots where coast live oak was recorded.....122

Figure B3 Comparisons of annual stem mortality rates of sudden oak death species.....124

Figure B4 Contemporary comparison of annual basal area mortality rates of epidemiologically important sudden oak death species.....125

Figure B5 Comparisons of local annual basal area mortality rates to estimated mortality rates from 1994-2004.....126

Figure B6 Comparisons of annual basal area mortality from this study to regional mortality rates predicted out to 2014.....127

Figure B7 Comparisons of annual basal area mortality rates from this study to estimated regional mortality rates from 1994-2004.....128

CHAPTER 1. INTRODUCTION

Emerging infectious diseases threatening human well-being are exacerbated by rapidly increasing global connectivity, human population growth, and climate change (Chapin III et al. 1997, Parmesan and Yohe 2003, Ellis et al. 2010). They are often noticed because they threaten our socio-ecological systems, either directly to human health, or indirectly through impacts to food security or valued biodiversity. While much attention and research is spent on diseases that directly impact human health (e.g. Lyme's, malaria, influenza, HIV/AIDS), we also face indirect threats from diseases that are particular to animals and plants. Crop and animal diseases threaten our food security, and diseases of wild plants and animals may dramatically alter landscapes, reducing the biodiversity and resiliency of ecosystems we depend upon. Promoting and ensuring the health of our socio-ecological systems in the face of diseases threatening our well-being requires implementing effective management and prevention. The key to effective management, especially in cases of novel emerging infectious disease where knowledge is typically limited, is gaining an understanding of the interactions between the disease and its environment across complex and changing landscapes (Plantegenest et al. 2007, Meentemeyer et al. 2012).

Any disease can be described by the disease triangle, consisting of a pathogen, susceptible hosts, and environmental conditions. Without the favorable interaction of all three factors there will not be disease. While conceptually simple, efforts to study host-pathogen-environment relationships are complicated by interactions among processes that differentially affect the pathogen, the host(s), and environmental conditions across space and time. Developing an understanding of these relationships for a single host, single pathogen system with a narrow environmental envelope is no simple task, and unfortunately many

diseases that threaten our socio-ecological systems do not fall into this category. Disease systems are frequently multi-host and may exhibit different characteristics across a broad range of environmental gradients.

Forests are complex and dynamic ecosystems supporting diverse communities of life from microscopic bacteria and fungi to some of the largest and longest living organisms on earth in their trees. These systems are often characterized by ecological disturbance regimes (e.g. flooding, wildfire, or drought) that have shaped ecosystem processes by altering resource availability, modifying physical and hierarchical ecosystem structure, and creating new spatial patterns (Spies et al. 1994, Turner et al. 2003). Impacts to these systems from an emerging infectious disease may interact with existing disturbance regimes, causing novel changes to the relationships between the pathogen, host(s), and environment (Burdon et al. 2006, Jones et al. 2008). The changes to wildland landscapes wrought by these novel host-pathogen-environment interactions are also likely to have a prominent impact on socio-ecological systems from local to global scales (Turner 2010). Understanding and managing the impacts of these disease systems requires disentangling processes driven by host-pathogen-environment interactions across a broad range of spatial and temporal scales.

In my dissertation, I aim to develop empirical knowledge of host-pathogen-environment relationships in a wildland disease system in order to test epidemiological theory, improve parameterization of dynamic models, and address impacts to social-ecological systems caused by disease. To accomplish this, I utilize landscape epidemiological approaches to examine disease-environment relationships of the plant pathogen *Phytophthora ramorum* in forest ecosystems. My dissertation is organized into three chapters addressing these research objectives, with each chapter intended to be a published manuscript

in a peer-reviewed journal. In my first chapter, I examine the influence of the spatial scale of empirical host density measurements on the inference and conclusions drawn from models of disease intensity. For my second chapter, I assess the relative influence of direct and indirect effects from biotic and abiotic factors on pathogen spillover. In my third chapter, I examine the influence of *P. ramorum* on coexistence among tree species in disease-impacted communities.

CHAPTER 2. PERSPECTIVES OF SPATIAL SCALE IN A WILDLAND FOREST EPIDEMIC

This chapter has been published in the European Journal of Plant Pathology. Citation: Dillon, W.W., S.E. Haas, D.M. Rizzo, and R.K. Meentemeyer. (2014). Perspectives of spatial scale in a wildland forest epidemic. Eur. J. Plant Pathol. 138:449-465.

Abstract

The challenge of observing interactions between plant pathogens, their hosts, and environmental heterogeneity across multiple spatial scales commonly limits our ability to understand and manage wildland forest epidemics. Using the forest pathogen *Phytophthora ramorum* as a case study, we established 20 multi-scale field sites to analyze how host-pathogen-environment relationships vary across spatial scales of observation in a wildland disease system. We developed statistical models of disease intensity across five nested levels of spatial aggregation, from an individual host through four broader spatial extents of observation. Analyses were conducted from two spatial perspectives: a *focal view*, where disease intensity at one scale was examined as a function of broader-scale landscape conditions, and an *aggregate view*, where disease intensity and landscape conditions are observed at the same scale of spatial aggregation. For each perspective, separate models were developed to compare direct field measurements of host density versus less expensive remotely sensed estimates of host habitat as predictors of disease in landscape-scale studies. From both perspectives, models using direct measurements of host density performed better than models using remotely sensed estimates of host habitat across all four spatial extents. We found no significant difference in model performance at the individual level. From the

focal view, the performance of host density models declined with increasing spatial extent, whereas the performance of host habitat models improved with spatial extent. These results illustrate how the scale of observation – both spatial extent and measurement detail – can influence conclusions drawn from epidemiological models of wildland disease systems.

Introduction

The landscapes of wildland plant disease systems exhibit substantial environmental heterogeneity compared to agricultural croplands or intensively managed ecosystems, such as tree plantations. The increased complexity and cross-scale interactions in these landscapes make it challenging to measure and analyze the drivers of disease dynamics. Even when measurements of environmental heterogeneity are undertaken there is rarely a single correct scale of observation that is known a priori for a given disease system (Meentemeyer et al. 2012; Fig. 2.1). Meanwhile, host-pathogen interactions are intricately embedded within communities, ecosystems, and entire landscapes, so it is essential that we understand the role that environmental heterogeneity across multiple scales plays in the spread and persistence of wildland diseases (Ostfeld et al. 2005; Burdon et al. 2006). In addition, the scale of observation and analysis has been recognized as influential results and conclusions drawn from models (Wiens, 1989; Plantegenest et al. 2007; Chave, 2013). Still, our best empirical understanding of host-pathogen-environment interactions is predominantly derived from analyses conducted at single (and small) spatial scales.

The emerging discipline of landscape epidemiology provides concepts and tools for analyzing the role that environmental heterogeneity plays in the development of epidemic trajectories across space and time. Yet, in a recent review of 143 landscape epidemiological

studies, Meentemeyer et al. (2012) found that only 13% utilized a multi-scale approach. Perhaps the slow progress toward understanding scale-dependent processes in wildland disease systems stems from the more complex spatial heterogeneity of biotic and abiotic conditions compared to experimental and intensely managed settings. These circumstances present a special challenge for studying wildland pathogens across large geographic areas, because our ability to collect data of direct epidemiological relevance decreases as study extents increase. For example, our ability to directly measure environmental heterogeneity (e.g., solar radiation and host density) in the field across multiple scales becomes progressively less tenable as study extents expand in scope and duration. As a compromise, multi-scale disease studies in natural ecosystems often resort to using indirect measures of environmental heterogeneity (e.g., elevation and land cover), which serve as surrogates for the underlying epidemiological processes. Thus, the scale of observation may especially affect our understanding of host-pathogen-environment interactions in wildland settings.

In this study, we compare the performance of landscape epidemiological models parameterized with direct field measurements to those using indirect measurements of biotic environmental heterogeneity across multiple spatial extents. We focus on a heterogeneous forested landscape infested by the emerging wildland plant pathogen *Phytophthora ramorum* (Phylum *Oomycota*), the causal agent of sudden oak death in North America (Rizzo and Garbelotto 2003). *P. ramorum* was discovered in the mid-1990s in the greater San Francisco Bay Area of California (Rizzo and Garbelotto 2003; Rizzo et al. 2005), and spread rapidly via local and long-distance dispersal events, resulting in current infestations from southwestern Oregon to the Big Sur region of California (Václavík et al. 2012). This pathogen causes diseases expressed in two ways: stem canker infections, and foliar and twig

infections (Rizzo et al. 2005). Canker infections have led to extensive mortality of trees throughout coastal forests of California and Oregon, particularly coast live oak (*Quercus agrifolia*), California black oak (*Quercus kellogii*), as well as tanoak (*Notholithocarpus densiflorus*) (Rizzo et al. 2005; Meentemeyer et al. 2008a). The infectious inoculum from this pathogen is produced through sporulation from the nonlethal foliar infections, predominantly on non-canker host species (Rizzo et al. 2005). Although recognized as a generalist pathogen with an incredibly broad range of hosts (>130 confirmed host species; APHIS, 2013), the abundant inoculum production responsible for driving epidemic spread across the landscape arises predominantly from two highly-competent foliar host species: California bay laurel (*Umbellularia californica*) and tanoak. Tanoak is unique in this disease system as the only species known to be susceptible to lethal canker infections as well as function as a competent foliar host for inoculum production.

During previous studies on *P. ramorum* researchers found that the majority of pathogen transmission occurs locally (<10-m), though dispersal may occur regularly within a 200-m radius of infected sites (Davidson et al. 2005; Swiecki and Bernhardt 2007; Mascheretti et al. 2008). Rare long-distance dispersal events (>1-km) are the most likely cause of the patchy distribution of this pathogen across northern California and into southern Oregon (Meentemeyer et al. 2004; Meentemeyer et al. 2008a; Ellis et al. 2010; Václavík et al. 2012). Although there have been a number of studies focusing on the epidemiology of the *P. ramorum* disease system – elucidating some general disease-environment relationships – most of these have been spatially implicit and/or used a single resolution and extent (e.g. Hansen et al. 2008; Cobb et al. 2010; Haas et al. 2011; Hüberli et al. 2011; Metz et al. 2012). We recognized two studies of this system that applied multi-scale approaches by examining

relationships across either local to landscape (Condeso and Meentemeyer 2007) or local to regional scales (Cushman and Meentemeyer 2008). Of these, Condeso and Meentemeyer (2007) provided the most compelling study on disease-environment relationships of *P. ramorum* across multiple scales. The authors used high-resolution forest cover data to examine the relationship between the proportion of forested area (host habitat) and disease intensity in focal plots across nested spatial scales of increasing extent. They discovered that the explanatory power of their models improved when host habitat at broader scales was included as an explanatory variable up to a 200-m radius around focal plots.

Although forest cover proved to be useful for explaining disease severity in the study by Condeso and Meentemeyer (2007), it is an indirect measure of the mechanism(s) involved in the underlying process of disease transmission. Specifically, host habitat cover may be considered a surrogate for host density, however high amounts of host habitat cover do not necessarily confer high host density. Thus, using host habitat as a surrogate for host density may limit our understanding of disease dynamics in disease systems regulated by density-dependence mechanisms. Furthermore, the spatial variability in disease intensity of disease systems that are influenced by diversity-disease risk processes, such as sudden oak death (Haas et al. 2011), may also be better understood by examining the relationship between the disease and host density at multiple scales.

Here, we examine host-pathogen-environment relationships across multiple spatial scales in a wildland *P. ramorum* disease system. Our goal is to understand how the perspective of scale used for observation and analysis influences the inference and conclusions drawn from landscape epidemiological models. Using a field-based sampling strategy, we collected data on the pathogen, hosts, and environmental heterogeneity across

five levels of spatial aggregation: individual host stems and four broader (nested) spatial extents. We analyze these data from two spatial perspectives: a *focal view*, where disease intensity at one scale is examined as a function of broader-scale landscape conditions, and an *aggregate view*, where disease intensity and landscape conditions are observed at the same scale of spatial aggregation. For each perspective, we develop multiple models in order to compare direct field measurements of host density versus less expensive remotely sensed estimates of host habitat as predictors of disease in landscape-scale studies.

Methods

Data Collection

We designed and implemented a field-based sampling strategy to capture the spatial heterogeneity of host-pathogen interactions across multiple spatial scales. During the spring of 2010, we established 20 multi-scale sites on the western side of Sonoma Mountain in southeastern Sonoma County, California (Fig. 2.2). At each site we collected data on disease intensity and host density at nested extents of 15-m x 15-m, 60-m x 60-m, 140-m x 140-m, and 220-m x 220-m. We performed a census of all stems within the 15-m extent, recording the diameter at breast height (DBH; breast height = 1.4-m) on stems of the four main *P. ramorum* host species that measured ≥2-cm DBH. We also recorded the presence of stems of other species that measured ≥5-cm DBH.

A complete census across all extents at each site was considered cost-prohibitive, so we quantified host density and disease intensity at the 60-m, 140-m, and 220-m extents using the point-quarter transect sampling method (Cottam et al. 1953, Cottam and Curtis 1956).We established 36 evenly spaced satellite plots around the 15-m extent at each site using line

transects (Morrison 1996) (Fig. 2.3a). Each satellite plot was divided into quadrants, the distance from the center of each satellite plot to the nearest stem ≥5-cm DBH in each quadrant was measured, and species of that stem was recorded (Fig. 2.3b). To calculate bay laurel density across the three broader extents, we first calculated an estimate of the total stem density at each extent using the point to plant distances measured at the satellite plots within that extent in the following equation,

$$\textit{Total stem density} = 1/(\textit{mean point-to-stem distance})^2 \quad \text{Eq. 2.1}$$

The denominator is an estimate of the area occupied per stem, which is the reciprocal of the density (Cottam and Curtis 1956).

We then calculated the relative density of bay laurel stems at each extent as the number of bay laurel stems divided by the total number of stems of all species. In order to calculate and estimate bay laurel stem density at each extent, we applied the relative density of bay laurel stems and total stem density in the following equation,

$$\textit{Bay laurel stem density} = \textit{relative density of bay laurel stems} * \textit{total stem density} \quad \text{Eq. 2.2}$$

resulting in the number of stems per square meter at each extent. At the 15-meter extent we only applied Eq. 2.2 because the census we conducted at that extent meant that the total stem density was empirically derived and so Eq. 2.1 was unnecessary. When we calculated the estimates of bay laurel density at the larger spatial scales, we included the stems recorded at

the 15-m extent in the calculation of relative density. Thus, the host density estimate calculated for each extent was composed of data aggregated from each smaller extent.

To assess disease intensity we conducted 60-s counts of leaves exhibiting *P. ramorum* symptoms on all bay laurel stems encountered at each site (Condeso and Meentemeyer 2007). The disease intensity at each extent was calculated as the total number of symptomatic leaves by summing the number of symptomatic leaves across the nested scales. For example, the disease intensity at the 15-m extent was the sum total of the leaf counts within that extent, while the disease intensity at the 60-m extent was the sum of the leaf counts at 15-m plus the sum of the leaf counts from the satellite plots at the 60-m extent.

We used a geographic information system to calculate the proportion of host habitat and the average elevation at each extent across the 20 multi-scale sites. The proportion of host habitat was calculated by extracting the number of cells within each extent that were classified as host habitat from a 5-m resolution grid and dividing this value by the total number of cells in that area. This host habitat surface was originally developed from 1-m resolution ADAR imagery (see Condeso and Meentemeyer 2007). Average elevation in meters was calculated from a 10-m resolution United States Geological Survey digital elevation model by averaging the values of the cells within each extent.

Analysis

We modeled disease intensity as a function of elevation, and either bay laurel density or the proportion of host habitat, across the five levels of spatial aggregation: individual bay laurel stems, and the four spatial extents. At each of the four spatial extents, we examined disease intensity as a function of the predictor variables observed at the same extent (*aggregate*

view), as well as at each larger extent (*focal* view), using separate ordinary least squares regression models (OLS). For example, disease intensity at the 60-m extent was modeled as a function of the predictors at that same extent (aggregate view models), and then in two other models using observations of the predictor variables at each of the larger extents (focal view models). We ran paired models at each extent (one using host density and one using host habitat) in order to compare the effect on model performance of directly measured host density versus the host habitat surrogate. Elevation was included as a predictor variable in each model in order to account for some of the variation in the physical environment across this landscape. To satisfy assumptions of normality for these extent-level models, we applied transformations to the disease intensity, host density, and host habitat variables (i.e. symptomatic leaf count, bay laurel density, and the proportion of host habitat). Disease intensity and host density were transformed using the natural logarithm, and host habitat was arcsine transformed.

Disease intensity at the individual level was measured as the symptomatic leaf count of an *individual* bay laurel stem from the census at the 15-m extent across the 20 multi-scale sites. We modeled the individual's disease intensity from the focal view as a function of the DBH of the individual stem, and either host density or host habitat, and elevation in separate models that used the predictor variables observed at each of the four spatial extents. In order to model disease intensity at the level of individual stems we needed to account for the grouping of the individual stems within the same extent at each site, so we used a generalized linear mixed effects modeling approach (Gelman and Hill 2007). This is similar to generalized linear models where the family of distributions (e.g. binomial or Poisson) of the response variable is designated, but also provides the additional benefit of including random

effects that account for unobserved variance resulting from hierarchical structuring of data, e.g. clustering of individuals within sites (Gelman and Hill 2007, Bolker et al. 2009). In our case, we needed to account for the unobserved variance affecting stems grouped within the same extent at each site, so we identified the 'site' as a random effect. Since we were modeling count data, we specified the Poisson family of distributions (Bolker et al. 2009, O'Hara and Kotze 2010). Preliminary analysis revealed that our count data were overdispersed, so we included a data-level variance component, 'stem', as an additional random effect (Gelman and Hill 2007, pp. 325-331). The Poisson model for disease intensity on stem *i* in plot *j* can be written as:

$$Y_{ij} \sim Poisson\left(\mu + X_{ij}\beta_{ij} + Z_j\alpha_j\right) + \epsilon_{ij} \quad \text{Eq. 3}$$

where Y_{ij} is the disease intensity (symptomatic leaf count) on stem *i* in plot *j*, μ is the intercept, X_{ij} is the vector of predictor variables for stem *i* in plot *j* with the coefficient(s) β_{ij} estimated from the data, Z_j is the vector of plot indicators (plot identifier) with the coefficient $\alpha_j \sim N(0, \sigma_\alpha^2)$, and ϵ_{ij} allows for overdispersion and is modeled as $\epsilon_{ij} \sim N(0, \sigma_\epsilon^2)$.

All variables were standardized prior to running the models, because our goal was to compare the inference, statistical significance, and relative influence of the covariates, as well as the goodness-of-fit and/or explanatory power of the models. We assessed and compared the goodness-of-fit of the mixed effects regression models (individual-level, focal view) using the Akaike information criterion (AIC; Akaike, 1974). This information theoretic approach offsets the log-likelihood of a model with a penalty for each predictor variable, enabling the identification of which model of a set is most likely capable of reproducing the

observed data (Burnham and Anderson 2002). Lower AIC values indicate better model fit, and a change in AIC of four may indicate a significantly better model (Burnham and Anderson 2002, p. 446). The performance of ordinary least squares regression models were assessed based on explanatory power (the adjusted R^2), as well as their goodness-of-fit, measured as AICc. The AICc metric is an extension of AIC for small sample sizes, and as sample size increases AICc converges to AIC (Burnham et al. 2010). We used AICc to assess the models of disease intensity at the four spatial extents because there were only 20 replicates at these levels (i.e. one for each site), compared to 331 stems across all the sites for the individual level models.

We also examined the collinearity among predictor variables, selecting a correlation threshold of |0.50| for variable inclusion in the same model. All statistical analyses were conducted using the R Statistical Software, version 3.0.2 (R Core Team 2013). Generalized linear mixed effects models were implemented using the 'glmer' function in the 'lme4' package (Bates et al. 2013) and ordinary least squares regression models were implemented using the 'lm' function in the base 'stats' package. The 'AICc' function from the 'MuMIn' package (Barton 2013) was used for calculating AICc of the OLS regressions.

Results

Across the four spatial extents (15-m, 60-m, 140-m, 220-m) at all 20 multi-scale sites, bay laurel density ranged from 0.0014 to 0.1867 stems/m^2; the proportion of host habitat ranged from 0.11 to 1; elevation ranged from 273-m to 691-m; and disease intensity ranged from 64-8936 symptomatic leaves (Fig. 2.7). Disease intensity on the individual bay laurel stems from the censuses at the 15-m extents ranged from 0 to 257 symptomatic leaves (mean = 58) and

the DBH of these stems ranged from 2-cm to 105.3-cm (mean = 21.9). Correlation tests between predictor variables in the same models resulted in a maximum Pearson's coefficient of less than 0.40 During this analysis we found that bay laurel density had a strong positive relationship with the proportion of host habitat, especially at the broader 140-meter and 220-meter extents where Pearson's correlation coefficients were > 0.75 (Fig. 2.8).

Our analyses showed that the effectiveness of host density or host habitat for predicting disease intensity varied with the scale of aggregation of the response and predictor variables. In the next two sections, we describe the results from the models of disease intensity at the individual level ("Individual-level Models") and for the suite of models at each of the four spatial extents examined from the focal and aggregate views ("Extent-level Models").

Individual-level Models

After accounting for elevation, stem DBH, and the variability captured in the random effects of 'site' and 'stem', neither host density nor host habitat measured at any extent were statistically significant ($p<0.1$) in their respective models (Table 2.1). Based on AIC scores, the best model was with host habitat at the 15-meter extent, however the change in AIC across models was ≤2 (Table 2.1; Fig. 2.4). Although the differences were small, elevation was relatively more influential at smaller extents in the host density models, whereas it was relatively more influential at broader extents in the host habitat models (Fig. 2.4).

Extent-level Models: Focal and Aggregate Views

From both perspectives, we found that using host density in models of disease intensity provided more explanatory power (higher adjusted R^2) and better goodness-of-fit (lower AICc) than models using host habitat at all spatial scales (Table 2.2; Figs. 2.5a-c & 2.6a-b). In comparing the models from the focal perspective, we found that host density models always performed better than host habitat models at each scale, however the performance of host density models within a focal extent declined as the scale at which the predictor variables were observed increased. Conversely, the performance of host habitat models at each scale tended to improve as the extent at which the predictor variables were observed increased (Table 2.2, Figs. 2.5a-c). From this perspective, the best performing host density and host habitat model (lowest AICc and highest adjusted R^2) was when disease intensity was modeled at the 140-m extent as a function of predictors observed at the 220-m extent (Table 2.2, Fig. 2.5c). Host density was statistically significant ($p < 0.05$) in at least one model at each extent of disease intensity, whereas host density was significant only when observed at 220-m for models of disease intensity at 60-m and 140-m.

To compare the host density to host habitat models from the aggregate perspective, we plotted the adjusted R^2 and AICc (Fig. 2.6a), and the standardized beta coefficients of the predictor variables (Fig. 2.6b) from the models at each extent. Similarly to the focal perspective, models parameterized with host density provided greater explanatory power and better goodness-of-fit than models parameterized with host habitat at each extent (Table 2.2, Fig. 2.6a). The model using host density at the 15-m extent produced the best model of disease intensity from this perspective, as well as best model overall ($R^2 = 0.74$, AICc = 39.03; Fig. 2.6a, Table 2.2), with both predictor variables statistically significant (Fig. 2.6b,

Table 2.2). This contrasts with the results from the focal perspective where the best models using either host density or host habitat were at the broadest spatial scale, although the best host habitat model was still at the broadest extent (220-m) from this perspective.

The R^2 as well as AICc of the host density models decreased at the 60-m extent, although explanatory power then increased marginally at the 140-m and 220-m extents. The AICc of the host density models showed no notable difference across the 60-m to 220-m extents. The host density predictor variable was statistically significant in models at each extent, while elevation was statistically significant only in models at the 15-m and 60-m extents. In comparison, the explanatory power of host habitat models consistently increased across the four spatial extents from an R^2 of 0.11 at 15-m to an R^2 of 0.49 at 220-m (Table 2.1; Fig. 2.6a). The goodness-of-fit of the host habitat models also improved with increasing extent from an AICc of 63.43 at 15-m to an AICc of 52.55 at 220-m, a notably better fit compared to models at the 15-m and 60-m extents (ΔAIC >4; Burnham and Anderson 2002, p. 446). The relative influence of the host habitat predictor variable increased with increasing extent, but was statistically significant only at the 140-m and 220-m extents (Fig. 2.6b). The elevation predictor variable was statistically significant only at the 15-m and 60-m extents in the host habitat models.

Discussion

Issues of spatial scale are a key consideration in studying disease epidemics (Real and McElhany 1996; Jeger et al. 2007), and may be especially important for improving our understanding of disease dynamics in wildland disease systems (Holdenrieder et al. 2004; Kauffman and Jules 2006). Equally important is the selection of epidemiologically relevant

variables that provide accurate inference and interpretable results for the efficacious management of diseases in natural ecosystems (Meentemeyer et al. 2012). In this study, we found that the scale of observation – spatial extent and measurement detail – affected model outcomes.

Our results concur, as well as provide novel insight, to findings from the multi-scale study on *P. ramorum* by Condeso and Meentemeyer (2007). Their study area occurred in the same geographic region as ours, so underlying differences in habitat type and invasion history do not confound comparisons of results. By including the proportion of host habitat surrounding focal plots (a *focal view*) at increasing spatial extents as a predictor variable, Condeso and Meentemeyer (2007) found an improvement in explanatory power of infection severity with increasing scale between 50-m and 200-m. We found a similar relationship in our host habitat models, where model fit improved with increasing scale of host habitat measurements around the focal extent (though not in models at the individual stem level). Our correlation analysis of the proportion of host habitat and bay laurel density suggested that the high-resolution forest cover data may be a reasonable surrogate for host density, yet our measurements of host density revealed a relationship with disease intensity that was strongest at the focal extent, suggesting that local dispersal mechanisms may be driving disease dynamics in the *P. ramorum* disease system. In particular, the results from models of disease intensity at the 15-m extent suggest that there may be a spatial threshold between 60-m and 140-m beyond which the impacts of host density on focal epidemiological processes are substantially diminished.

The fluctuation in the explanatory power of the host density models as scale increased from the aggregate perspective may in part be a product of our multi-scale sampling design.

That is, the 60-m extent has proportionally the least amount of data, with only four satellite plots plus the 15-m census informing the host density and disease intensity calculations for the entire area (3600-m^2). With less data there is perhaps less of the variability in disease intensity captured at this extent, resulting in the least explanatory power of the models (lowest adjusted R^2), however the fit of the model to the data is in fact no worse than at the 140-m and 220-m extents (ΔAICc < 2). Along these lines, the model at the 15-m extent is informed by the stem census at that scale (the most complete data for any extent), likely contributing to this being the model with the best performance. The results from this aggregate view indicate that the relationship between disease intensity and host density is best described by observation of these variables at the same extent.

The mechanism underlying the relationship between host density and disease intensity is in the processes of dispersal and transmission of inoculum. More competent hosts in a given area is likely to result in more inoculum production and therefore greater disease risk, but it may also be that host density alters physical microclimate conditions in the forest understory. This affects the physiology and vigor of pathogen reproduction and survival, as *P. ramorum* has been shown to be sensitive to soil moisture, humidity, and light levels (Englander et al. 2006; Tooley et al. 2008). The modest improvement of host habitat models across increasing extents may be due to this same mechanism, where greater forest cover leads to more favorable microclimate conditions for the pathogen.

At the individual level, host-pathogen interactions are driven by interactions between multiple environmental, ecological, and genetic factors (Morrison 1996; Anacker et al. 2008). After accounting for individual stem characteristics (DBH) and physical properties (elevation) of the sites we found no effect of either host density or host habitat measured at

any extent on the infection intensity of individual bay laurel stems. This would indicate that while the aggregate disease intensity at a site is influenced by the biotic conditions, the intensity of disease on individuals might be more strongly shaped by the individual's characteristics. The negative relationship observed between stem DBH and disease intensity could be in part due to the nearly complete fire suppression across this region over the past 65 years, which has resulted in the expansion of woodlands into areas previously dominated by grassland and chaparral (Meentemeyer et al. 2008b). As a result, the abundance and density of *P. ramorum* host species, including bay laurel, has increased over time because stems with smaller DBH are surviving longer (Meentemeyer et al. 2008b). Moreover, these smaller stems are generally located in the forest understory where they experience less exposure to solar irradiation and overall conditions that are more favorable for pathogen survival. In turn, the positive relationship with elevation would indicate that individuals in locations that are generally cooler and wetter exhibit higher disease intensity.

Our findings add to the growing body of literature indicating that spread of *P. ramorum* is a predominantly local process (Davidson et al. 2005; Swiecki and Bernhardt, 2007; Davidson et al. 2008; Mascheretti et al. 2008). Because plants are sessile and *P. ramorum* exhibits limited long-distance dispersal, the environmental conditions in small habitat patches may be sufficient to cause variation in infection on a local scale. The diminishing model fit we found between host density and disease intensity across increasing spatial scales from the focal perspective is similar to models of other passively-dispersed organisms (Mundt and Sackett 2012). Because of the opposite inference (increasing model performance with extent) from the host habitat models, we feel it is important to note that host habitat and host density may each be considered surrogate measures of infection

pressure, but each provides distinct insights into disease dynamics (Burdon and Chilvers 1982). High resolution surfaces of host habitat may be an appropriate variable for examining disease-environment relationships in some instances, especially at broad spatial scales, but the measurement of factors such as host density that are more proximal to epidemiological processes can provide more meaningful insight in to the disease dynamics of wildland disease systems.

Emerging infectious pathogens are recognized as a powerful force in shaping natural plant communities around the world, with long-term and largely unknown consequences to biodiversity and ecosystems services (Dinoor & Eshed, 1984; Gilbert, 2002; Burdon et al. 2006; Meentemeyer et al. 2012 Burdon et al. 2013). In a world with increased human mobility and international plant trade, it is imperative that we gain a better understanding of the diverse factors governing the dynamics of wildland disease systems from local to global scales, including interactions with other disturbances (Metz et al. 2011; Dillon et al. 2013). Here we have illustrated how the scale of observation – the spatial extent and the measurement detail – can influence conclusions drawn from epidemiological models of wildland disease systems. Improved ecological forecasts of disease dynamics will require well-parameterized models that consider a range of causal factors with direct epidemiological relevance across multiple spatial scales.

CHAPTER 3. RELATIVE INFLUCENCES OF THE BIOTIC AND ABIOTIC ENVIRONMENT ON PATHOGEN SPILLOVER

Abstract

Pathogen spillover occurs when disease epidemics are driven by an alternate reservoir host population, yet there is limited understanding of how environmental variation influences this process. While studies of disease systems with pathogen spillover frequently examine the biotic environment (host community), the abiotic environment is seldom accounted for simultaneously. We applied 10 years of microclimate, disease, and community data in a path analysis to investigate the relative influence of biotic and abiotic factors on pathogen spillover for the emerging infectious forest disease sudden oak death. We found that biotic factors were stronger drivers, but abiotic factors significantly influenced the success of spillover events. Greater exposure to hot summer temperatures reduced pathogen loads the following spring, while exposure to optimal pathogen sporulation conditions increased oak infection. Simultaneously examining biotic and abiotic influences in disease can enhance control efforts of emerging infectious diseases by informing predictive models and focusing direct management efforts.

Introduction

Pathogen spillover is a characteristic of multi-host disease systems where disease transmission is driven by an alternate reservoir host population (Power and Mitchell 2004). This process arises due to asymmetry in infectious competency of the pathogen hosts. The *reservoir* host maintains a high level of the pathogen population relative to *non-reservoir*

host species. Non-reservoir hosts experience higher infection rates in communities where the reservoir host is present, because the pathogen is amplified within the reservoir host and then spills over to the non-reservoir host. Power and Mitchell (2004) demonstrated this experimentally in the barley yellow dwarf plant disease system, where the presence of a single reservoir host in the community increased the proportion of susceptible species that were infected compared to communities where the reservoir host was absent. In the realm of zoonotic disease, Kilpatrick et al. (2006) showed that American robins (*Turdus migratorius*) are a reservoir host for West Nile virus (WNV), because they are more frequently fed upon by WNV transmitting mosquitoes relative to their abundance, and thus infect a higher proportion of vectors. The pathogen then spills over from American robins to other hosts. Some additional disease systems where pathogen spillover occurs include Lyme disease (*Borrelia burgdorferi*; Brisson *et al.* 2008), bovine tuberculosis (Nugent 2011), and the Ebola virus (Chowell and Nishiura 2014), demonstrating that pathogen spillover is a significant epidemiological process in a variety of multi-host disease systems directly and indirectly affecting human health.

Plants cannot move to avoid contact with infected individuals, therefore environmental effects on the pathogen and hosts may play a larger role in disease spread than among mobile animal hosts. In plant disease systems with pathogen spillover we expect that when the local community includes relatively high abundance of the reservoir host, and environmental conditions are favorable for the pathogen, then disease transmission to the non-reservoir species will increase. Despite the essential role environmental conditions play in disease dynamics at multiple temporal and spatial scales (Meentemeyer et al. 2012), the

effects on pathogen production and host susceptibility have seldom been examined simultaneously.

Most studies of pathogen spillover have focused on the dominant community dynamics, sometimes including a broad scale temperature or moisture index to assess the relationship between the disease and the physical environment. The dearth of studies examining the influence of environmental conditions on pathogen spillover is in part due to a lack of environmental and ecological data collected at spatial and temporal scale(s) appropriate for the disease system. Understanding environmental controls of pathogen spillover requires disentangling the host-pathogen-environment interactions across space and time, which necessitates long-term monitoring of disease dynamics under naturally changing environmental conditions (Jules et al. 2002, Holdenrieder et al. 2004, Rohr et al. 2011, Meentemeyer et al. 2012).

We investigated how the landscape, community, and local microclimate simultaneously influenced pathogen spillover in the sudden oak death (SOD) disease system (Rizzo and Garbelotto 2003). This forest disease has killed millions of trees in coastal forests of California and southwestern Oregon since its introduction in the mid-1990s (Meentemeyer *et al.* 2008; Lamsal *et al.* 2011) and is emblematic of pathogen spillover. The pathogen, *Phytophthora ramorum*, causes two host-dependent diseases: 1. lethal canker infections on the stems of a certain *Quercus spp.* and tanoak (*Notholithocarpus densiflorus*; Manos et al. 2008), and 2. non-lethal foliar infections on a wide range of other species (APHIS 2013). Tanoak is unique in this system because it is the only species known to be susceptible to both types of infection. Pathogen transmission is driven by foliar host species, especially California bay laurel (*Umbellularia californica*) and tanoak (Rizzo et al. 2005, Cobb et al.

2010). Pathogen spillover from foliar hosts causes canker infections and mortality of susceptible *Quercus* host species (coast live oak, *Q. agrifolia*; California black oak, *Q. kellogii*; and canyon live oak, *Q. chrysolepsis*), which do not support pathogen sporulation (Rizzo et al. 2005, Swiecki et al. 2016). Meanwhile, foliar infection on bay laurel does not negatively impact this host (DiLeo et al. 2009).

While asymmetric host competency and susceptibility clearly indicate a reservoir host (California bay laurel) and non-reservoir hosts (*Quercus spp.*), the temperature and moisture sensitivity of *P. ramorum* make this a useful system to study abiotic effects on pathogen spillover. Experimental and observational studies indicate that temperature extremes (hot or cold) and/or lack of moisture reduces sporulation, and therefore transmission, of *P. ramorum* (experimentally: Englander et al. 2006, Tooley et al. 2008; observationally: Davidson et al. 2005, 2008, Eyre et al. 2013). We aimed to disentangle the relative contributions of biotic and abiotic environmental factors on pathogen spillover in this disease system. Our overarching hypothesis is that biotic factors will outweigh abiotic factors, however, the abiotic factors will have a significant influence on pathogen spillover.

The inherent complexity of ecological systems presents analytical challenges, because multiple factors have direct and indirect causal relationships within and across ecological hierarchies. We addressed this analytical challenge using path analysis, which enables the examination of direct and indirect effects of multiple variables within a confirmatory causal framework. Specifically, we examined the influence of topography, understory microclimate, and the tree community on pathogen spillover resulting in oak infection in the sudden oak death disease system. Our results offer insight into the relative effects of biotic and abiotic

environmental drivers of disease dynamics and highlight that understanding these effects can improve disease control and management efforts.

Methods

Study Area

During 2003-2004, we established 202 plots (each 225-m^2) in potential *P. ramorum* host habitat (i.e. forests or woodland) across a 275-km^2 study area in southeastern Sonoma County, CA (Fig. 3.2).Plots were located on public and private lands with varying levels of forest cover and development in the surrounding landscapes. Elevation at plot centroids ranged from 55 m to 800 m (mean 378 m). Vegetation is diverse across this landscape, including stands of mixed evergreen forest dominated by oak species and bay laurel, as well as stands dominated by coast redwood (*Sequoia sempervirens*). Chaparral, characterized by manzanita (*Arctostaphylos sp.*), chamise (*Adenostoma fasciculatum*), and *Ceanothus* shrub species interspersed with a few oak species, occurs at higher elevations of the Mayacama Mountain range along the eastern border of the study area. Tanoak is relatively rare across this study area, only found in eight plots, typically occurring with coast redwood or Douglas-fir (*Pseudotsuga menziesii*). This region of California has a Mediterranean climate with distinct wet and dry seasons. Precipitation predominantly falls as rain from October through April, followed by a dry season with higher temperatures and lower humidity from May through September.

Data Collection

After plot establishment, we collected data annually each spring through 2012, and then began sampling every other year, with the most recent data used in this analysis collected during the spring of 2014. During annual surveys, we recorded individual host stem characteristics, disease intensity and prevalence, and understory microclimate temperature in each plot. During each visit, we assessed stems measuring ≥2-cm diameter at breast height (DBH; breast height = 1.4-m) of five epidemiologically important host species: coast live oak, California black oak, canyon live oak, tanoak, and California bay laurel. Some species commonly form multi-stemmed trees, so a stem was defined as a major branching that separated from the base or main trunk of the tree below breast height. We quantified disease intensity on bay laurel by counting the number of symptomatic leaves on bay laurel stems for 60 seconds (Condeso and Meentemeyer 2007). Prevalence of infected oak species was determined by visual inspection for cankers characteristic of *P. ramorum* infection on main stems or major branches. At plot establishment, the stems of all other tree species rooted in the plot and ≥5 cm DBH were identified to species, assessed as alive or dead, and their DBH was recorded.

The ambient understory temperature was recorded in each plot using HOBO temperature loggers (during 2003-2008 model: H08-032-08, during 2008-2016 model: UA-001-64, Onset Computer Corp. Bourne, MA, USA) housed inside a solar radiation shield (model RS1, Onset Computer Corp. Bourne, MA, USA) secured 1-m above the ground on a pole located in the center of each plot. The temporal resolution of these data sometimes changed between years and some data were missing each year. Missing records were due to user error, logger malfunction, and/or battery failure (also cows). Using methods described in

Tonini et al. (2016), we created a data set of temperature measurements at an hourly resolution for each plot for the entire study period. We also recorded rainfall using tipping-bucket rain gauges (model RG3, Onset Computer Corp. Bourne, MA, USA) at 14 locations capturing the topographic variability across the study area. Using these data we developed variables representing the landscape context, plant community, and local climate that are relevant to the epidemiology of this disease system.

Landscape context

Landscape context, such as topography, influences moisture persistence at a site, as well as the vegetation community and, indirectly, disease dynamics. To account for the influence of topography in the sudden oak death disease system we calculated the topographic wetness index for each plot from a 15-m resolution digital elevation model using the r.topidx function (Cho 2000) implemented in GRASS GIS (GRASS Development Team 2016). The topographic wetness index (TWI) was developed as part of estimating flow from a catchment during a rainfall event using physical characteristics of topography and soil transmissivity (Beven and Kirkby 1979). The index is calculated by dividing the upslope contributing area of a location on the landscape by the tangent of the local slope gradient (in radians) assuming soil transmissivity is constant (Moore et al. 1991):

$$w = \ln\left(\frac{A_s}{\tan\beta}\right) \quad \text{Eq. 1}$$

where w is the wetness index, A_s is the catchment area, and β is the local slope gradient. Higher index values indicate the potential for more water to flow through or accumulate at a location, prolonging moisture persistence, which is favorable for pathogen reproduction and

survival. The topographic structure indicated by TWI values is also related to the local microclimate of a site, with cool air pooling at higher values (Dobrowski 2011).

Community

We calculated tree species diversity in each plot as Shannon's Diversity Index, also called the Shannon-Wiener function (Krebs 1999, p. 444-445). This index quantifies the uncertainty in correctly predicting the species of the next individual collected, and is calculated using the following equation:

$$H' = -\sum_{i=1}^{s}(p_i)(\log_2 p_i) \quad \text{Eq. 2}$$

where H' is the Shannon's Diversity Index, s is the number of species, and p_i is the proportion of the total sample belonging to the i-th species. Larger values of H' indicate greater uncertainty and therefore a more diverse community. We used the 'diversity' function implemented in the 'vegan' package (Oksanen et al. 2016) within R statistical computing environment (R Core Team 2016) to calculate Shannon's index for each year that data on all tree species was collected (2005, 2012, and 2014). Index values were strongly correlated between these years (Pearson's $r > 0.9$), so we selected the values from the 2005 sample year for use in our analysis, because this enabled retaining the most complete data set.

We estimated reservoir host density using the number of bay laurel stems ≥2-cm rooted in each plot. First, we calculated the number of stems per square meter based on plot area (225-m^2), and then scaled this to the common forestry standard of stems per hectare.

Local climate

Moisture and temperature are key factors in the epidemiology of sudden oak death, influencing the population of *P. ramorum* on timescales of weeks to months (Davidson et al. 2005), and of the host trees over years to decades. We investigated the influence of the local climate on the pathogen using the high-resolution rainfall and microclimate data collected across the study area. Based on relationships established in prior research on sudden oak death epidemiology, we calculated two different variables to capture effects of local climate variability on foliar pathogen load and oak infection at each plot: 1. heat exposure, and 2. exposure to warm and wet conditions. For heat exposure, we calculated the number of hours that were above 25 °C during the dry season (June - September) prior to sampling during the following spring. We chose this threshold because inoculum is reduced with greater exposure to high temperatures due to increased leaf abscission and direct mortality of the pathogen (Davidson et al. 2005, Englander et al. 2006, Tooley et al. 2008). For warm & wet conditions, we calculated the average number of hours that the temperature was between 14 and 22 °C on days with recorded precipitation (>0.25 mm) during the wet season (November – May) of the current and previous sample year for each plot. A plot was determined to have a "wet-day" if its nearest-neighbor rain gauge recorded precipitation for that day. We developed this variable based on warmer and wetter average temperatures during two consecutive years increasing the likelihood of oak infection (Haas et al. 2016), and that pathogen sporulation was greater in this temperature range in controlled experiments (Englander et al. 2006).

Pathogen spillover

We quantified two key parts of pathogen spillover during each sampling season for each plot: the pathogen load and disease prevalence. We estimated the plot-level pathogen load by summing the symptomatic leaf counts on bay laurel stems that were rooted within, or had foliage overhanging, the plot boundary. We calculated disease prevalence for susceptible oak species as the ratio of infected oak stems to uninfected oak stems based on observed canker symptoms.

Modeling Framework

Path analysis (Wright 1921, Shipley 2004) is a type of structural equation modeling (SEM) without latent variables. As a methodology, SEM is ideal for conceptualizing and understanding the direct and indirect effects of multiple processes in ecological systems (Grace et al. 2010). The philosophical underpinnings of SEM as a confirmatory approach means that the fit of a SEM is assessed based on whether or not the complete set of hypotheses that make up the structural model are supported by the data. This is unlike null hypothesis testing where the test is to see if the data fit the developed model better than an alternative "null model." In other words, an acceptable path model will result in statistical insignificance at a level selected a priori, e.g. $p > 0.05$. The interpretation of an acceptable model should be tentative, because there may be other model structures that are also supported by the data. If the initial model structure is not fully supported and/or the data suggests an alternative structure (i.e. statistically significant missing paths between variables), then the new structure may be assessed, but this should be considered an

exploration of the relationships in the system. Ideally, the new structure would then be tested using an independent data set for further confirmation (Grace et al. 2010).

We used path analysis in a confirmatory approach to assess a hypothesized set of direct and indirect effects of landscape context, species diversity, and local climate variation, on the process of pathogen spillover for a single structural model (Fig. 3.1). Based on published knowledge of sudden oak death disease dynamics, we developed a set of epidemiologically relevant variables to apply to this framework using 10 years of data from a long-term study in California, USA.

Path Analysis

We applied these data in our path model describing hypothesized direct and indirect relationships between the landscape, local climate, tree community, and disease (Fig. 3.1). In a path analysis, response variables have one or more arrows pointing toward them from predictor variables, and can be a predictor variable for another part of the model. We assessed the path model using the 'piecewiseSEM' package version 1.1 (Lefcheck 2015) in R. This package implements the steps for assessing path model structures using the d-sep (short for "directed separation") test (Shipley 2000, 2009; Appendix C).

Rooted in graph theory, the d-sep test assesses independence claims between pairs of unconnected variables (or nodes) in a directed acyclic graph (DAG). The independence between variables suggested by the topology of the graph is translated to a predicted statistical independence between random variables, i.e., variables without a direct connection are conditionally independent. These conditional independence claims are tested by applying the set of variables that are causal to each of the variables assumed to be independent

together in the same model. For example, in Fig. 3.1 species diversity is independent of heat exposure conditional on the landscape context. To test this conditional independence claim, heat exposure is modeled as a function of species diversity and landscape context and if the p-value of the species diversity variable is statistically significant then it is not conditionally independent of heat exposure. The p-values of the independence claims are combined into Fisher's *C*-statistic (Shipley 2000, 2004) to assess the overall fit of the path model (we selected a threshold of $p<0.05$ for statistical dependence of each claim). One or more violations of independence claims may result in the test of Fisher's *C* having a small p-value, indicating the data do not support the model structure. The necessary steps for performing the d-sep test are listed in Appendix C.

An advantage of the d-sep test is that different model types can be used to appropriately analyze the response variable, e.g., generalized linear and mixed-effects models can be used as needed to assess the different pieces of the path model (Shipley 2009). Thus, a variable with a binomial distribution can be assessed in the same path model as a normally distributed variable. In our analysis, disease prevalence was observed as an aggregation of yes/no observations of oak infection in each plot, so it is appropriately modeled as a binomial response; and most measurements were repeated in each plot for each year resulting in crossed data. We used mixed-effects models with scalar random effects for the sample year and plot, which account for this cross-replication by allowing the intercepts for these grouping factors to vary. The random effect for year accounts for correlation between measurements made during the same year, while the random effect for plot accounts for correlation between the measurements from the same plot. Accounting for this induced

correlation provides more accurate estimates of statistical significance by preventing variation being inappropriately attributed to measured variables.

The 'piecewiseSEM' package enables approximation of correlated errors between variables that are not causal to each other, but have a shared driver, by excluding them from the basis set and calculating a significance test on the bivariate correlation (Lefcheck 2015). In our model, we assumed correlation between the local climate variables, indicated by the curved and double-headed arrow (Fig. 3.1), because the shared driver of these phenomena is the regional climate pattern, so neither is causal to the other.

We modeled all of the response variables, with the exception of oak infection, as normally distributed. To better meet assumptions of normality, we natural logarithm transformed the pathogen load, host density, and warm & wet conditions variables. We fit models appropriate to each response variable in the R statistical computing environment. Since diversity for each plot was calculated from a single year (not a repeated measurement) and had a single predictor variable we fit an ordinary least squares regression model via the 'lm' function. We modeled the repeatedly measured symptomatic leaf count and the local climate variables using linear mixed-effects regressions with random effects for sample year and plot, implemented with the 'lmer' function from the 'lme4' package (Bates et al. 2015):

$$(\mathbf{y}|\mathrm{B} = \mathbf{b}) \sim N(\mathbf{X} \times \boldsymbol{\beta} + \mathbf{Z} \times \mathbf{b} + \mathbf{e}) \quad \text{Eq. 3}$$

$$\mathrm{B} \sim N(0,\mathbf{D}) \quad \text{Eq. 4}$$

$$\mathbf{e} \sim N(0,\sigma^2) \quad \text{Eq. 5}$$

where $\mathbf{y}$ is the n-length vector of observed values for the response variable, which is multivariate normal conditional on $\mathrm{B} = \mathbf{b}$; $\mathbf{X}$ is the $n \times p$ fixed-effects matrix of predictor variables, with p equal to the number of explanatory variables; $\boldsymbol{\beta}$ is the p-length vector of

fixed-effects coefficients to be estimated that apply to all years and plots; **Z** is the $n \times q$ random-effects model matrix for the q-dimensional unobserved random-effects variable B whose value is fixed at **b**, where q is the total number of levels in the grouping factors. B has an unconditional multivariate normal distribution with a mean of zero and covariance matrix **D** (Bates et al. 2015). The simple scalar random effects terms for sample year and plot result in the covariance matrix **D** having diagonal structure with the variance (diagonal matrix values) estimated within each group and the covariance (off-diagonal matrix values) equal to zero. The n-length vector **e** is the residual error in the model (unexplained variation in **y**), and assumed to be normally distributed with a mean of zero and a variance σ^2.

We fit a binomial generalized linear mixed-effects regression with random effects for plot and sample year using the 'glmer' function from the 'lme4' package to model oak infection:

$$(\mathbf{y}|B = \mathbf{b}) \sim \text{Binomial}(\mathbf{n}, \mathbf{p}|\mathbf{b}) \quad \text{Eq. 6}$$

$$\text{logit}(\mathbf{p}|\mathbf{b}) = \mathbf{X} \times \boldsymbol{\beta} + \mathbf{Z} \times \mathbf{b} \quad \text{Eq. 7}$$

where **y** is binomially distributed with an occurrence probability **p**, which is modeled as a function of linear predictors using the logit link function (Eq. 7). The details of the linear predictors in Eq. 7 are the same as those in Eq. 3 and 4 above.

We assessed collinearity of the predictor variables prior to inclusion in each of the regression models to assure that Pearson's r was <|0.5|, and examined residual plots of each model for heteroscedasticity that would indicate violation of model assumptions. We tested the fit of the path model structure using the 'sem.fit' function, which implements the d-sep test (Shipley 2000, 2009), from the 'piecewiseSEM' package (Lefcheck 2015) with an *a priori* threshold p-value >0.05 as an acceptable fit. We fit the models using unstandardized

variables, and then extracted the raw and standardized (mean = 0, variance = 1) coefficient values using the 'sem.coefs' function in the 'piecewiseSEM' package. The implementation of the 'sem.coefs' function for "scaled" variables results in standardizing all continuous variables in the path model to a mean of zero and standard deviation of one. In our model the binomial oak infection response remains unaltered. We report both raw and standardized coefficients for the path model.

Path coefficients are interpreted as the direct and/or indirect effects on the response variables, where direct effects are from variables that point directly to a response variable. Variables with indirect effects are those that are at least once removed from another response variable. For example, landscape context indirectly affects disease prevalence through direct effects on species diversity and heat exposure (Fig. 3.1). Indirect effects are calculated by multiplying the coefficients along the path to the response variable. The total effect of a variable is the sum of the direct and indirect effects. The relative strength of direct and indirect effects on a response variable can be assessed using standardized coefficients.

Results

We tested our path model structure using data from 164 plots sampled between 2005 and 2014 (n=1433 observations) that met the criteria of having one or more susceptible oak trees and found an acceptable fit (p=0.22, Fig. 3.3, Table 3.1). While the biological variables had stronger effects on pathogen spillover, the physical environmental variables still had significant influence (Fig. 3.3, Table 3.2 & 3.3). More time at temperatures >25 °C during June-September reduced symptomatic leaf count the following sample season, resulting in less pathogen spillover as indicated by the net negative effect on oak infection. However, this

was countered by the strong positive effect of bay laurel density on pathogen load. Greater exposure to temperatures between 14 and 22 ºC on wet days had a positive, but weak, direct effect on symptomatic leaf count ($p=0.068$, Table 3.2), however, the direct effect of this variable on oak infection was positive, indicating that warm and wet conditions facilitated the success of pathogen spillover to susceptible oak species. Species diversity had a dilution effect, indicated by the strong negative effect on oak infection.

Direct effects of the topographic index indicate that locations with higher potential soil moisture were less diverse and had fewer hours with temperatures >25 °C during the dry-season. The net effect on pathogen spillover was positive, indicating that oak trees located in areas with greater potential for moisture persistence are more likely to become infected.

Discussion

Many emerging infectious diseases (EIDs) involve multiple hosts and are characterized by pathogen spillover. While prevention and control of EIDs is a common goal, more research is needed to understand how environmental variation can affect these efforts by simultaneously affecting the pathogen load on reservoir host(s) and the susceptibility of non-reservoir host(s). Studies on pathogen spillover frequently focus on the relationship between the reservoir and non-reservoir host, but seldom include effects of the physical environment. Plant disease systems, such as sudden oak death, are useful for investigating these relationships because the host species do not move and are typically long-lived, so variation in disease-environment relationships can be more easily monitored. In addition to improving disease management for the focal systems, studies of plant disease systems can provide

insights into the types and frequency of data collection necessary for effective prevention and control of other diseases.

Pathogen spillover in the sudden oak death disease system was more strongly influenced by vegetation community characteristics, but still significantly affected by variation in the local climate and physical environment. Higher densities of the reservoir host increased pathogen load, which increased disease prevalence on oak species (i.e. pathogen spillover), but this was countered by the strong dilution effect of species diversity. The local climate simultaneously influenced reservoir host pathogen load and non-reservoir host infection, with heat exposure reducing pathogen load, but warm and wet conditions increasing disease prevalence. The community and local microclimate were affected by the landscape context, where areas with greater potential for moisture accumulation and persistence ultimately having a positive effect on pathogen load and disease prevalence.

The negative relationship between disease prevalence and species diversity is evidence for the dilution effect, whereby species diversity reduces disease risk (Keesing et al. 2006, 2010), which was previously shown in the sudden oak death disease system (Haas et al. 2011, 2016). Analyzing data at the individual stem level collected through 2010 from the same region as the present study, Haas et al. (2016) found positive effects of the two-year mean for temperature and precipitation calculated from coarse climate data that was downscaled, and the size of individual trees on likelihood of infection, with a relatively weaker dilution effect. We found similar relationships in our analysis using additional years of data capturing the onset of drier than average conditions (Fig. 3.4) and a later stage of invasion, but found relatively stronger dilution effect (Fig. 3.3). These minor differences may be partly due to the levels of aggregation of the response variables (individual stems vs. our

aggregation to the plot), or the higher resolution abiotic variables we used. By aggregating disease prevalence across all stems of all susceptible oak species we obscured the variation among species' and individual's disease resistance, susceptibility, and tolerance that may be conferred by genetic differences (Dodd et al. 2005). Since this individual variation exists, efforts that preserve the genetic diversity of susceptible species are key for enhancing resilience to this and other diseases. While not accounting for this variation may influence the magnitude of the estimated effects on oak infection, these estimates may also be affected by cryptic infections making visual detection more difficult (Swiecki et al. 2016). Haas et al. (2016) showed that coast live oak individuals had greater probability of infection than black oak, but also noted the caveat of visual detection potentially influencing this result. Still, the dilution effect of diversity reducing disease in the SOD system appears to be consistent in oak-dominated stands.

We also confirmed that density of bay laurel was the strongest driver of pathogen load (total symptomatic leaf count) in the plot, but local climatic conditions were also significant. Plot-level pathogen loads on bay laurel in this region have been shown to be sensitive to climatic conditions (Condeso and Meentemeyer 2007, Anacker et al. 2008). Again, our aggregation to the plot obscures individual variation in bay laurel susceptibility (Anacker et al. 2008, Hüberli et al. 2011), however, the variation between individuals in these studies was based on lesion sizes from detached leaf assays. While larger lesions produce more inoculum, the differences between susceptibility of individual trees were overridden at the landscape scale by local climatic conditions (Anacker et al. 2008). This supports our analysis of effects on pathogen load at the plot-level. Still, the individual variation in susceptibility indicates the possibility of superspreader (Heesterbeek et al. 2015)

bay laurels existing in the population or particular plots that we did not detect using these methods, which is an area of research that could be further explored.

In addition to the hosts and pathogen, local climate conditions are the other key part of disease dynamics. We confirmed that heat exposure during the summer reduced pathogen spillover by reducing pathogen inoculum load the following spring, corroborating findings showing that *P. ramorum* survival on bay laurel leaves decreased during the summer months (Davidson et al. 2005) and with the number of days exceeding 30 ºC (DiLeo et al. 2014). Several experimental studies also showed decreased survival of *P. ramorum* exposed to high constant temperatures for several hours (Tooley et al. 2008, 2014, Tooley and Browning 2015). Although infection on California bay laurel leaves can rebound quickly following drought conditions (Eyre et al. 2014), based on our results this may not necessarily lead to increased pathogen spillover. According to our results, disease prevalence was greater when temperatures are consistently warm and wet, meanwhile, hotter summer temperatures indirectly reduced disease prevalence by lowering the pathogen inoculum load. These effects suggest that warmer temperatures during the wet season will increase the success of pathogen spillover, but a generally warming climate may also increase heat exposure, thereby reducing the pathogen load and limiting spillover.

In a review of studies examining the relationship between drought and plant diseases Desprez-Loustau et al. (2006) found that 67% showed evidence for drought favoring disease, and in some cases the interaction was synergistic. However, only 50% of the studies on *Phytophthora* related diseases reported positive drought-disease interactions. Increases in disease severity were frequently attributed to indirect effects of drought on the pathogen by altering host physiology and increasing susceptibility. Using observations of disease

prevalence and environmental variation in a natural landscape over multiple years we found evidence for an antagonistic interaction between drought and infection for a *Phytophthora* related disease, where hot and dry conditions reduced pathogen spillover from the reservoir to non-reservoir hosts. This is partly due to bay laurel leaves damaged by the pathogen being abscised during hot summers, as well as the pathogen being killed directly or forced into dormancy due to the prolonged heat exposure and dry conditions. The susceptible oak tree species are also resilient to drought and commonly occur where rainfall is generally lower than in our study area (Lamsal et al. 2011). Since we modeled infection and not mortality of infected oaks, it is still possible that sudden oak death has a positive interaction with drought in terms of increasing mortality of infected trees.

Landscape context such as local and regional topography influences biotic and abiotic environmental conditions through orographic effects, cool air pooling, and soil moisture. Higher values of TWI (greater potential moisture) indirectly increased pathogen spillover by reducing species diversity and heat exposure, promoting higher pathogen load and increasing susceptibility of oak trees. Locations with higher TWI values experience persistent soil moisture and cool air pooling, both of which reduce the moisture deficit and can enhance pathogen sporulation and persistence. Persistent moisture also increases the likelihood that *P. ramorum* spores will survive long enough to encounter an opening on the surface of an oak tree and start an infection without altering the physiological susceptibility of the host.

The sensitivity of *P. ramorum* to heat exposure confirmed in our model suggests that management actions to slow disease spread and protect valuable oak trees may be especially effective during seasonal drought conditions when the pathogen load has already been reduced. Slowing the spread can primarily be achieved through removal of bay laurel, which

would also worsen microclimate conditions for the pathogen on any remaining susceptible host species. These efforts could simultaneously reduce and restructure potential fuel loads, helping prevent large wildfires (Metz et al. 2011). Low-intensity prescribed fire may in fact be an effective tool for thinning forest understory that is dominated by California bay laurel, although this species can sprout prolifically following fire (personal observation). In these cases, the substrate for *P. ramorum* to survive at relatively high levels during the dry summer months would be at least temporarily removed, thus reducing the inoculum available to seed epidemic spread during the following wet season. By assessing the simultaneous influence of biotic and abiotic environmental factors on pathogen spillover we have provided further understanding into the relative effects of disease drivers while also gaining insight that may enhance the efforts to control emerging infectious diseases.

CHAPTER 4: SPILLOVER OF AN EXOTIC FOREST PATHOGEN PROMOTES ITS NATIVE RESERVOIR HOST

Abstract

Pathogens play a significant role in structuring communities by mediating competition between species. The outcome of this apparent competition either facilitates or hinders coexistence of the competing species. We investigated the consequences of apparent competition caused by the exotic, generalist plant pathogen *Phytophthora ramorum* by analyzing a decade of change in susceptible and non-susceptible species in natural forest communities in California. In this region, *P. ramorum* causes the canker disease sudden oak death on susceptible oak species, however, pathogen transmission is driven by the tolerant reservoir host species, California bay laurel (*Umbellularia californica*). Based on this relationship, we used path analysis in a confirmatory approach to test hypothesized relationships among five tree species in these forest communities. We also examined the relationship between pathogen load and species diversity of the entire tree community. We confirmed our hypothesis that spillover of *P. ramorum* from bay laurel to susceptible oak species favors the reservoir host. Increases in the tolerant reservoir host are related to greater losses of susceptible oak in places with higher pathogen loads. This relationship was also moderated by the local climate conditions, where hotter locations had lower pathogen loads and smaller increases in bay laurel. Disease impacts also favored persistence of non-susceptible oak species, but had no effect on Douglas-fir (*Pseudotsuga menziesii*), a low-competency host species encroaching into oak woodlands in the region. Finally, we found a negative trend in the relationship between pathogen load and species diversity that appeared

to grow stronger over time. This may be an indication of *P. ramorum* ultimately reducing species diversity by reducing the competitive ability of susceptible oak species. Our results indicate that this exotic, generalist pathogen is negatively effecting existing coexistence mechanisms, suggesting these forests are on a trajectory toward a new community structure of species coexistence.

Introduction

Diseases affect their host communities by modifying host fitness and mediating competition. These effects on fitness and competition either facilitate or hinder coexistence through two mechanisms: 1. *stabilizing* mechanisms increase intraspecific competition relative to interspecific competition, and 2. *equalizing* mechanisms minimize fitness differences between species (Chesson 2000). Pathogens facilitate coexistence when they are either stabilizing, by limiting the growth of their host as it becomes more abundant, or equalizing by minimizing fitness differences between competitors. Coexistence is hindered when a pathogen increases fitness differences or creates positive feedbacks that increase interspecific competition relative to intraspecific competition leading to competitive exclusion of the less abundant species (Mordecai 2011).

A pathogen's effect on coexistence mechanisms is influenced by its host-specificity (specialist vs. generalist), whether it is exotic vs. endemic or naturalized, and whether it causes epidemic disease (Alexander and Holt 1998, Gilbert 2002, Mordecai 2011, Salkeld et al. 2016). Host-specific pathogens (*specialists*) promote coexistence by limiting their preferred host as it becomes more abundant (*stabilizing*), thereby favoring rare species in the community (Janzen-Connell hypothesis; (Janzen 1970, Connell 1971)). Meanwhile, multi-host pathogens (*generalists*) can have a similar or opposite impact (Mordecai 2011). Exotic

pathogens are frequently recognized for their destabilizing impacts to their novel environments, while endemic or naturalized pathogens are key ecosystem components that maintain coexistence (Hansen and Goheen 2000). Epidemic disease is not part of regular ecosystem dynamics and frequently has negative effects on coexistence mechanisms. Disease epidemics often result from major changes to the system, such as introductions (e.g. exotic pathogens), landscape modifications, and/or stochastic climate events (Hansen et al. 2001, Stenlid and Oliva 2016, Stephens et al. 2016). For example, the introduction of the exotic fungus *Cryphonectria parasitica* caused an epidemic decimating the American chestnut tree that had previously dominated Appalachian forests of the eastern United States, leading to new communities dominated by hemlock and oak species (Paillet 2002).

Hosts of generalist pathogens tend to respond differently to their shared pathogen. Asymmetries in transmission competency and tolerance of infection can result in pathogen spillover, which is when a reservoir host species drives pathogen transmission and disease in non-reservoir hosts (Power and Mitchell 2004). Depending on the details of the disease system, pathogen spillover may facilitate or hinder coexistence mechanisms for competing species. Mordecai (2013) provided an example of facilitation via stabilization, where the reservoir host (the invasive cheat-grass *Bromus tectorum*) experienced a net cost of infection by the endemic fungal pathogen black fingers of death (BFOD, *Pyrenofora semeniperda*; (Medd et al. 2003), relative to a native perennial bunch grass (*Elymus elymoides*) that was less susceptible to infection. In this case, the pathogen reduced the competitive ability of the reservoir host, facilitating coexistence with the competing host species. Borer et al. (2007) found a similar effect in their examination of the relationship between the barley-yellow dwarf viruses and introduced and native grass hosts in California. In that case, coexistence

was promoted because the disease facilitated invasion of the introduced grass species by increasing its competitive ability relative to the native grass species.

Rapid transportation has enabled the introduction of an increasing number of exotic species to novel ecosystems during the past 100 years (Aukema et al. 2010, Bradley et al. 2012). Exotic pathogens are numerous (Jones et al. 2008), difficult to detect, and can have dramatic impacts, including permanently restructuring forest communities (e.g. American chestnut blight; Paillet 2002). Exotic pathogens are often epidemic in their novel environments, so pathogen spillover can reverse the stabilizing and/or equalizing mechanisms of coexistence in naïve communities. Previous research has demonstrated that *Phytophthora ramorum*, the invading generalist forest pathogen that causes sudden oak death (Rizzo and Garbelotto 2003), altered the competitive dominance of a native tree species (Cobb et al. 2010, 2012). The native reservoir host, California bay laurel (*Umbellularia californica*), has high host competency and is very tolerant of infection (DiLeo et al. 2009), and therefore drives pathogen transmission to other host tree species that are susceptible to mortality from infection. This is an example of apparent competition, defined as indirect interspecific interactions that affect the relative abundances of the competing species (Holt 1977).

We investigated the consequences of apparent competition for coexistence of overstory tree species due to impacts from the exotic plant pathogen *P. ramorum* across a landscape where oak species (*Quercus spp.*) susceptible to sudden oak death (SOD) are common. Sudden oak death is a multi-host forest disease caused by an exotic generalist pathogen that has killed millions of trees in coastal forests of California and southwestern Oregon since its introduction in the mid-1990s (Meentemeyer et al. 2008c, Lamsal et al.

2011). Previous studies showed that this pathogen catalyzed dramatic changes to naïve forest communities, especially those where tanoak is abundant (Cobb et al. 2010, 2012, Metz et al. 2011, 2012, 2013). The amount of pathogen inoculum is likely to affect disease severity (Davidson et al. 2005, Haas et al. 2016) and have cascading impacts to community composition and diversity, yet most studies in this system have used the density, abundance, or prevalence of infected trees as a proxy for pathogen load (but see Haas et al. 2016 and Chapter 3 herein).

Using a decade of field measurements where we recorded disease levels and community changes, we provide detailed evidence of how SOD is affecting forest communities where the most susceptible oak species, coast live oak (*Q. agrifolia*) and California black oak (*Q. kellogii*) are abundant. In addition to observations of the biotic community, we collected local microclimate data enabling us to account for influences of the abiotic environment on the hosts and pathogen. We developed a path analysis (Fig. 1) guided by asking the following questions: 1. Did losses in the density and/or dominance of standing live susceptible non-reservoir host species correlate to gains in the reservoir host species? (i.e. apparent competition favoring the bay laurel) and 2. Did other commonly occurring non-host or weakly competent species increase, decrease, or remain unaffected (i.e. apparent competition favoring other species in the community)?

Methods

Study Area

We collected data at 202 plots (each 225-m^2) across a 275-km^2 study area in southeastern Sonoma County, CA described in Haas et al. (2016) and Chapter 3 herein (Fig. 2). The

landscape is topographically diverse and captures a mix of urban, agriculture, and wildland areas. Most of the forested landscape is a mix of evergreen species with stands dominated by oak species (*Quercus sp.*), bay laurel, and Douglas-fir (*Pseudotsuga menziesii*). Pacific madrone (*Arbutus menziesii*) and California buckeye (*Aesculus californica*) are also common overstory tree species. This region of California has a Mediterranean climate with distinct wet and dry seasons, where precipitation predominantly falls as rain from October through April.

Study system

P. ramorum is moisture, temperature, and light sensitive, thriving in warm and wet conditions (Davidson et al. 2005, Englander et al. 2006, Tooley et al. 2008). The most competent host tree, California bay laurel, is also very tolerant of infection, so while the majority of transmission occurs within this species it experiences few ill-effects (DiLeo et al. 2009). Pathogen spillover from bay laurel results in deadly canker infections on neighboring susceptible oak species that are otherwise incompetent hosts (Rizzo et al. 2005, Swiecki et al. 2016), providing a useful system for examining the consequences of pathogen-mediated apparent competition

Data collection

Following plot establishment (2003-2004), we collected disease, temperature, and rainfall data annually through the 2012 sampling season, and then began sampling every other year. The most recent data used in this analysis was collected during the spring of 2016. Each year, we recorded individual host stem characteristics, disease intensity and disease prevalence, as

well as understory microclimate temperature in each plot. In order to track community changes, we censused all trees in each plot during establishment, 2012, 2014, and 2016. During these visits, we recorded the diameter at breast height (DBH; breast height = 1.4-m) of standing live and dead stems of five epidemiologically important host species (bay laurel, black oak, coast live oak, canyon live oak, and tanoak) with a DBH ≥2-cm, and of all other standing tree or shrub stems with a DBH ≥5-cm. During each visit we quantified pathogen load on California bay laurel by counting the number of symptomatic leaves on bay laurel stems rooted in or overhanging the plot for 60 seconds (Condeso and Meentemeyer 2007).

We recorded the ambient understory temperature in each plot using HOBO data loggers (during 2003-2008 model: H08-032-08, during 2008-2016 model: UA-001-64, Onset Computer Corp. Bourne, MA, USA) housed inside a solar radiation shield (model RS1, Onset Computer Corp. Bourne, MA, USA) secured 1-m above the ground on a pole located in the center of each plot. Missing temperature data were interpolated and resolved to hourly observations using methods described in Tonini et al. (2016). We recorded rainfall using tipping-bucket rain gauges (model RG3, Onset Computer Corp. Bourne, MA, USA) at 14 locations capturing the topographic variability across the study area.

Analyses

Using these data, we calculated the density, dominance, and importance value of living stems for each species in 2005, 2012, 2014, and 2016, as well as the change in these values from 2005 to 2016, for each plot. We also calculated the average pathogen load between 2005 and 2016 and average temperature between 2005 and 2014 for each plot. In all of our calculations we lumped non-susceptible oak species (*Q. garryana*, *Q. lobata*, and *Q. douglasii*) into a

"white oak" designation due to similar ecological and epidemiological traits, and difficulty in accurately identifying the species during data collection. Our study area is a zone of hybridization for these species, adding to the challenge. Typically, a single member of this group was represented when present in a plot, but species diversity may be underestimated in some locations. In calculating change in species and averages of pathogen load and temperature, we excluded plots that had missing tree community data due to collection errors in either 2005 or 2016, as well as plots where mechanical removal was noted at any time during the study period. These limitations ensured that calculations of change represented ecological effects, and resulted in 182 plots available for our analysis.

Stem density for each species was calculated for each plot as the number of stems per plot area (225-m^2) and stem dominance as the total basal area in square meters of each species in each plot, i.e.:

$$BA_S = \sum_{i=1, i \in S}^{n} (\pi * DBH_i/40000) \quad \text{Eq. 1}$$

where BA_S is the basal area of species S, DBH is measured in centimeters for each stem i belonging to species S, and n is the total number of stems for each species in each plot. The importance value combines the relative density and relative dominance of a species, providing insight into how changes in species with different life history strategies alter the community characteristics:

$$IV_S = 0.5 * (relative\ density_S + relative\ dominance_S) \quad \text{Eq. 2}$$

with

$$relative\ density_S = number\ of\ stems_S / total\ number\ of\ stems \quad \text{Eq. 3}$$

and

$$relative\ dominance_S = basal\ area_S / total\ basal\ area \quad \text{Eq. 4}$$

where IV_S is the importance value for each species S in each plot, and ranges from 0 to 1. While useful, importance value obscures details of whether the change in one species is purely relative to the change in another, or if the species is actually responding with absolute changes in its density and/or dominance. We calculated the change from 2005 to 2016 in each of these metrics by subtracting the values calculated for 2005 from the values calculated for 2016, resulting in a single observation of change for each of the 182 plots. Missing values in change calculations due to a species absent from a plot in both 2005 and 2016 were replaced with zeroes (i.e. interpreted as neither loss nor gain).

We also examined changes in community diversity indices. For each of the years we collected data on all the overstory species (2005, 2012, 2014, and 2016) we calculated Shannon's Diversity Index, Simpson's Diversity Index, and Pielou's Evenness Index for each plot using the 'diversity' function in the 'vegan' (Oksanen et al. 2016) package implemented in the R statistical computing environment (R Core Team 2016):

$$H' = -\sum_{i=1}^{S} p_i * ln(p_i) \quad \text{Eq. 5 (Shannon's Diversity Index)}$$

$$D = 1 - \sum_{i}^{S} p_i^2 \quad \text{Eq. 6 (Simpson's Diversity Index)}$$

$$J = H'/ln(S) \quad \text{Eq. 7 (Pielou's Evenness)}$$

where p_i is the proportion of the total sample belonging to the *i*-th species and S is the number of species. Larger values of H' or D indicate greater species diversity and should be strongly correlated, however, H' is more sensitive to changes in rare species, while D is more sensitive to changes in abundant species (Krebs 1999, p. 440-444). Values for Pielou's

Evenness range from 0-1, with 1 indicating complete equitability in the abundance of two or more species and 0 indicating complete dominance by a single species. To gain inference on how sudden oak death is impacting the community diversity we summarized indices across the plot network for each DBH census year, and conducted a paired *t*-test comparing the 2016 data to the 2005 data.

We used path analysis (Wright 1921, Shipley 2000, 2004) to assess the direct and indirect effects of the average temperature and pathogen load on changes in the most commonly occurring species (*U. californica*, *Q. agrifolia*, *Q. kellogii*, *P. menziesii*), and the white oak species group in our study area. Although the tree and shrub species pool is diverse (21 species) across the entire plot network, this subset of species included the three most epidemiologically important species in the study area, and the species for which we were most likely to be able to detect a statistically robust response due to occurrence. We developed a path model structure hypothesizing how changes in species, and therefore the community demographics, were expected to respond to disease impacts (Fig. 1).

Path analysis is a type of structural equation modeling and characteristically is useful for understanding direct and indirect effects of multiple system processes (Grace et al. 2010). The philosophical underpinnings of SEM as a confirmatory approach means that the fit of a SEM is assessed based on whether or not the complete set of hypotheses that make up a model are supported by the data. An acceptable model structure will result in statistical insignificance at a level selected *a priori*, e.g. $p > 0.05$, but the interpretation of an acceptable model should be still be tentative. There may be other model structures that are also supported by the data, emphasizing the need to carefully think about the processes being represented by the model structure and the inference you intend to gain.

Our metrics for investigating effects on coexistence were the change in species dominance (basal area) or density (number of stems in the plot). We also explored the change in importance value of Douglas-fir and white oak species using a revised path model structure, because initial analyses resulted in non-significant paths to the change in density or dominance of these species. We calculated variables for use in our path model (Fig. 1) corresponding to a single observation for each of the 182 plots: *Heat Exposure* was the averaged daily maximum temperature during the rainy season (November-May) for sample years 2005 through 2014, *Pathogen Load* was the averaged total symptomatic leaf count for sample years 2005 through 2016, and *Susceptible Oaks* was the change in density or basal area of either coast live oak or California black oak calculated as the difference between the 2005 and 2016 measurements. Changes for bay laurel, white oaks, and Douglas-fir were calculated in the same manner.

We conducted a confirmatory test of the path model structure by applying the d-sep test of conditional independence (Shipley 2000, 2004; Appendix C) implemented in the 'piecewiseSEM' package (Lefcheck 2015) in the R statistical computing environment (R Core Team 2016). The d-sep test translates topological independence claims of the path model structure to statistical independence claims enabling assessment of the model structure by combining exact p-values estimated for variables assumed to be independent. We chose an *a priori* p-value >0.05 as an indication of overall acceptable fit for the path model structure.

Each component model in the path analysis was assessed as a linear relationship using ordinary least squares regression:

$$\mathbf{y} \sim N(\mathbf{X} \times \boldsymbol{\beta} + \mathbf{e}) \quad \text{Eq. 8}$$

$$\mathbf{e} \sim N(0,\sigma^2) \quad \text{Eq. 9}$$

We natural-log transformed the *Pathogen Load* variable to better approximate a Gaussian distribution in the response variable. This transformation was maintained when *Pathogen Load* was used as a predictor variable and when assessing the correlation with change in bay laurel. We fit the models using unstandardized variables, and then extracted the raw and standardized coefficient values using the 'sem.coefs' function in the 'piecewiseSEM' package. The implementation of the 'sem.coefs' function for extracting "scaled" variables results in standardizing all continuous variables in the path model (mean = 0, variance = 1), so the relationships between predictor and response variables are in terms of changes in standard deviations for both sets of variables. We report the standardized and unstandardized path coefficients for all models. For each model, we examined plots of residual error to ensure that there were no violations of assumptions of homoscedasticity.

The 'piecewiseSEM' package enables approximation of correlated errors between variables that are not causal to each other, but have a shared driver, by excluding them from the basis set and calculating a significance test on the bivariate correlation. In our model, we assumed a non-causal correlation between the average pathogen load and change in bay laurel basal area. Because these species don't all commonly occur together, we tested the model structure using all available data and subsets of data that were limited to plots where each species occurred in at least 2005 or 2016.

We also compared annual mortality rates of key host species calculated from this study to pre-epidemic (pre-1995) mortality rates calculated across species' host ranges in California (Barrett 2006) and two other studies in this region conducted prior to (Brown and Allen-Diaz 2009), and overlapping with (McPherson et al. 2010) our study period. We matched these studies by calculating the arithmetic annual mortality rate from 2005 to 2016,

i.e. the number of trees that were alive in 2005 that died by 2016 divided by 11 years. McPherson et al. (2010) calculated separate mortality rates for SOD-symptomatic and asymptomatic trees, so we averaged the symptomatic and asymptomatic mortality rates to get an overall mortality rate similar to our calculations and the calculations from the other two studies (Barrett 2006; Brown and Allen-Diaz 2009). Since there was no asymptomatic mortality rate for black oaks in McPherson et al. (2010), we used the pre-epidemic estimate from Barrett (2006) to calculate the presumed overall mortality rate. Barrett (2006) and McPherson et al. (2010) calculated stem mortality rates, while Brown and Allen-Diaz (2009) calculated basal area mortality rates, so, we compared basal area and stem mortality rates separately. Also, Brown and Allen-Diaz (2009) calculated mortality rates across two time periods (observed 1994-2004 and predicted 1994-2014) and two of their eight sites occurred within our study area. Thus, we compared our mortality rates with the rates for each time period and either the average rate of the two sites within our study area, or all eight of their sites in the region separately.

Results

Across the 182 plots used in our analysis, the most commonly occurring overstory species was California bay laurel, followed by coast live oak, Douglas-fir, white oak species, and California black oak. The most susceptible oak host species, coast live oak and California black oak, both declined in their occurrence over time. Meanwhile, the occurrence of California bay laurel and Douglas-fir showed a net increase (Fig. 4.3).

Changes in Species Diversity

Species diversity and evenness indices generally declined across the plot network from 2005 to 2016. Pathogen load tended to be lower in plots with greater diversity, and this relationship grew stronger through time as indicated by the slope of the linear regression lines (Fig. 4.4). Using paired *t*-tests to compare the 2005 metrics to the 2016 metrics we found that the trend in diversity was statistically significant while the trend in evenness was not ($p<0.05$; Table 1).

Change in importance value, basal area, and density

From 2005 to 2016 there was a net loss in total live stem abundance for all of these species, except California bay laurel, while, total live basal area had a net increase for all of these species, except California black oak (Fig. 4.5). Douglas-fir stem abundance declined by 0.9%, coast live oak by 5.5%, and white oaks by 13%, meanwhile, total bay laurel stem abundance increased by 10.9%. In contrast, basal area increased for Douglas-fir by 16.7%, coast live oak by 4.9%, bay laurel by 21.5%, and white oaks by 2.7%, while California black oak basal area declined by 16.7%. From 2005 to 2016, mortality of coast live oak, California black oak, and bay laurel stems continued to accumulate at varying rates across the study area (Fig. 4.5). Coast live oak lost 9.3% (0.8% yr-1) of basal area that was alive in 2005, California black oak lost 24% (2.2% yr-1), and bay laurel lost 2% (0.19% yr-1). Stem mortality showed a similar pattern: 17.8% (1.6 % yr-1) of coast live oak stems died, 30.4% (2.8% yr-1) of black oak, and 10% (0.9% yr-1) of bay laurel stems alive in 2005 were dead by 2016. Since we did not keep records for individual stems of Douglas-fir and white oak,

only standing dead stems of these species were counted at the time of measurements, so we did not calculate their mortality rates.

Compared to pre-epidemic stem mortality rates of coast live oak, black oak and bay laurel, we observed rates that were respectively, 3.2, 4.8, and 2 times greater (Fig. 5b). We also compared our observed mortality rates with those from two other studies, one with observations made prior to our study period and one with observations that overlapped part of our study period. Brown and Allen-Diaz (2009) conducted a study that examined mortality rates of species basal area at eight sites in the north San Francisca Bay area from 1994-2004 and the predicted the overall rate from 1994-2014 by reconstructing 1994 stand conditions during observations made in 2004. We observed lower mortality rates for coast live oak and bay laurel compared to the average of the two sites that fell within our study area, as well as the average across all eight of their sites for both the reconstructed 1994-2004 period and the prediction out to 2014. In contrast, we observed a greater mortality rate of black oak compared to their prediction out to 2014 for sites within our study area as well as across the area, however, we observed a lower mortality rate compared to the reconstructed period (1994-2004) for this species. Comparing stem mortality rates with McPherson et al. (2010), we observed similar rates for coast live oak, but a greater rate for black oak in our study area.

These population-level changes manifested from varying amounts of change in live stem density and basal area at the plot-level from 2005 to 2016 (Fig. 4.6). Means and standard errors of the measurements are reported here. Douglas-fir nearly doubled in basal-area (94±30%) in plots where it occurred, coast live oak gained 58±55%, black oak lost 18±6%, bay laurel gained 44±6%, and white oak species increased by 12±8% on average. The average change in stem density for Douglas-fir increased by 13±10%, decreased for

coast live oak by 2±6%, decreased for black oak by 33±5%, increased for bay laurel by 23±5%, and decreased for white oak species by 10±5%. These changes in stem density and basal area resulted in the majority of plot-level changes in the importance value of California bay laurel and Douglas-fir being positive, while the most susceptible oak species, coast live oak and California black oak, had negative change in importance value. On average, white oak species showed very little change in its importance value in plots where it occurred (Fig. 4.6).

Path models

We tested our structural model (Fig. 4.1) using either change in density or change in basal area of species, with separate models fit for coast live oak and California black oak. Results of the d-sep tests and coefficient estimates with standard errors and p-values for each model reported on here are in Tables A1-A7 (Appendix A). None of the data applied to this model structure resulted in statistically significant path coefficients to the change in Douglas-fir or white oak species. Using the change in coast live oak basal area and data from 182 plots resulted in a significant path to the change in bay laurel, and revealed a missing path between the averaged daily maximum temperature during the rainy season and the change in bay laurel basal area (Fig. 7, open arrow). Cooler locations had higher pathogen loads, more negative change in coast live oak basal area, and greater positive change in bay laurel basal area. We had similar results when applying data subset to plots where bay laurel or coast live oak were present in either or both 2005 and 2016 (Appendix B). Using the change in coast live oak density instead of basal area resulted in weak relationships with the change in basal area or density of other species ($p>0.11$ $|ß|<0.12$). Relationships were also statistically

insignificant when using the change in density or basal area of California black oak instead of the change in coast live oak basal area (Tables A6-A7).

Since California black oak occurred in fewer plots, which can affect the ability to gain statistical inference especially due to assigned zeroes where it was absent, we assessed the effect of the change in California black oak on other species using data subset to plots where black oaks were present (n = 67). Similar to results from other models, the path to the change in bay laurel basal area was negative, while the effects on other species were not significant (Fig. 8). Although, the relationship between symptomatic leaf count and change in black oak basal area was not statistically significant at the $p<0.05$ level, a trend was suggested ($p=0.07$; Fig. 8).

Since changes in density and dominance of the susceptible oak species did not have significant effects on the change in density or dominance of Douglas-fir or white oak species, we explored influences on these species importance values. As part of this exploratory analysis, we selected variables for the changes in the host species based on the strength of their Pearson's correlations while also minimizing collinearity between predictor variables. Using data only from plots where Douglas-fir occurred, we found a significant negative relationship between the change in bay laurel basal area and the importance value of Douglas-fir (Fig. 9). We also found a negative relationship between the change in coast live oak stem density and Douglas-fir importance value, but it was statistically weak ($p=0.08$).

Using data only from plots with white oak species and selecting variables using the same criteria as above for Douglas-fir, we found significant negative effects from change in coast live oak basal area and California black oak density to the change in white oak importance value (Fig. 10). Symptomatic leaf count had a significant negative affect on coast

live oak basal area, but no effect on black oak density in these plots. Consistent with results from other models, cooler locations had higher pathogen loads and declines in coast live oak. Here, these effects resulted in more positive changes to white oak importance value. The change in California black oak density had a relatively stronger direct negative effect on the change in white oak importance value compared to the change in coast live oak basal area (Fig. 10).

Discussion

Coexistence between forest tree species depends on the outcome of competition for soil area, nutrients, water, and light. Outcomes of competition depend on life history strategies, and in our rapidly changing world, how species respond to novel disturbances. Increasingly, forest communities are being altered by novel disturbances, or changes to existing disturbance regimes, such as increased frequency of fire and drought, and introductions of exotic pests and pathogens. Exotic pests and pathogens in particular have the capability to negatively effect existing community coexistence mechanisms by altering fitness differences and therefore competition between species (Mordecai et al. 2011). Although pathogens play a substantial role competition between species, the outcome for the community is not always certain, especially in variable environments. In addition, when dealing with generalist pathogens the effects on coexistence mechanisms can be either negative or positive depending on the other details of the disease system. The multiple possible outcomes of pathogen-driven apparent competition indicate a need to examine pathogen effects on coexistence in natural settings for a variety of disease systems.

In this study, we investigated how the exotic, generalist forest pathogen *P. ramorum*

has affected coexistence between its tolerant native reservoir host and oak tree species susceptible to sudden oak death across a heterogeneous landscape in California. Results from our path analysis indicate that this pathogen is negatively affecting existing coexistence mechanisms in oak woodland communities across this area. Testing our path model structure with multiple subsets of data consistently showed that increases in the dominance of the pathogen reservoir host, California bay laurel, was related to decline in coast live oak dominance. The decline in coast live oak dominance was in turn related to higher pathogen loads in cooler locations. The asymmetries in tolerance and competency of the reservoir host and the non-reservoir oak host species have resulted in spillover of this exotic pathogen producing a positive feedback favoring its native reservoir host in a case of apparent competition.

Across the plot network, we found a significant negative effect of pathogen load on coast live oak dominance. The pathogen load did not have a strong or significant effect on susceptible oak species in some subsets of data, which may be due to the exclusion of some of the plots with susceptible oak species in some cases, i.e. subsets based on non-oak species being present. Although the effect of pathogen load on changes in California black oak dominance was statistically weak, the p-value of 0.07 when analyzing data from 67 plots with black oak (Fig. 7) suggests that the pathogen is still likely affecting the change in this species, as indicated by other studies (Brown and Allen-Diaz 2009, McPherson et al. 2010). Our sampling of this species may have been insufficient for clear statistical inference. These results may also be indicative of differences in resistance, tolerance, and susceptibility between coast live and black oak species, as well as individual trees. Black oak trees were less likely to be infected compared to coast live oak (Haas et al. 2016), however, this could

also be an issue of detection due to cryptic or asymptomatic infections. Seeing infections on coast live oak trees may simply be easier than seeing infections on black oak trees. Finally, by analyzing data at the plot and species levels we did not explicitly capture individual genetic variability in resistance, tolerance, and susceptibility that may be genetically conferred (Dodd et al. 2005).

We gained insight into how non-susceptible oak species and Douglas-fir (a common, but weakly competent host) respond to changes in susceptible oak species and the bay laurel reservoir host. Since there were no significant direct effects on the absolute changes in the dominance or density of these species, we examined their change in importance value. This is a relative metric that changes simultaneously for other species as one species has gains or losses in abundance or dominance.

Douglas-fir importance value

Despite the relationship between the change in coast live oak density and Douglas-fir importance value being statistically weak (Fig. 9), it does suggest competition between these species. Based on the very weak relationship between symptomatic leaf count and coast live oak density in this model, it is likely that Douglas-fir is generally outcompeting oak trees directly. Douglas-fir is a fast growing species that can attain great heights, and quickly become dominant in the overstory. It also can support pathogen sporulation, but is a weakly competent host compared to bay laurel. Still, it is possible that in addition to directly outcompeting coast live oak stems for canopy exposure, Douglas-fir also derives some benefit from disease impacts to oaks where these species occur together. In these cases, it is likely that bay laurel are a component of the understory, however, independence of bay laurel

basal area and coast live oak density in this model (Fig. 9) indicate that these species don't commonly occur together in plots with Douglas-fir. Where Douglas-fir occurs with more dominant bay laurel trees (larger basal area) it tends to decline in importance. This may be due to pathogen spillover from the very competent and very tolerant bay laurel to the somewhat less tolerant Douglas-fir, and/or large bay laurel continuing to directly outcompete smaller Douglas-fir for canopy position.

White oak importance value

While the pathogen is affecting the coexistence of coast live oak with white oak species (Fig. 10), our results indicate that it does not play a significant role in competition between white oaks and California black oak. Together with the insignificant effects on changes in white oak basal area or density, these relationships suggest that white oak species are persisting, but have not made substantial gains in density or dominance where coast live oak or black oak declined.

Temperature also plays a significant role in sudden oak death disease dynamics, affecting pathogen sporulation and infection risk of susceptible oak species (Davidson et al. 2005, Haas et al. 2016, Chapter 3 herein). Locations with hotter temperatures had lower pathogen loads and smaller gains in bay laurel dominance, with a net indirect effect of promoting coast live oak dominance (Fig. 7). With climate change forecasts predicting higher temperatures for this region it is possible that pathogen loads will be decreased, however, this will be heavily dependent on changes in precipitation patterns that have greater uncertainty (Micheli et al. 2012).

Species Diversity

We found evidence for decreasing species diversity in plots with higher pathogen load. The decline in species diversity in locations with higher pathogen loads since plots were established in 2005 indicates that sudden oak death may be reducing tree community diversity via mortality of susceptible oak species (Fig. 3). Loss of unsusceptible oak tree species (Fig. 4), as well as other less common species, due to competitive interactions unrelated to sudden oak death would also contribute to the decline in diversity. Our model did not provide an explanation for the loss of unsusceptible oak stems, suggesting that other factors such as environmental conditions or self-thinning may have a substantial effect in some locations.

The increase in basal area of California bay laurel corresponding to decreases in susceptible oaks, especially when the pathogen is abundant, indicates that the disease is favoring this tolerant reservoir host species. Bay laurel persisted and increased its dominance in plots where susceptible oak species declined (Figs. 8 and 9), supporting our hypothesis that this pathogen is promoting its native reservoir host. The opposing patterns in total abundance (loss) and basal area (gain) for coast live oak (Fig. 4.5) seem confounding, but are likely due to local plot conditions. The net loss in living coast live oak stem abundance across the plot network is most likely occurring where coast live oak is less abundant and dominant than other species (especially bay laurel). Since larger oak trees are often more susceptible to infection (Haas et al. 2016), this can translate to a large negative change in importance value of coast live oak (Fig. 4.6) in these plots, especially if there are only a few large trees. The net average increase in coast live oak basal area is likely driven by gains in plots where coast live oak stems dominate and continue to increase in diameter with low risk

of infection.

Comparing Mortality Rates

While all post-epidemic mortality rates were greater compared to the pre-epidemic rates, comparing post-epidemic produced some interesting differences (Appendix B Figs. B3-B7). In most cases we observed lower mortality rates for coast live oak and bay laurel, but a greater rate for black oak, compared to other post-epidemic studies. Notable, is the apparent over-estimation of coast live oak mortality and under-estimation of black oak mortality within our study area by Brown and Allen-Diaz (2009; Fig. B4). The over-estimation for coast live oak may in part be due to their assumption that 100% of the trees that were symptomatic in 2004 would die by 2014. The comparative under-estimation for black oak mortality is perhaps partly due to the low abundance of this species in their sites. It is also possible that fewer black oak species were infected as of 2004, or that cryptic/asymptomatic infections affected estimated future mortality. Comparison of stem mortality rates with a study in Marin County that ran from 2000-2008 (McPherson et al. 2010) showed a similar pattern, but with a much smaller difference (0.2% yr^{-1}) in coast live oak mortality rate (Fig. B3). Their lower observed mortality rate for black oak could be in part due to the low relative abundance of this species at these sites.

The reduction in basal area mortality rate of coast live and black oak we observed compared to the 1994-2004 rate reported in Brown and Allen-Diaz (2009) for sites within our study area may largely be due to the stage of invasion (Figs. B5 and B7). Studies have shown that larger trees are more susceptible to SOD-induced mortality (Cobb et al. 2012, Haas et al. 2016), so many larger oak trees may have died at the beginning of the epidemic with

progressively smaller trees being lost later in the epidemic.

Individual genetic variability in disease tolerance and susceptibility of *P. ramorum* hosts (Dodd et al. 2005), likely explains some of the difference between our observed mortality rate and the rate predicted by Brown and Allen-Diaz. Calculating overall mortality rates also incorporates factors other than *P. ramorum*, e.g., other pests and pathogens, herbivory, water stress, contributing to tree death. While the SOD epidemic is the most noticeable change in these forests, variation in these other factors would also influence the mortality rates.

Overall, these results indicate that this exotic, generalist forest pathogen is destabilizing coexistence mechanisms in these forest communities via pathogen spillover from its highly competent, but also tolerant, reservoir host. Observed increases in the density and dominance of bay laurel over ten years corresponded to higher pathogen loads. Higher pathogen loads were also related to lower tree species diversity, indicating the broad impacts to stabilizing mechanisms of coexistence. Managing the spread and impacts of generalist pathogens is inherently difficult, and *P. ramorum* has the widest host range of any plant pathogen for which intense regulation and management as been attempted (Rizzo et al. 2005). Forest pathogens are an added challenge because their hosts are frequently interspersed. Although eradication of *P. ramorum* is unattainable (Cunniffe et al. 2016), efforts to slow the spread and protect valued oak trees can still be successful. Our results indicate that reducing bay laurel will offer protection to susceptible oak trees by directly reducing pathogen load. Removing dominant or co-dominant bay laurel trees would also increase the local temperature, which we found was also related to lower pathogen loads. By assessing biotic and abiotic relationships of disease systems across large landscapes we gain

better insights into how management challenges can be effectively met, and what our landscapes might look like in the future in the absence of action.

CHAPTER 5: CONCLUSION

In these three research projects I explored host-pathogen-environment relationships in the sudden oak death disease system. In Chapter 2, I examined how the spatial scale of host density measurements can affect inference from models of disease intensity. I systematically collected data across five nested spatial scales at 20 sites to assess relationships between disease intensity, host density, and environmental variation using either field measurements or remotely sensed estimates of host density. Model results showed that using direct measurements of host density performed better than remotely sensed estimates, and that explanatory power of models decreased with increasing spatial extent. Although expensive, this highlights that direct measurements can provide better insight into the spatial scales at which disease dynamics are operating relative to remotely sensed data.

In Chapter 3, I assessed the influence of direct and indirect effects from the biotic and abiotic environment on pathogen spillover in the sudden oak death disease system. Using current knowledge of sudden oak death disease dynamics, I developed a path analysis to test these relationships using epidemiologically relevant variables derived from 10-years of field measurements. Biotic factors characterizing the tree community were stronger drivers of pathogen spillover, but abiotic factors still significantly influenced this process. Examining biotic and abiotic factors simultaneously provided insights that could enhance disease management and control efforts.

In Chapter 4, I explored how the exotic plant pathogen is affecting coexistence among tree species in disease-impacted forest communities. I analyzed 10 years of change in the density and dominance of common tree species in forest stands impacted by sudden oak death. Using a confirmatory path analysis, I showed that spillover of *P. ramorum* is reducing

dominance of coast live oak, and causing a positive feedback that is increasing dominance of its reservoir host, California bay laurel. These results indicate that disease is destabilizing existing community dynamics, and that these forests are likely on a trajectory toward a new community structure of species coexistence.

Increasing our knowledge about disease dynamics in uncontrolled environments is imperative in the face of emerging infectious diseases, which are on the rise across the plant and animal kingdoms. Plant disease systems are especially useful for examining environmental influences on disease since most of the host species are stationary. What we learn from these systems, including the most appropriate spatial and temporal scales for monitoring and management, can inform data collection and analysis efforts in other plant, human, and animal disease systems. In an era of climate change that is breaking the bounds of the historical range of variability, understanding how diseases are responding to biotic and abiotic environmental variation is essential to prevent severe negative impacts to human well-being.

REFERENCES

Akaike, H. 1974. A new look at the statistical model identification. IEEE Transactions on Automatic Control 19:716–723.

Alexander, H. M., and R. D. Holt. 1998. The interaction between plant competition and disease. Perspectives in Plant Ecology, Evolution and Systematics 1:206–220.

Anacker, B. L., N. E. Rank, D. Hüberli, M. Garbelotto, S. Gordon, T. Harnik, R. Whitkus, and R. K. Meentemeyer. 2008. Susceptibility to Phytophthora ramorum in a key infectious host: landscape variation in host genotype, host phenotype, and environmental factors. New Phytologist 177:756–766.

APHIS. 2013. Plant health: Phytophthora ramorum/sudden oak death. http://www.aphis.usda.gov/plant_health/plant_pest_info/pram/index.shtml.

Aukema, J. E., D. G. McCullough, B. Von Holle, A. M. Liebhold, K. Britton, and S. J. Frankel. 2010. Historical Accumulation of Nonindigenous Forest Pests in the Continental United States. BioScience 60:886–897.

Barton, K. 2013. MuMIn: Multi-model inference.

Bates, D., M. Mächler, B. Bolker, and S. Walker. 2015. Fitting Linear Mixed-Effects Models Using lme4. Journal of Statistical Software 67.

Bates, D., M. Maechler, B. Bolker, and S. Walker. 2013. lme4: Linear mixed-effects models using Eigen and S4.

Beven, K. J., and M. J. Kirkby. 1979. A physically based, variable contributing area model of basin hydrology / Un modèle à base physique de zone d'appel variable de l'hydrologie du bassin versant. Hydrological Sciences Bulletin 24:43–69.

Bolker, B. M., M. E. Brooks, C. J. Clark, S. W. Geange, J. R. Poulsen, M. H. H. Stevens, and

J.-S. S. S. White. 2009, March. Generalized linear mixed models: a practical guide for ecology and evolution.

Borer, E. T., P. R. Hosseini, E. W. Seabloom, and A. P. Dobson. 2007. Pathogen-induced reversal of native dominance in a grassland community. Proceedings of the National Academy of Sciences USA 104:5473–8.

Bradley, B. a., D. M. Blumenthal, R. Early, E. D. Grosholz, J. J. Lawler, L. P. Miller, C. J. B. Sorte, C. M. D'antonio, J. M. Diez, J. S. Dukes, I. Ibanez, and J. D. Olden. 2012. Global change, global trade, and the next wave of plant invasions. Frontiers in Ecology and the Environment 10:20–28.

Brisson, D., D. E. Dykhuizen, and R. S. Ostfeld. 2008. Conspicuous impacts of inconspicuous hosts on the Lyme disease epidemic. Proceedings. Biological sciences / The Royal Society 275:227–35.

Brown, L. B. B., and B. Allen-Diaz. 2009. Forest stand dynamics and sudden oak death: Mortality in mixed-evergreen forests dominated by coast live oak. Forest Ecology and Management 257:1271–1280.

Burdon, J. J., and G. A. Chilvers. 1982. Host Density as a Factor in Plant Disease Ecology. Annual Review of Phytopathology 20:143–166.

Burdon, J. J., P. H. Thrall, and A. L. Ericson. 2006. The current and future dynamics of disease in plant communities. Annual review of phytopathology 44:19–39.

Burdon, J., P. Thrall, and L. Ericson. 2013. Genes, communities & invasive species: understanding the ecological and evolutionary dynamics of host-pathogen interactions. Current opinion in plant biology 16:400–405.

Burnham, K., and D. Anderson. 2002. Model selection and multi-model inference: a practical

information-theoretic approach. 2nd edition. Springer-Verlag, New York, NY.

Burnham, K. P., D. R. Anderson, and K. P. Huyvaert. 2011. AIC model selection and multimodel inference in behavioral ecology: some background, observations, and comparisons. Behavioral Ecology and Sociobiology 65:23–35.

Chave, J. 2013. The problem of pattern and scale in ecology: What have we learned in 20 years? Ecology Letters 16:4–16.

Chesson, P. 2000. Mechanisms of maintenance of species diversity. Annual review of Ecology and Systematics 31:343–66.

Cho, H. 2000. GIS Hydrological Modeling System by Using Programming Interface of GRASS. Kyungpook National University, Korea.

Chowell, G., and H. Nishiura. 2014. Transmission dynamics and control of Ebola virus disease (EVD): a review. BMC medicine 12:196.

Cobb, R. C., J. A. N. Filipe, R. K. Meentemeyer, C. A. Gilligan, and D. M. Rizzo. 2012. Ecosystem transformation by emerging infectious disease: loss of large tanoak from California forests. Journal of Ecology.

Cobb, R. C., R. K. Meentemeyer, and D. M. Rizzo. 2010. Apparent competition in canopy trees determined by pathogen transmission rather than susceptibility. Ecology 91:327–333.

Condeso, T. E., and R. K. Meentemeyer. 2007. Effects of landscape heterogeneity on the emerging forest disease sudden oak death. Journal of Ecology 95:364–375.

Connell, J. H. 1971. On the role of natural enemies in preventing competitive exclusion in some marine animals and in rain forest trees. Proc. Adv. Study Inst. Dynamics Numbers Popul.:298–312.

Cottam, G., and J. Curtis. 1956. The use of distance measures in phytosociological sampling. Ecology 37:451–460.

Cottam, G., J. Curtis, and B. Hale. 1953. Some sampling characteristics of a population of randomly dispersed individuals. Ecology 34:741–757.

Cunniffe, N. J., R. C. Cobb, R. K. Meentemeyer, D. M. Rizzo, and C. A. Gilligan. 2016. Modeling when, where, and how to manage a forest epidemic, motivated by sudden oak death in California. Proceedings of the National Academy of Sciences:201602153.

Cushman, J. H., and R. K. Meentemeyer. 2008. Multi-scale patterns of human activity and the incidence of an exotic forest pathogen. Journal of Ecology 96:766–776.

Davidson, J. M., H. A. Patterson, and D. M. Rizzo. 2008. Sources of inoculum for Phytophthora ramorum in a redwood forest. Phytopathology 98:860–866.

Davidson, J. M., A. C. Wickland, H. A. Patterson, K. R. Falk, and D. M. Rizzo. 2005. Transmission of Phytophthora ramorum in mixed-evergreen forest in California. Phytopathology 95:587–596.

Desprez-Loustau, M.-L., B. Marçais, L.-M. Nageleisen, D. Piou, and A. Vannini. 2006. Interactive effects of drought and pathogens in forest trees. Annals of Forest Science 63:597–612.

DiLeo, M., R. Bostock, and D. Rizzo. 2014. Microclimate Impacts Survival and Prevalence of Phytophthora ramorum in Umbellularia californica, a Key Reservoir Host of Sudden Oak Death in Northern. PloS one 9:1–6.

DiLeo, M. V, R. M. Bostock, and D. M. Rizzo. 2009. Phytophthora ramorum does not cause physiologically significant systemic injury to California bay laurel, its primary reservoir host. Phytopathology 99:1307–1311.

Dillon, W. W., R. K. Meentemeyer, J. B. Vogler, R. C. Cobb, M. R. Metz, and D. M. Rizzo. 2013. Range-wide threats to a foundation tree species from disturbance interactions. Madroño 60:139–150.

Dinoor, A., and N. Eshed. 1984. The Role and Importance of Pathogens in Natural Plant Communities. Annual Review of Phytopathology 22:446–66.

Dobrowski, S. Z. 2011. A climatic basis for microrefugia: the influence of terrain on climate. Global Change Biology 17:1022–1035.

Dodd, R. S., D. Hüberli, V. Douhovnikoff, T. Y. Harnik, Z. Afzal-Rafii, and M. Garbelotto. 2005. Is variation in susceptibility to Phytophthora ramorum correlated with population genetic structure in coast live oak (Quercus agrifolia)? New Phytologist 165:203–214.

Ellis, A. M., T. VaclavÌk, R. K. Meentemeyer, and T. Václavík. 2010. When is connectivity important? A case study of the spatial pattern of sudden oak death. Oikos 119:485–493.

Englander, L., M. Browning, and P. W. Tooley. 2006. Growth and sporulation of Phytophthora ramorum in vitro in response to temperature and light. Mycologia 98:365–73.

Eyre, C. A., K. J. Hayden, M. Kozanitas, N. J. Grunwald, and M. Garbelotto. 2014. Lineage, Temperature, and Host Species have Interacting Effects on Lesion Development in Phytophthora ramorum. Plant Disease 98:1717–1727.

Eyre, C. A., M. Kozanitas, and M. Garbelotto. 2013. Population dynamics of aerial and terrestrial populations of Phytophthora ramorum in a California forest under different climatic conditions. Phytopathology 103:1141–52.

Gelman, A., and J. Hill. 2007. Data Analysis Using Regression and Multilevel/Hierarchical Models. Page (R. M. Alvarez, N. L. Beck, and L. L. Wu, Eds.) Policy Analysis.

Cambridge University Press, New York, NY.

Gilbert, G. S. 2002. Evolutionary ecology of plant diseases in natural ecosystems. Annual review of phytopathology 40:13–43.

Grace, J., T. Anderson, H. Olff, and S. M. Scheiner. 2010. On the specification of structural equation models for ecological systems. Ecological … 80:67–87.

GRASS Development Team. 2016. Geographic Resources Analysis Support System (GRASS GIS) Software, Version 7.0.

Haas, S. E., J. H. Cushman, W. W. Dillon, N. E. Rank, D. M. Rizzo, and R. K. Meentemeyer. 2016. Effects of individual, community, and landscape drivers on the dynamics of a wildland forest epidemic. Ecology 97:649–660.

Haas, S. E., M. B. Hooten, D. M. Rizzo, and R. K. Meentemeyer. 2011. Forest species diversity reduces disease risk in a generalist plant pathogen invasion. Ecology Letters 14:1108–1116.

Hansen, A. J., R. P. Neilson, V. H. Dale, C. H. Flather, L. R. Iverson, D. J. Currie, S. Shafer, R. Cook, and P. J. Bartlein. 2001. Global Change in Forests: Responses of Species, Communities, and Biomes. BioScience 51:765.

Hansen, E. M., and E. M. Goheen. 2000. Phellinus Weirii and Other Native Root Pathogens As Determinants of Forest Structure and Process in Western North America. Annual review of phytopathology 38:515–539.

Hansen, E. M., A. Kanaskie, S. Prospero, M. McWilliams, E. M. Goheen, N. Osterbauer, P. Reeser, and W. Sutton. 2008. Epidemiology of Phytophthora ramorum in Oregon tanoak forests. Canadian Journal of Forest Research 38:1133–1143.

Heesterbeek, H., R. M. Anderson, V. Andreasen, S. Bansal, D. De Angelis, C. Dye, K. T. D.

Eames, W. J. Edmunds, S. D. W. Frost, S. Funk, T. D. Hollingsworth, T. House, V. Isham, P. Klepac, J. Lessler, J. O. Lloyd-Smith, C. J. E. Metcalf, D. Mollison, L. Pellis, J. R. C. Pulliam, M. G. Roberts, and C. Viboud. 2015. Modeling infectious disease dynamics in the complex landscape of global health. Science 347:aaa4339-aaa4339.

Holdenrieder, O., M. Pautasso, P. J. Weisberg, and D. Lonsdale. 2004. Tree diseases and landscape processes: the challenge of landscape pathology. Trends in Ecology & Evolution 19:446–452.

Holt, R. D. 1977. Predation, apparent competition, and the structure of prey communities. Theoretical Population Biology 12:197–229.

Hüberli, D., K. J. Hayden, M. Calver, and M. Garbelotto. 2011. Intraspecific variation in host susceptibility and climatic factors mediate epidemics of sudden oak death in western US forests. Plant Pathology 61:579–592.

Janzen, D. H. 1970. Herbivores and the number of tree species in tropical forests. American Naturalist 104:501–528.

Jeger, M. J., M. Pautasso, O. Holdenrieder, and M. W. Shaw. 2007. Modelling disease spread and control in networks: implications for plant sciences. The New phytologist 174:279–97.

Jones, K. E., N. G. Patel, M. a Levy, A. Storeygard, D. Balk, J. L. Gittleman, and P. Daszak. 2008. Global trends in emerging infectious diseases. Nature 451:990–3.

Jules, E., M. Kauffman, W. Ritts, and A. Carroll. 2002. Spread of an invasive pathogen over a variable landscape: a nonnative root rot on Port Orford cedar. Ecology 83:3167–3181.

Kauffman, M. J., and E. S. Jules. 2006. Heterogeneity Shapes Invasion: Host Size And Environment Influence Susceptibility To A Nonnative Pathogen. Ecological

Applications 16:166–175.

Keesing, F., L. K. Belden, P. Daszak, A. Dobson, C. D. Harvell, R. D. Holt, P. Hudson, A. Jolles, K. E. Jones, C. E. Mitchell, S. S. Myers, T. Bogich, and R. S. Ostfeld. 2010. Impacts of biodiversity on the emergence and transmission of infectious diseases. Nature 468:647–52.

Keesing, F., R. D. Holt, and R. S. Ostfeld. 2006. Effects of species diversity on disease risk. Ecology letters 9:485–98.

Kilpatrick, a M., P. Daszak, M. J. Jones, P. P. Marra, and L. D. Kramer. 2006. Host heterogeneity dominates West Nile virus transmission. Proceedings. Biological sciences / The Royal Society 273:2327–33.

Krebs, C. J. 1999. Ecological Methodology. Second. Addison-Wesley-Longman, New York, NY.

Lamsal, S., R. C. Cobb, J. Hall Cushman, Q. Meng, D. M. Rizzo, and R. K. Meentemeyer. 2011. Spatial estimation of the density and carbon content of host populations for Phytophthora ramorum in California and Oregon. Forest Ecology and Management 262:989–998.

Lefcheck, J. S. 2015. piecewiseSEM : Piecewise structural equation modeling in R for ecology, evolution, and systematics. Methods in Ecology and Evolution:1–7.

Manos, P. P. S., C. H. Cannon, and S. S.-H. Oh. 2008. Phylogenetic relationships and taxonomic status of the paleoendemic Fagaceae of western North America: recognition of a new genus, Notholithocarpus. Madroño 55:181–190.

Mascheretti, S., P. J. P. Croucher, A. Vettraino, S. Prospero, and M. Garbelotto. 2008. Reconstruction of the Sudden Oak Death epidemic in California through microsatellite

analysis of the pathogen Phytophthora ramorum. Molecular Ecology 17:2755–2768.

McPherson, B. a., S. R. Mori, D. L. Wood, M. Kelly, A. J. Storer, P. Svihra, and R. B. Standiford. 2010. Responses of oaks and tanoaks to the sudden oak death pathogen after 8y of monitoring in two coastal California forests. Forest Ecology and Management 259:2248–2255.

Medd, R. W., G. M. Murray, and D. I. Pickering. 2003. Review of the epidemiology and economic importance of Pyrenophora semeniperda. Australasian Plant Pathology 32:539–550.

Meentemeyer, R. K., B. L. Anacker, W. Mark, and D. M. Rizzo. 2008a. Early detection of emerging forest disease using dispersal estimation and ecological niche modeling. Ecological Applications 18:377–390.

Meentemeyer, R. K., S. E. Haas, and T. Václavík. 2012. Landscape Epidemiology of Emerging Infectious Diseases in Natural and Human-Altered Ecosystems. Annual Review of Phytopathology 50:379–402.

Meentemeyer, R. K., N. E. Rank, B. L. Anacker, D. M. Rizzo, and J. H. Cushman. 2008b. Influence of land-cover change on the spread of an invasive forest pathogen. Ecological Applications 18:159–171.

Meentemeyer, R. K., N. E. Rank, D. A. Shoemaker, C. B. Oneal, A. C. Wickland, K. M. Frangioso, and D. M. Rizzo. 2008c. Impact of sudden oak death on tree mortality in the Big Sur ecoregion of California. Biological Invasions 10:1243–1255.

Meentemeyer, R., D. Rizzo, W. Mark, and E. Lotz. 2004. Mapping the risk of establishment and spread of sudden oak death in California. Forest Ecology and Management 200:195–214.

Metz, M. R., K. M. Frangioso, R. K. Meentemeyer, and D. M. Rizzo. 2011. Interacting disturbances: wildfire severity affected by stage of forest disease invasion. Ecological Applications 21:313–320.

Metz, M. R., K. M. Frangioso, A. C. Wickland, R. K. Meentemeyer, and D. M. Rizzo. 2012. An emergent disease causes directional changes in forest species composition in coastal California. Ecosphere 3:art86.

Metz, M., J. Varner, and K. Frangioso. 2013. Unexpected redwood mortality from synergies between wildfire and an emerging infectious disease. Ecology 94:2152–2159.

Micheli, E., L. Flint, and A. Flint. 2012. Downscaling Future Climate Projections to the Watershed Scale: A North San Francisco Bay Case Study. San Francisco Estuary ….

Moore, I., R. Grayson, and A. Ladson. 1991. Digital terrain modelling: a review of hydrological, geomorphological, and biological applications. Hydrological processes 5:3–30.

Mordecai, E. 2011. Pathogen impacts on plant communities: unifying theory, concepts, and empirical work. Ecological Monographs 81:429–441.

Mordecai, E. A. 2013. Despite spillover, a shared pathogen promotes native plant persistence in a cheatgrass-invaded grassland. Ecology 94:2744–2753.

Morrison, J. 1996. Infection of Juncus dichotomus by the smut fungus Cintractia junci: an experimental field test of the effects of neighbouring plants, environment, and host plant genotype. Journal of Ecology 84:691–702.

Mundt, C. C., and K. E. Sackett. 2012. Spatial scaling relationships for spread of disease caused by a wind-dispersed plant pathogen. Ecosphere 3:1–10.

Nugent, G. 2011. Maintenance, spillover and spillback transmission of bovine tuberculosis in

multi-host wildlife complexes: A New Zealand case study. Veterinary Microbiology 151:34–42.

O'Hara, R. B., and D. J. Kotze. 2010. Do not log-transform count data. Methods in Ecology and Evolution 1:118–122.

Oksanen, J., F. G. Blanchet, M. Friendly, R. Kindt, P. Legendre, D. McGlinn, P. R. Minchin, R. B. O'Hara, G. L. Simpson, P. Solymos, M. H. H. Stevens, E. Szoecs, and H. Wagner. 2016. vegan: Community Ecology Package.

Ostfeld, R. S., G. E. Glass, and F. Keesing. 2005. Spatial epidemiology: an emerging (or re-emerging) discipline. Trends in ecology & evolution 20:328–36.

Paillet, F. L. 2002. Chestnut: history and ecology of a transformed species. Journal of Biogeography 29:1517–1530.

Plantegenest, M., C. Le May, and F. Fabre. 2007. Landscape epidemiology of plant diseases. Journal of the Royal Society, Interface / the Royal Society 4:963–72.

Power, A. G., and C. E. Mitchell. 2004. Pathogen spillover in disease epidemics. The American Naturalist 164:S79–S89.

R Core Team. 2013. R: A language and environment for statistical computing. R Foundation for Statistical Computing, Vienna, Austria.

R Core Team. 2016. R: A Language and Environment for Statistical Computing. Vienna, Austria.

Real, L., and P. McElhany. 1996. Spatial Pattern and Process in Plant-Pathogen Interactions. Ecology 77:1011–1025.

Rizzo, D. M., and M. Garbelotto. 2003. Sudden oak death: endangering California and Oregon forest ecosystems. Frontiers in Ecology and the Environment 1:197–204.

Rizzo, D. M., M. Garbelotto, and E. M. Hansen. 2005. Phytophthora ramorum: integrative research and management of an emerging pathogen in California and Oregon forests. Annual Review of Phytopathology 43:309–35.

Rohr, J. R., A. P. Dobson, P. T. J. Johnson, a M. Kilpatrick, S. H. Paull, T. R. Raffel, D. Ruiz-Moreno, and M. B. Thomas. 2011. Frontiers in climate change-disease research. Trends in ecology & evolution 26:270–7.

Salkeld, D. J., P. Stapp, D. W. Tripp, K. L. Gage, J. Lowell, C. T. Webb, R. J. Brinkerhoff, and M. F. Antolin. 2016. Ecological Traits Driving the Outbreaks and Emergence of Zoonotic Pathogens. BioScience:biv179.

Shipley, B. 2000. A New Inferential Test for Path Models Based on Directed Acyclic Graphs. Structural Equation Modeling: A Multidisciplinary Journal 7:206–218.

Shipley, B. 2004. Cause and Correlation in Biology: A User's Guide to Path Analysis, Structural Equations and Causal Inference. Page Cambridge University Press.

Shipley, B. 2009. Confirmatory path analysis in a generalized multilevel context. Ecology 90:363–8.

Shipley, B. 2013. The AIC model selection method applied to path analytic models compared using a d-separation test. Ecology 94:560–564.

Stenlid, J., and J. Oliva. 2016. Phenotypic interactions between tree hosts and invasive forest pathogens in the light of globalization and climate change. Philosophical Transactions of the Royal Society of London B 371.

Stephens, P. R., S. Altizer, K. F. Smith, A. Alonso Aguirre, J. H. Brown, S. A. Budischak, J. E. Byers, T. A. Dallas, T. Jonathan Davies, J. M. Drake, V. O. Ezenwa, M. J. Farrell, J. L. Gittleman, B. A. Han, S. Huang, R. A. Hutchinson, P. Johnson, C. L. Nunn, D.

Onstad, A. Park, G. M. Vazquez-Prokopec, J. P. Schmidt, R. Poulin, and H. Young. 2016. The macroecology of infectious diseases: a new perspective on global-scale drivers of pathogen distributions and impacts. Ecology Letters 19:1159–1171.

Swiecki, T., and E. Bernhardt. 2007. Increasing Distance from California Bay Laurel Reduces the Risk and Severity of Phytophthora ramorum Canker in Coast Live Oak. Page … Science Symposium, Santa Rosa, California. Albany, California, USA.

Swiecki, T. J., E. A. Bernhardt, K. Aram, and D. M. Rizzo. 2016. Phytophthora ramorum Causes Cryptic Bole Cankers in Canyon Live Oak:20–26.

Tonini, F., W. W. Dillon, E. S. Money, and R. K. Meentemeyer. 2016. Spatio-temporal reconstruction of missing forest microclimate measurements. Agricultural and Forest Meteorology 218–219:1–10.

Tooley, P., M. Browning, and D. Berner. 2008. Recovery of Phytophthora ramorum following exposure to temperature extremes. Plant Disease:431–437.

Tooley, P. W., and M. Browning. 2015. Temperature Effects on the Onset of Sporulation by *Phytophthora ramorum* on *Rhododendron* "Cunningham"s White'. Journal of Phytopathology 1931:n/a-n/a.

Tooley, P. W., M. Browning, and R. M. Leighty. 2014. The effect of temperature on germination of chlamydospores of Phytophthora ramorum. Mycologia 106:424–30.

Václavík, T., A. Kanaskie, E. M. Hansen, J. L. Ohmann, and R. K. Meentemeyer. 2010. Predicting potential and actual distribution of sudden oak death in Oregon: Prioritizing landscape contexts for early detection and eradication of disease outbreaks. Forest Ecology and Management 260:1026–1035.

Václavík, T., J. A. Kupfer, and R. K. Meentemeyer. 2012. Accounting for multi-scale spatial

autocorrelation improves performance of invasive species distribution modelling (iSDM). Journal of Biogeography 39:42–55.

Wiens, J. A. 1989. Spatial scaling in ecology. Functional ecology 3:385–397.

Wright, S. 1921. Correlation and causation. Journal of agricultural research 20:557–585.

TABLES

Table 2.1. Standardized coefficients and model fit for disease intensity on individual bay laurel stems.

Model extent	Stem DBH	Elevation	Bay laurel density	% host habitat	AIC
15-meters	-0.2287**	0.3089**	-0.1083	--	1545
	-0.2260**	0.2709**	--	-0.1605	1543
60-meters	-0.2278**	0.2813**	-0.0175	--	1545
	-0.2304**	0.3223**	--	-0.1211	1544
140-meters	-0.2286**	0.3041**	-0.1037	--	1545
	-0.2312**	0.3216**	--	-0.1181	1544
220-meters	-0.2286**	0.3158**	-0.1347	--	1544
	-0.2301**	0.3163**	--	-0.1064	1544

‘**’$p<0.05$

Table 2.2. Results from focal and aggregate-level models.

FOCAL PERSPECTIVE					
Model extent	Elevation	Bay laurel density	% host habitat	AICc	Adj. R^2
Disease Intensity at 15-meters					
60-meters	0.2136	0.4764*	--	59.58	0.26
	0.3936	--	0.1218	63.70	0.10
140-meters	0.2555	0.3815	--	61.34	0.20
	0.3936	--	0.1218	63.70	0.10
220-meters	0.2926	0.2897	--	62.56	0.15
	0.3413	--	0.2556	62.72	0.14
Disease Intensity at 60-meters					
140-meters	0.2202	0.5005**	--	51.66	0.40
	0.3524*	--	0.2754	56.31	0.24
220-meters	0.2412	0.4322*	--	53.79	0.33
	0.3262	--	0.3492*	54.94	0.29
Disease Intensity at 140-meters					
220-meters	0.0615	0.7170**	--	47.83	0.54
	0.2103	--	0.5589**	52.97	0.40
AGGREGATE PERSPECTIVE					
15-meters	0.2556*	0.8162**	--	39.03	0.74
	0.4358*	--	0.1550	63.43	0.11
60-meters	0.1662	0.6253**	--	46.39	0.54
	0.3601*	--	0.2687	56.40	0.23
140-meters	0.0685	0.7462**	--	45.23	0.60
	0.2274	--	0.5075**	54.71	0.35
220-meters	-0.0056	0.8572**	--	46.47	0.62
	0.1632	--	0.6920**	52.82	0.48

'*' $p<0.1$, '**' $p<0.05$

Table 3.1. Results from the d-sep test of the path model in Fig. 3.3 using unstandardized variables.

Missing Path	Conditioning Set	Estimate	SE	df	Crit.Value	p-value
Pathogen Load ~ Landscape Context	Reservoir Host Density, Heat Exposure, Warm & Wet, Species Diversity	-0.004	0.32	209.88	-0.01	0.991
Disease Prevalence ~ Landscape Context	Pathogen Load, Warm & Wet, Species Diversity	0.55	0.70	NA	0.77	0.436
Reservoir Host Density ~ Species Diversity	Landscape Context	1.10	0.49	161.33	2.27	0.025
Heat Exposure ~ Species Diversity	Landscape Context	1.89	22.71	159.84	0.08	0.934
Warm & Wet ~ Species Diversity	Landscape Context	0.21	0.18	169.05	1.14	0.254
Heat Exposure ~ Reservoir Host Density	Landscape Context	-1.80	2.70	149.64	-0.67	0.506
Warm & Wet ~ Reservoir Host Density	Landscape Context	-0.05	0.03	171.00	-1.78	0.077
Disease Prevalence ~ Reservoir Host	Landscape Context, Pathogen Load, Warm & Wet, Species Diversity	-0.003	0.09	NA	-0.03	0.973
Disease Prevalence ~ Heat Exposure	Landscape Context, Pathogen Load, Warm & Wet, Species Diversity	-0.001	0.001	NA	-1.32	0.187

Fisher's-*C*	df	p-value
21.86	18	0.238

Table 3.2. Standardized path coefficients from the fitted path model.

Response	Predictor	Estimate	SE	p-value
Species Diversity	Topographic Index	-0.24	0.07	0.002
Bay Laurel Density	Topographic Index	0.09	0.08	0.213
Symptomatic Leaf Count	Bay Laurel Density	0.78	0.03	0.000
Symptomatic Leaf Count	Summer Hours >25 ºC	-0.12	0.03	0.000
Symptomatic Leaf Count	Wet-Hours 14-22 ºC	0.03	0.02	0.068
Symptomatic Leaf Count	Shannon's Diversity Index	-0.04	0.03	0.226
Wet-Hours 14-22 ºC	Topographic Index	0.02	0.06	0.697
Summer Hours >25 ºC	Topographic Index	-0.22	0.06	0.000
Oak Infection	Pathogen Load	0.49	0.12	0.000
Oak Infection	Shannon's Diversity Index	-0.62	0.18	0.000
Oak Infection	Wet-Hours 14-22 ºC	0.20	0.07	0.004

Table 3.3. Unstandardized path coefficients from the fitted path model.

Response	Predictor	Estimate	SE	p-value
Shannon's Diversity Index	Topographic Index	-0.36	0.11	0.002
Bay Laurel Density	Topographic Index	0.89	0.71	0.213
Symptomatic Leaf Count	Bay Laurel Density	0.81	0.03	0.000
Symptomatic Leaf Count	Summer Hours >25 ºC	-0.002	0.00	0.000
Symptomatic Leaf Count	Wet-Hours 14-22 ºC	0.06	0.04	0.068
Symptomatic Leaf Count	Shannon's Diversity Index	-0.25	0.21	0.226
Wet-Hours 14-22 ºC	Topographic Index	0.10	0.26	0.697
Summer Hours >25 ºC	Topographic Index	-128.06	32.72	0.000
Oak Infection	Symptomatic Leaf Count	0.21	0.051	0.000
Oak Infection	Shannon's Diversity Index	-1.71	0.46	0.000
Oak Infection	Wet-Hours 14-22 ºC	0.19	0.07	0.004
~~ Summer Hours >25 ºC	~~ Wet-Hours 14-22 ºC	0.10	NA	0.000

Table 4.1. Paired t-tests comparing diversity metrics in 2005 to 2016.

Metric	Mean of the Differences	Lower CI	Upper CI	t	p-value
Shannon	-0.047	-0.077	-0.017	-3.128	0.002
Simpson	-0.022	-0.038	-0.0058	-2.681	0.008
Pielou	-0.016	-0.042	0.0097	-1.224	0.22

FIGURES

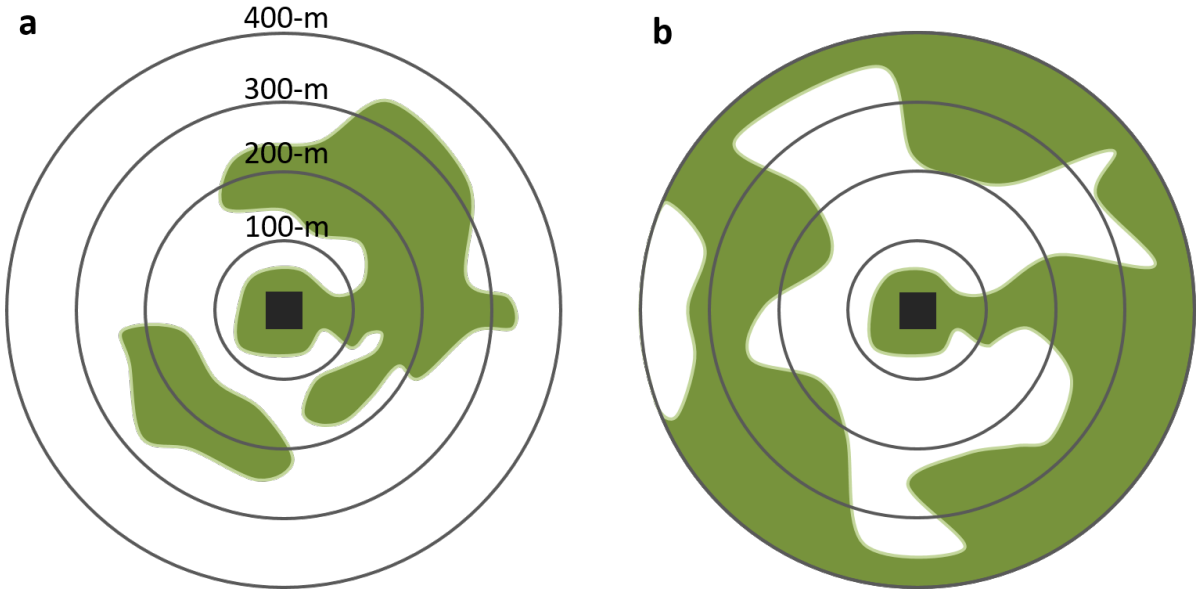

Figure 2.1. The selection of spatial extent for a given study may influence the model results and conclusions.

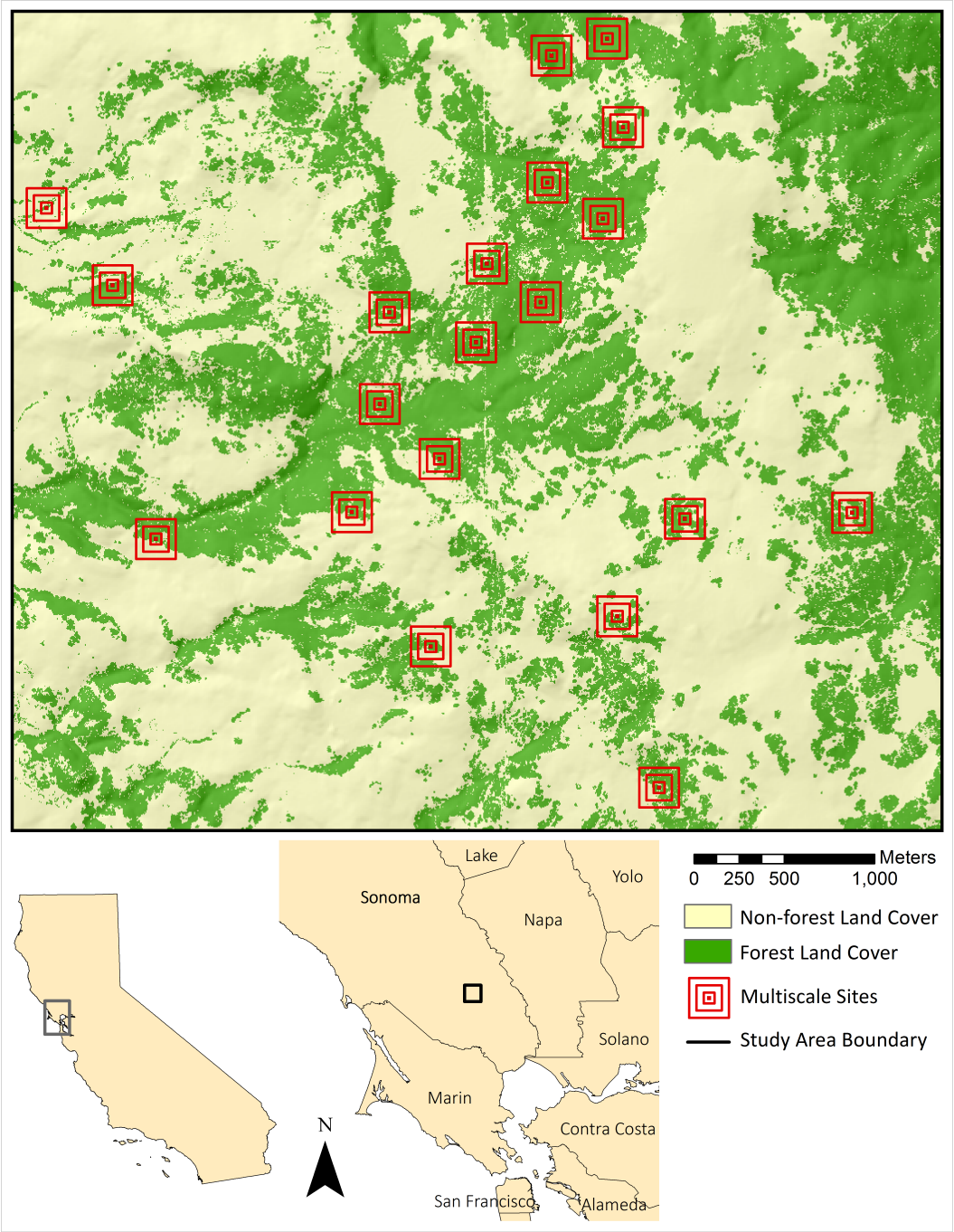

Figure 2.2. Study area and multiscale site locations in Sonoma County, California.

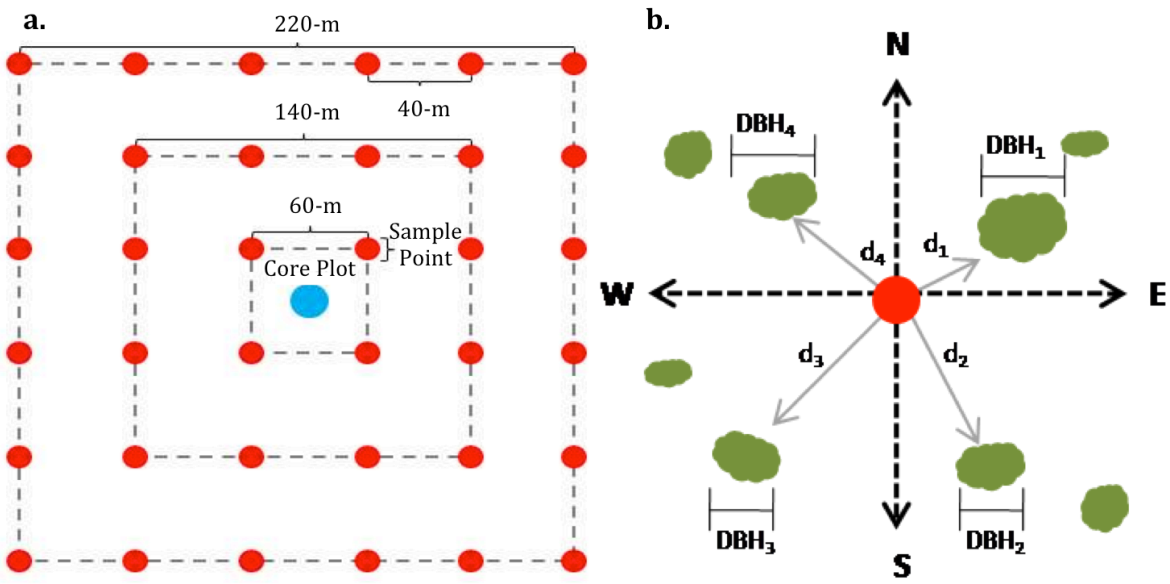

Figure 2.3. The point-quarter sampling diagram: (a) transects (b) point quarter sampling method.

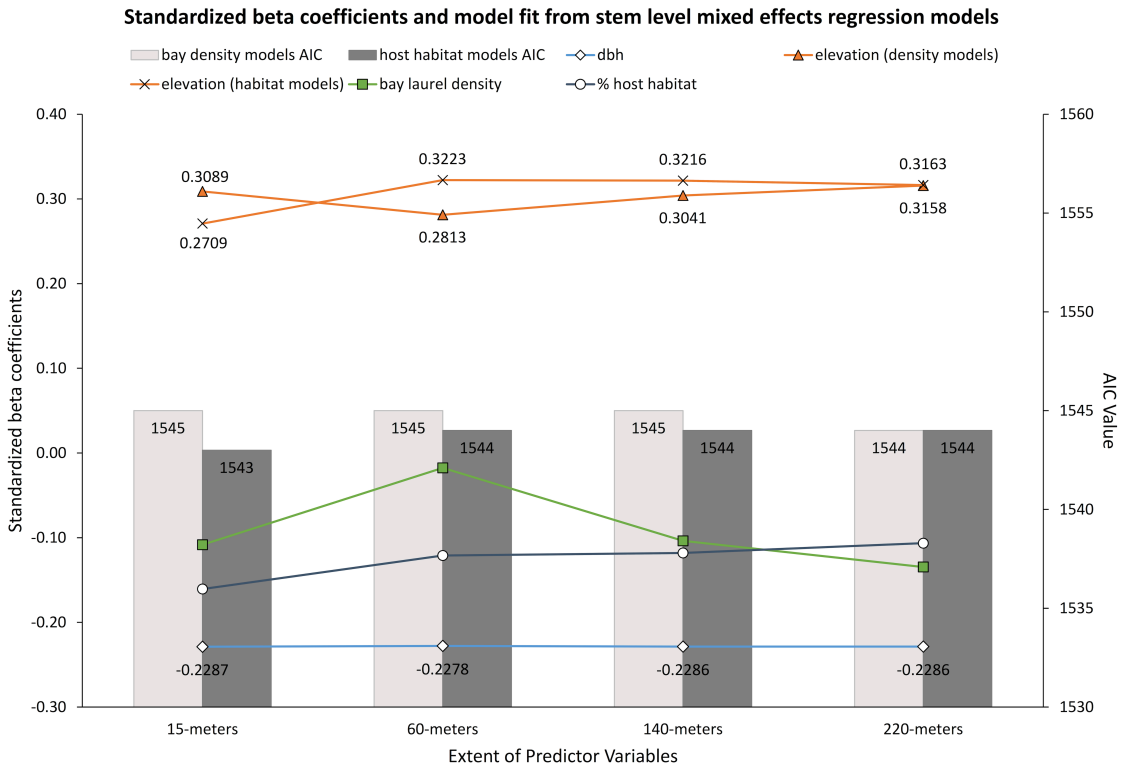

Figure 2.4. Stem-level model coefficients and AIC scores.

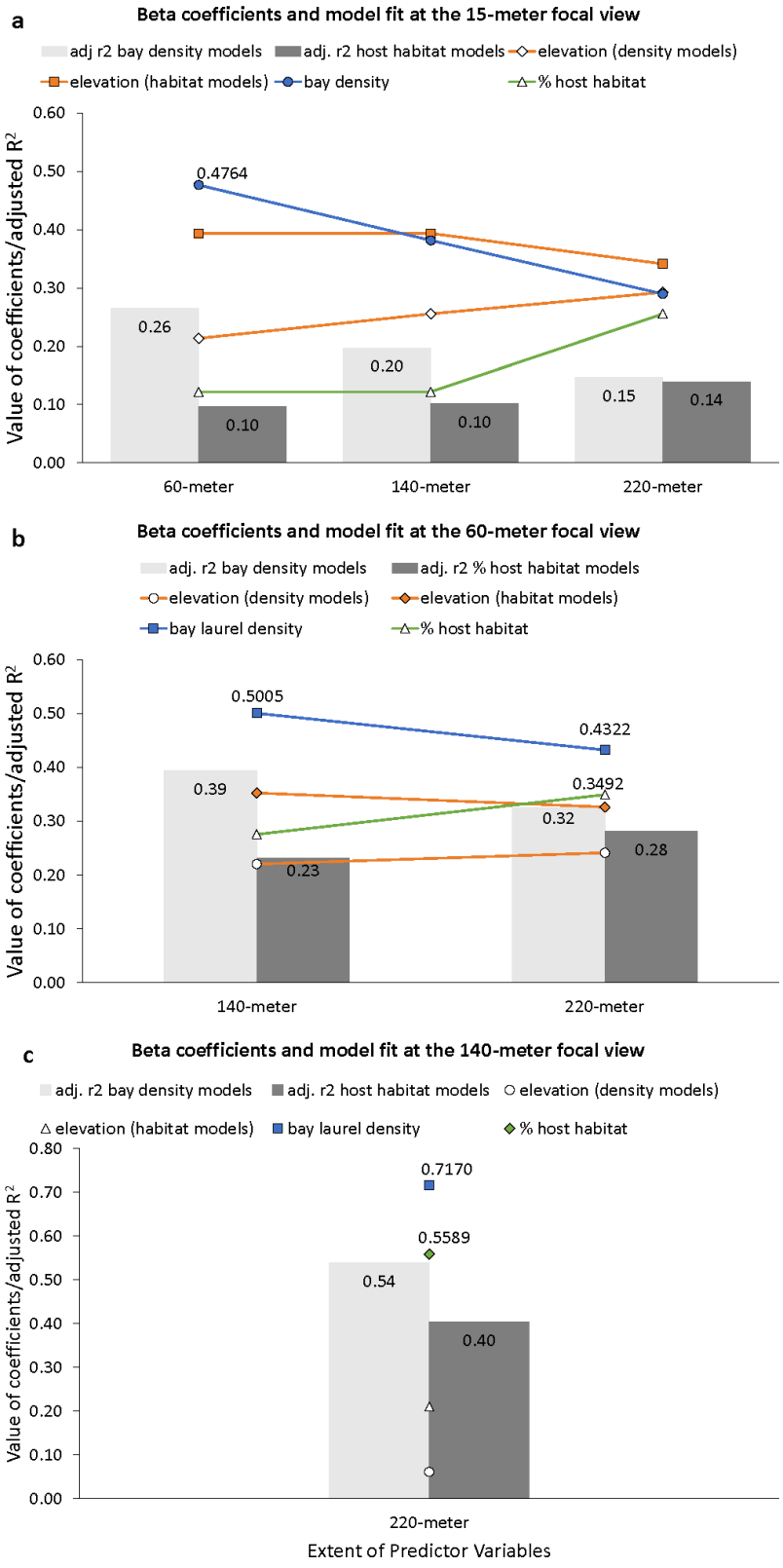

Figure 2.5. Focal-view model coefficients and R^2 values.

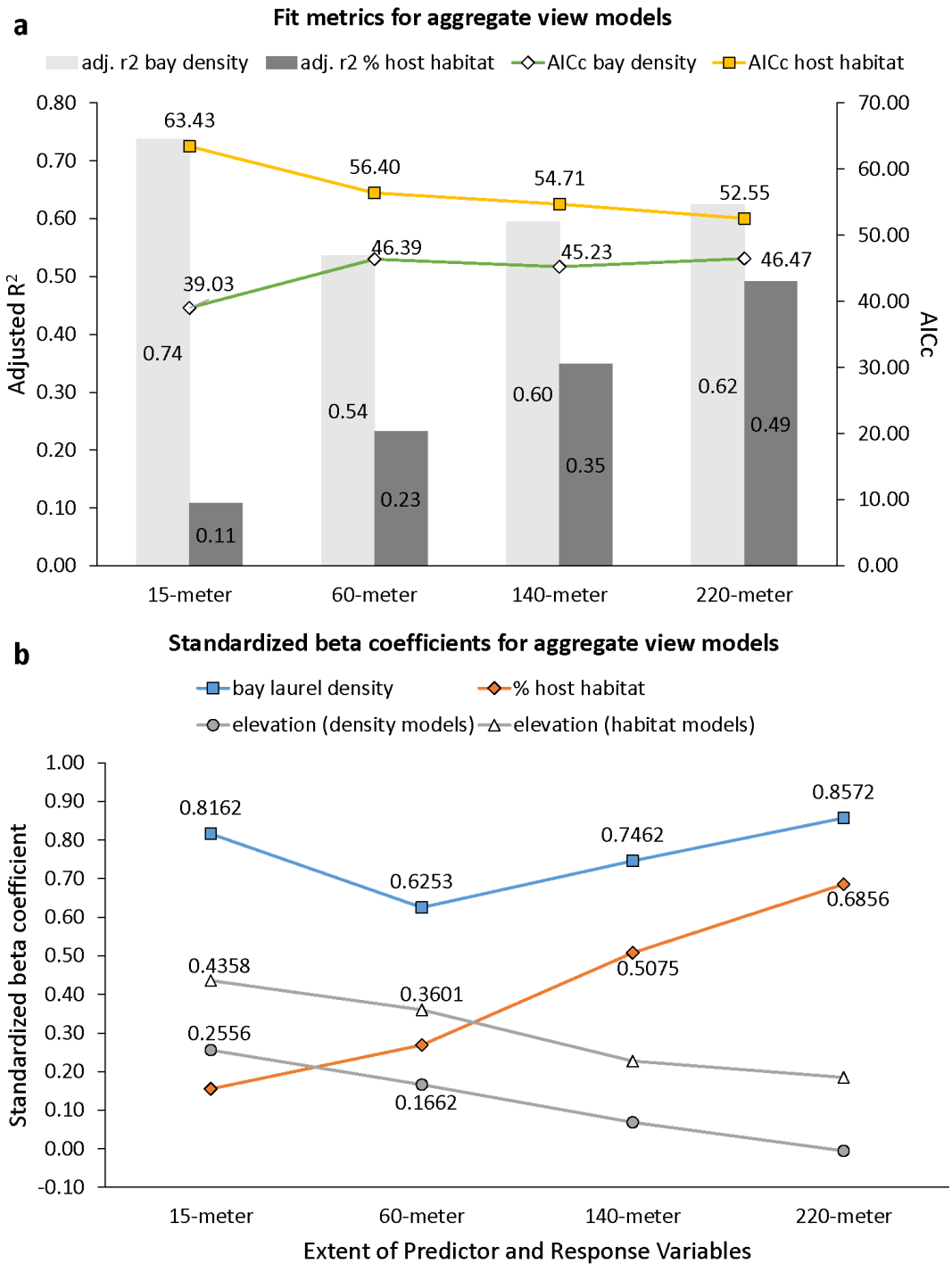

Figure 2.6. Aggregate-view model coefficients and R^2 values.

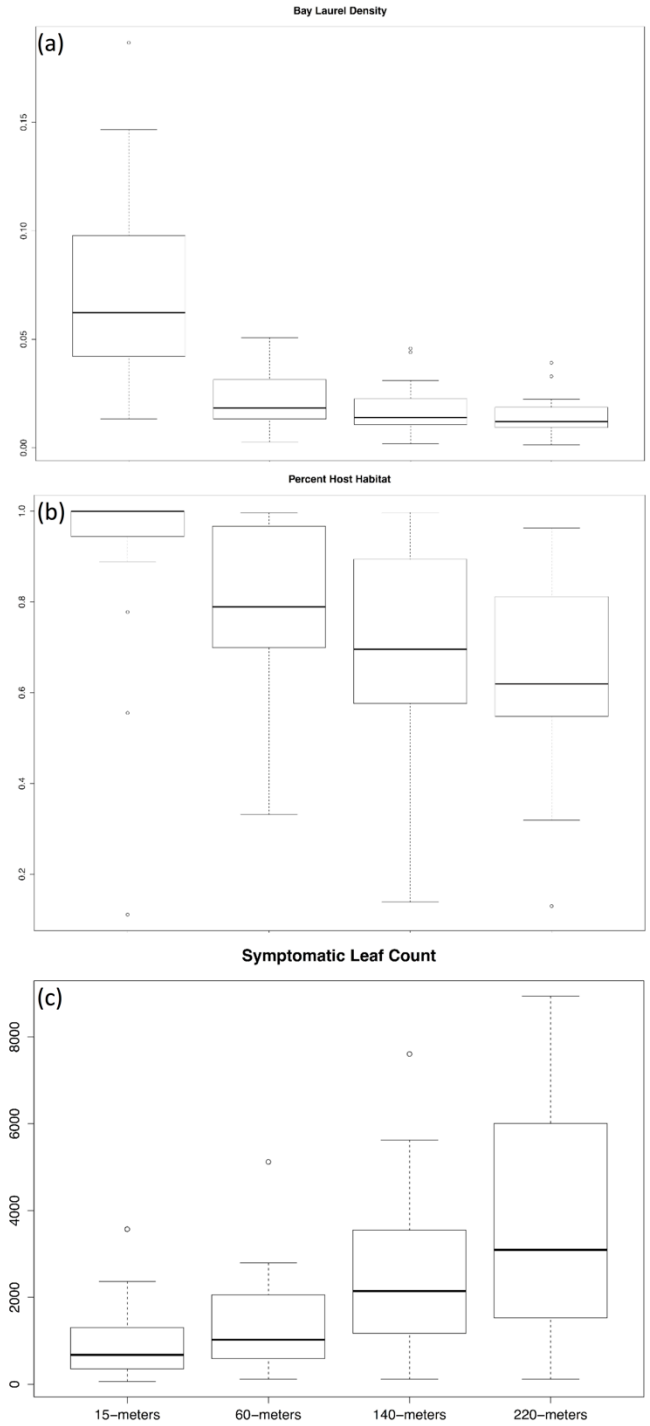

Figure 2.7. Bay laurel density, host habitat, and disease intensity.

Figure 2.8. Correlation matrix for bay laurel density and proportion of host habitat across spatial extents.

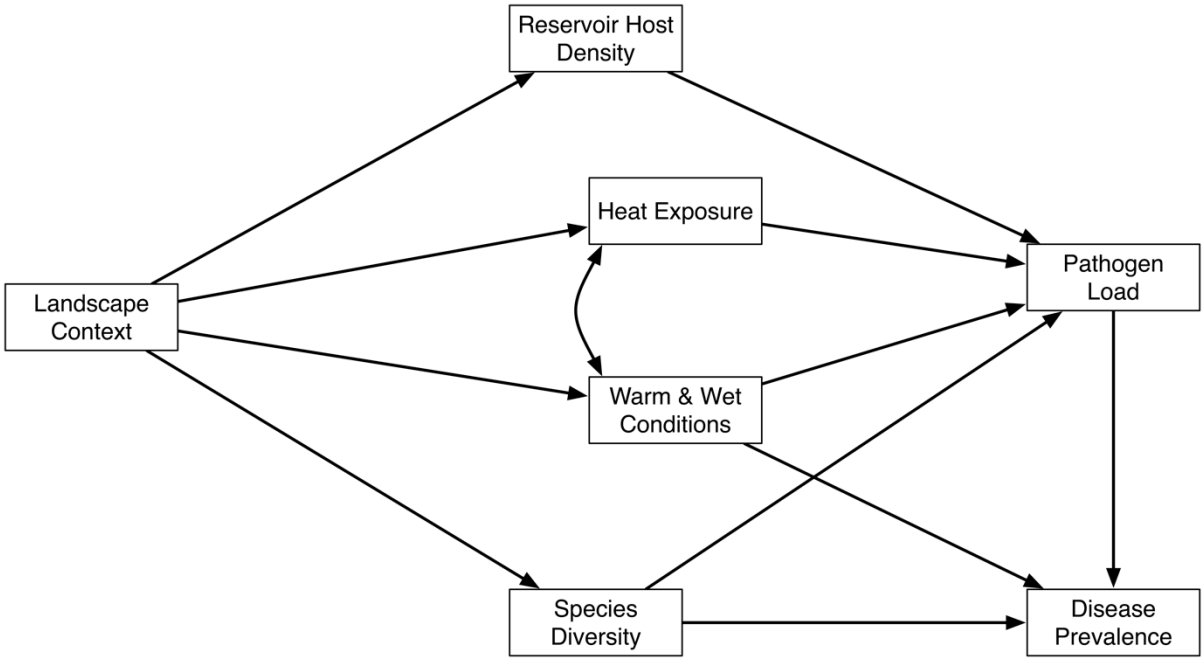

Figure 3.1. Conceptual path model of influences on pathogen spillover.

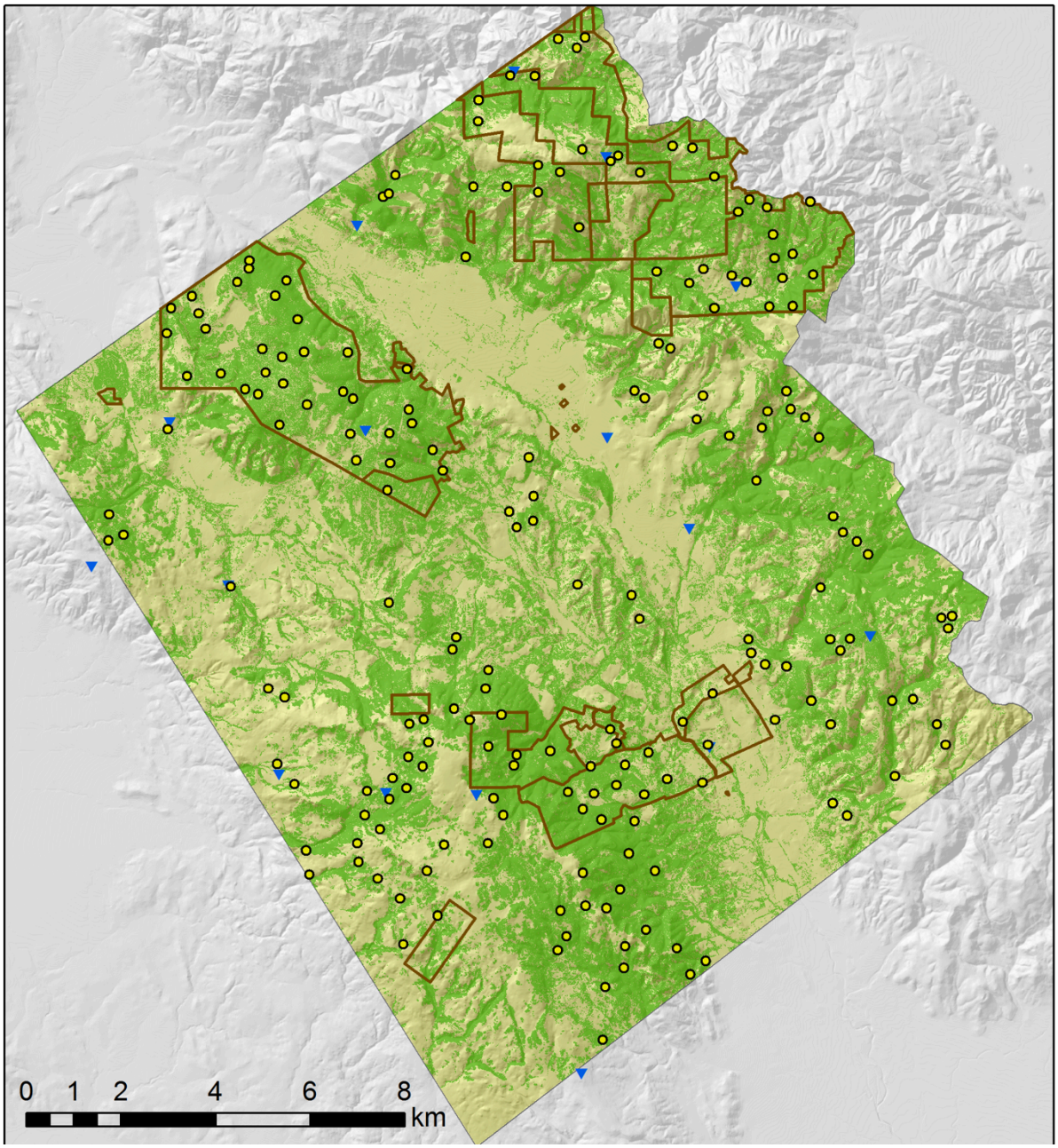

Figure 3.2. Study-area in Sonoma County, California with plot (yellow) and rain gauge (blue triangles) locations.

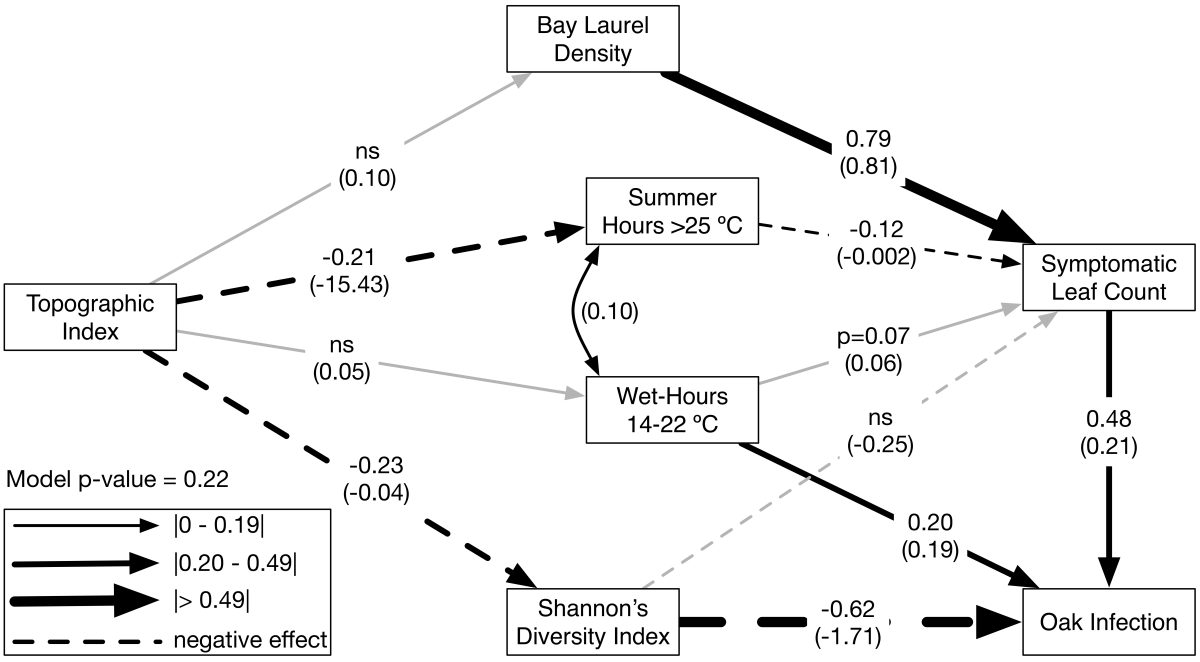

Figure 3.3. Results from path analysis with standardized and unstandardized coefficients.

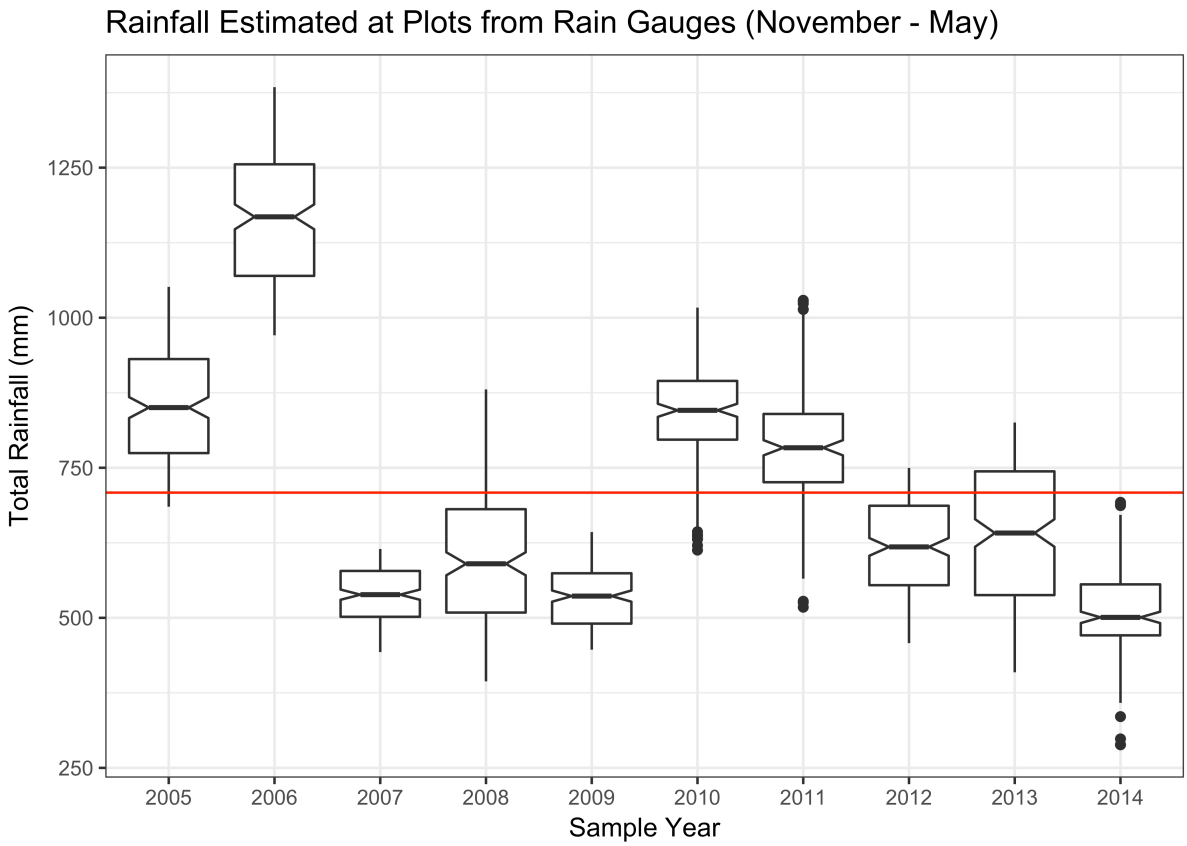

Figure 3.4. Total rainfall with 10-year average estimated at plot locations for the 2005-2014 rainy seasons.

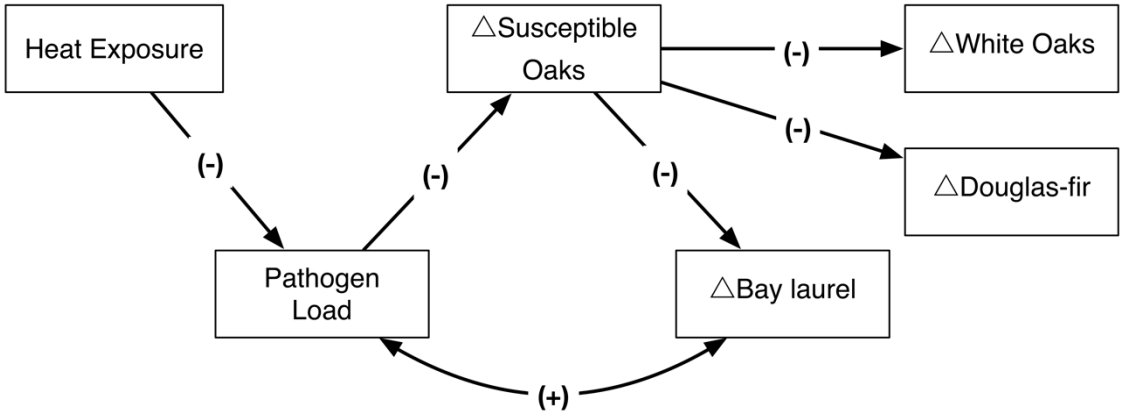

Figure 4.1. Structural path model of apparent competition.

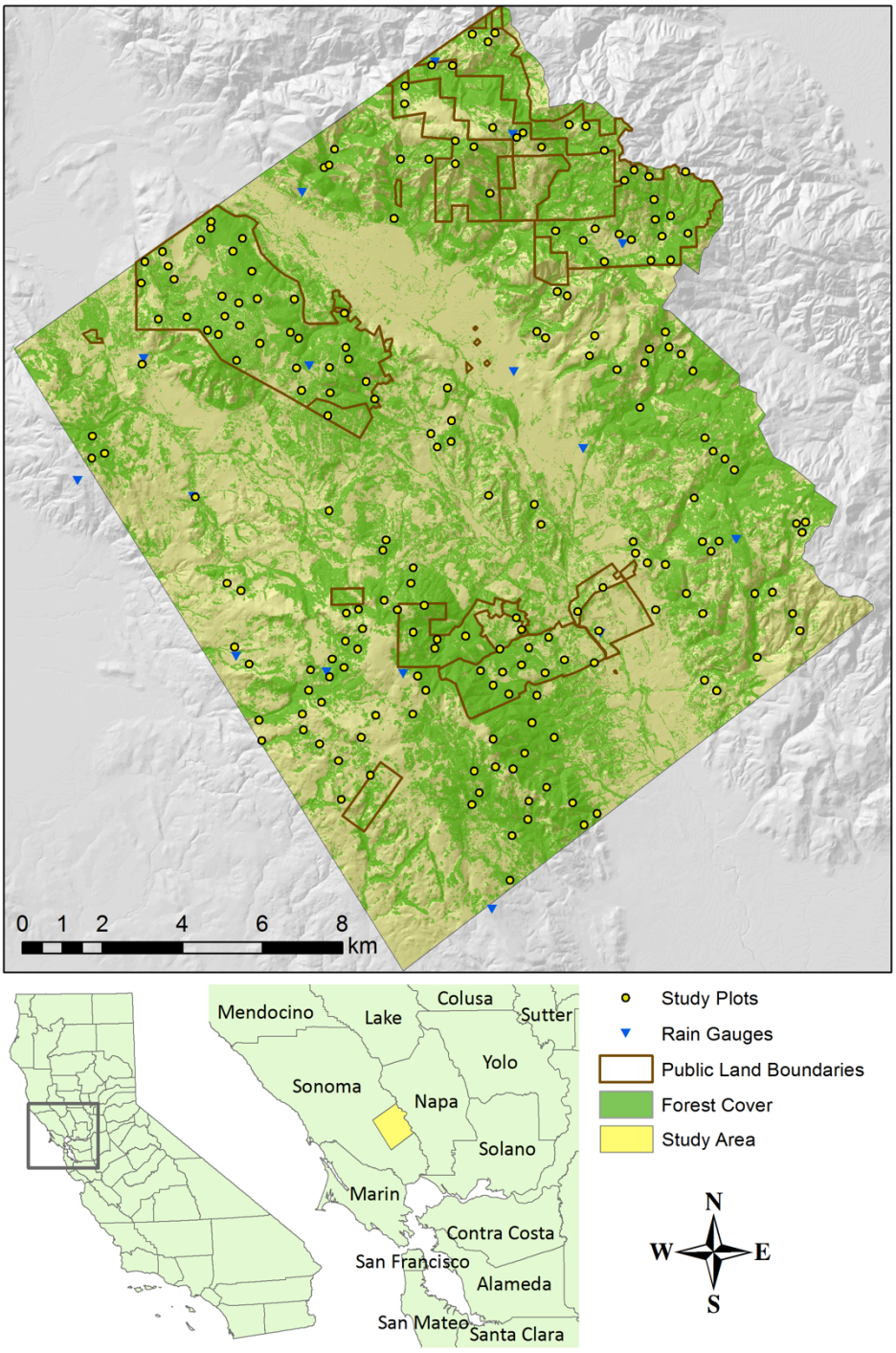

Figure 4.2. Study area in Sonoma County, California.

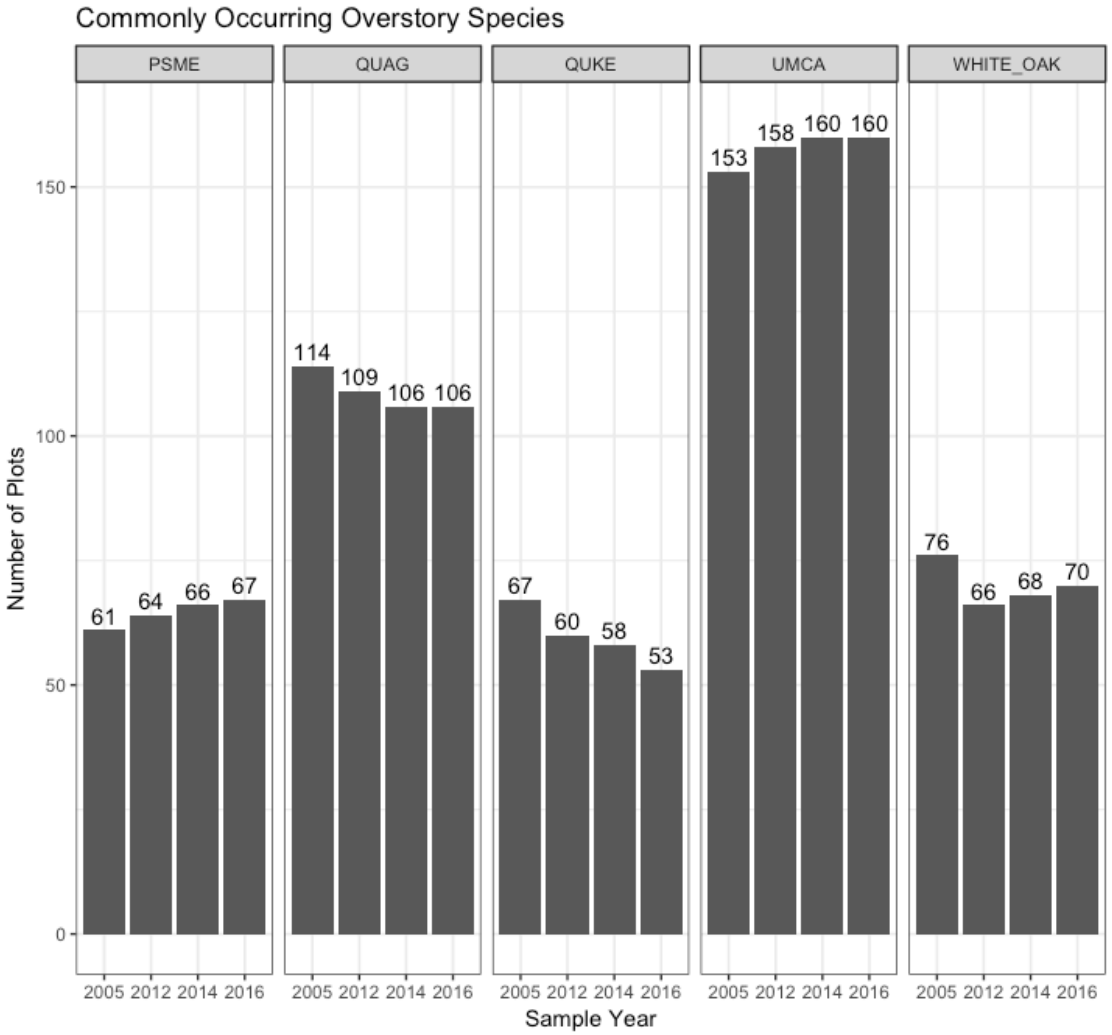

Figure 4.3. Species occurrence across the plot network.

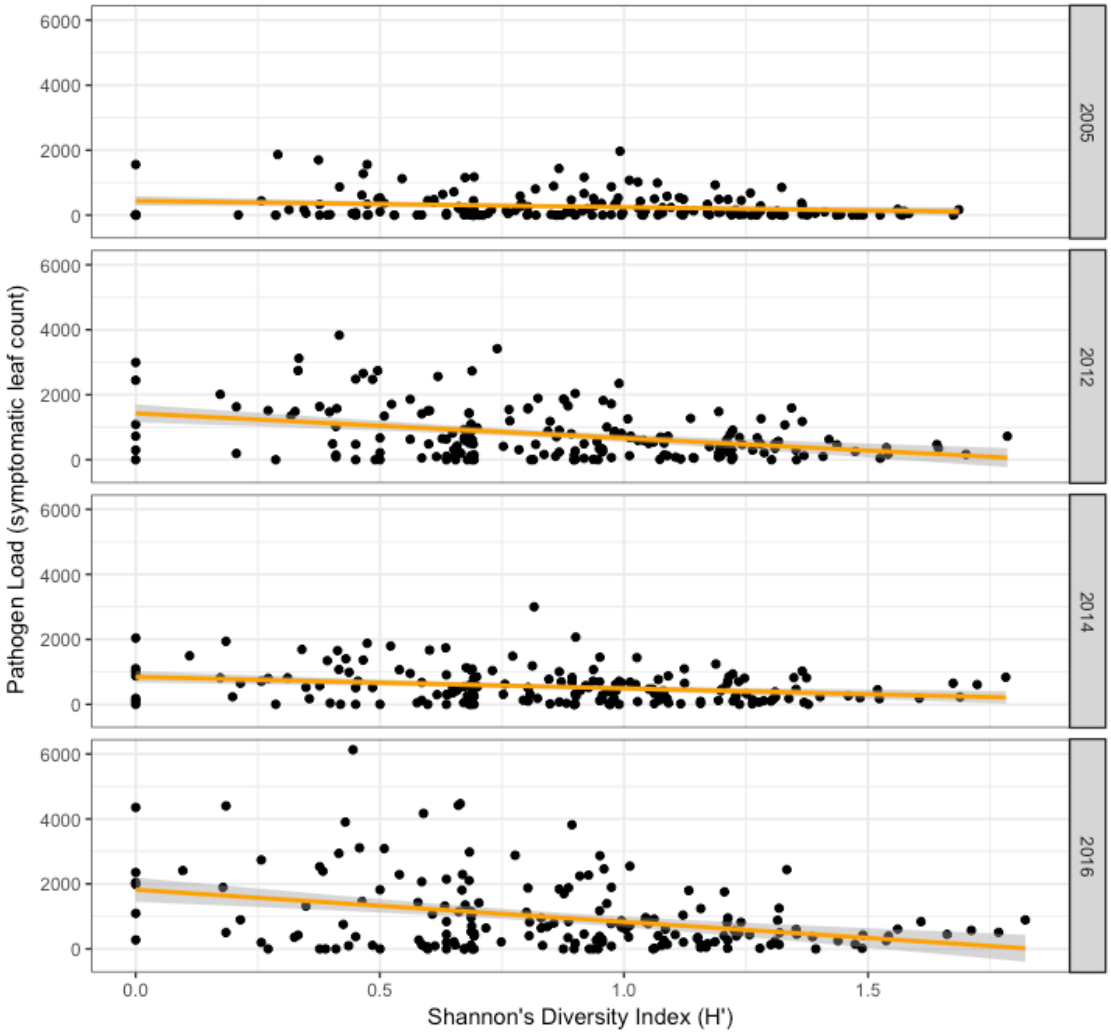

Figure 4.4. Relationship between pathogen load and species diversity.

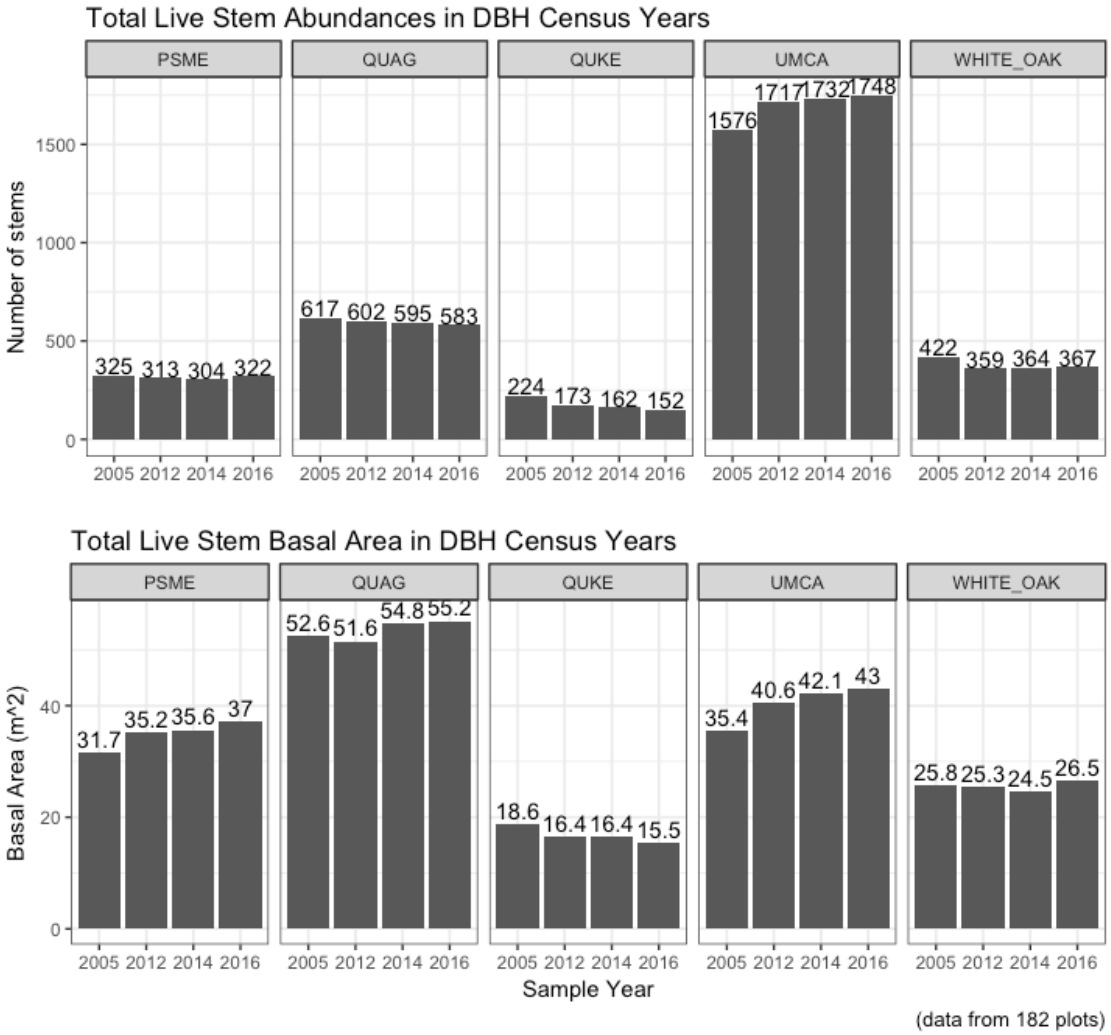

Figure 4.5. Total stem abundance and basal area across the plot network.

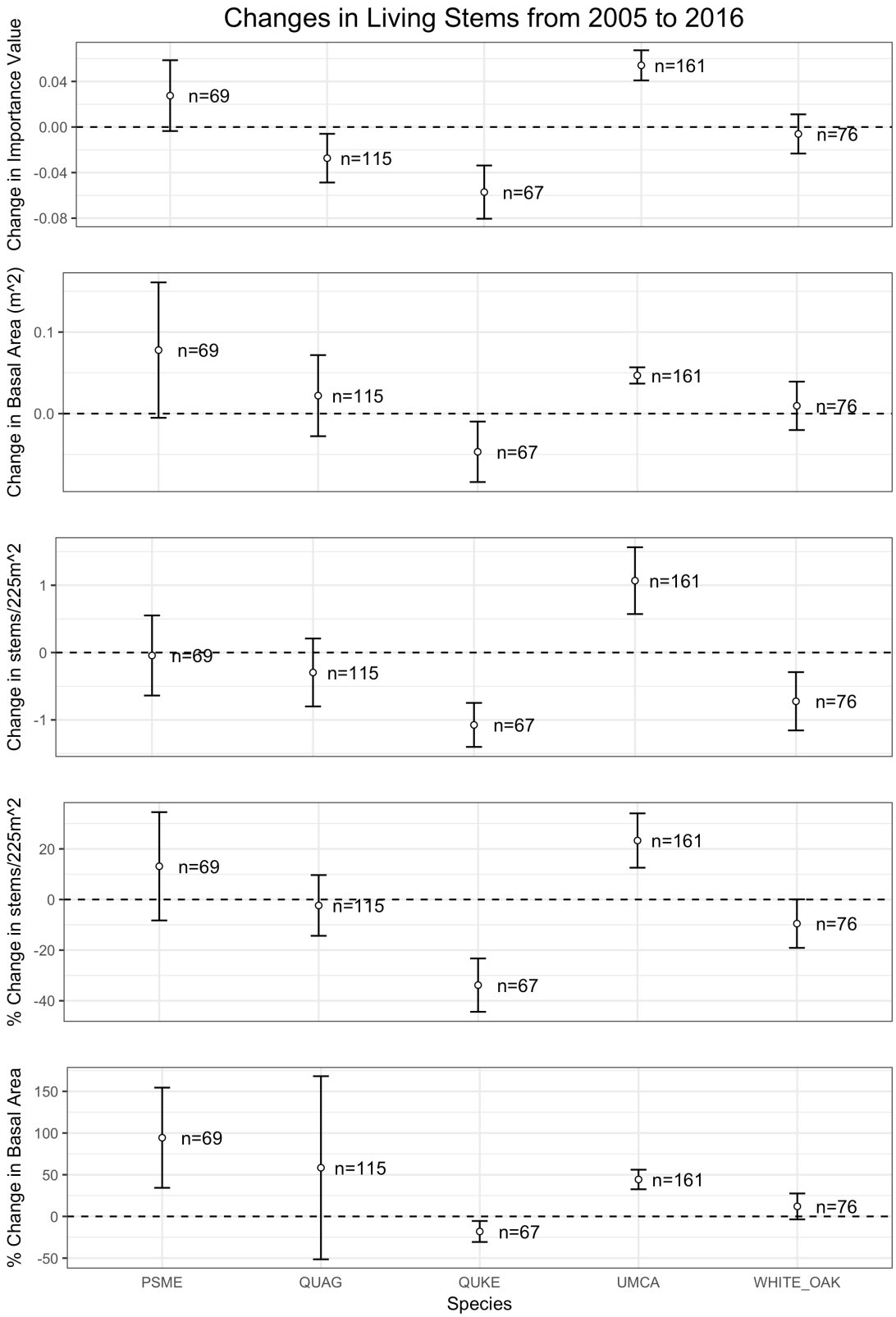

Figure 4.6. Change in importance value, basal area, and stem density.

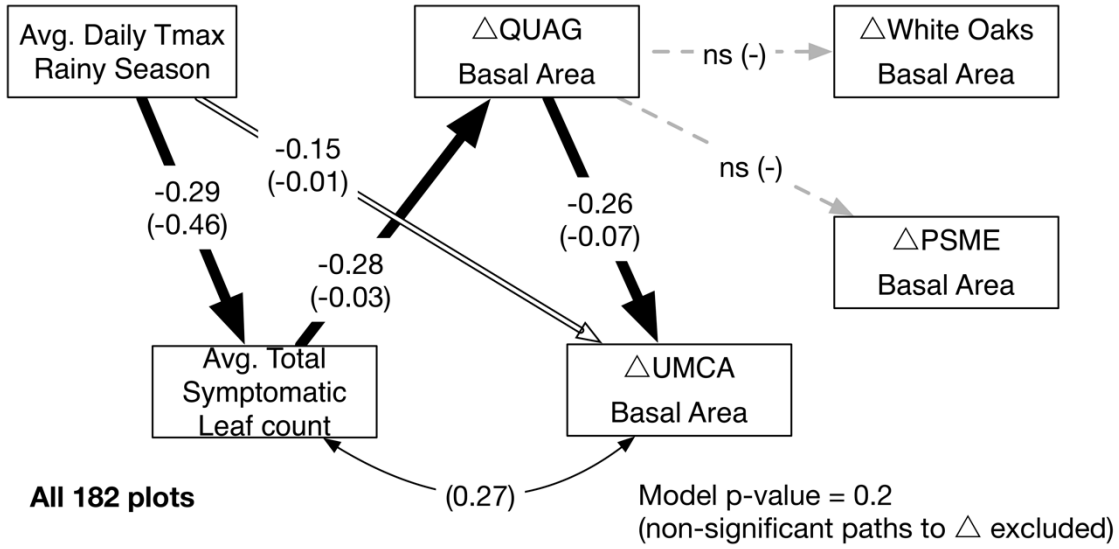

Figure 4.7. Apparent competition between coast live oak and bay laurel.

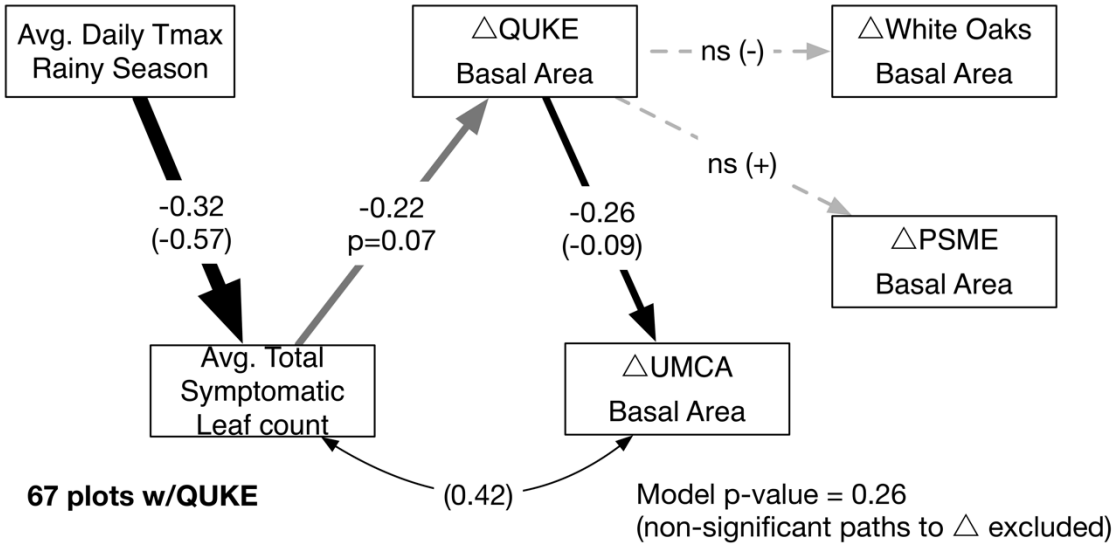

Figure 4.8. Apparent competition between California black oak and bay laurel.

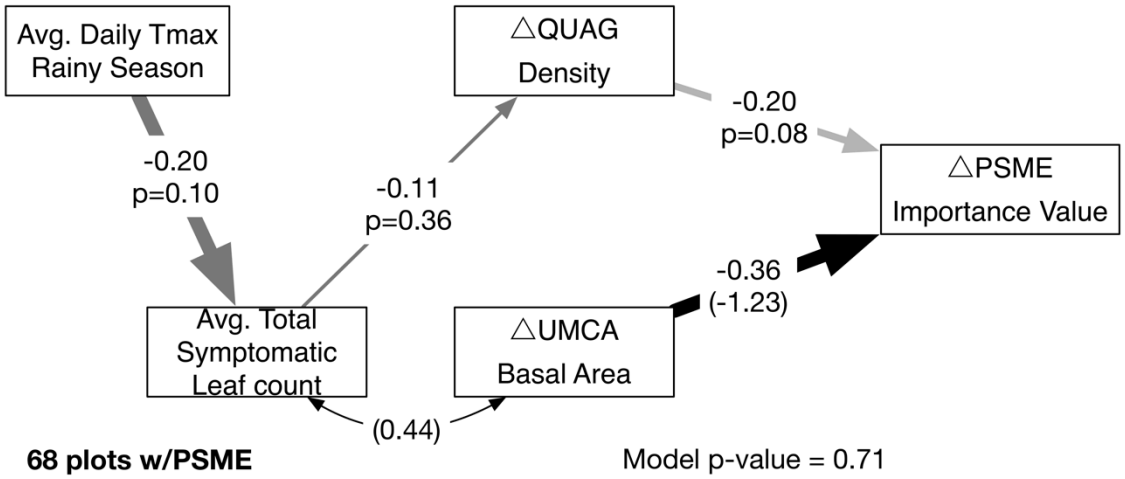

Figure 4.9. Effects on Douglas-fir importance value.

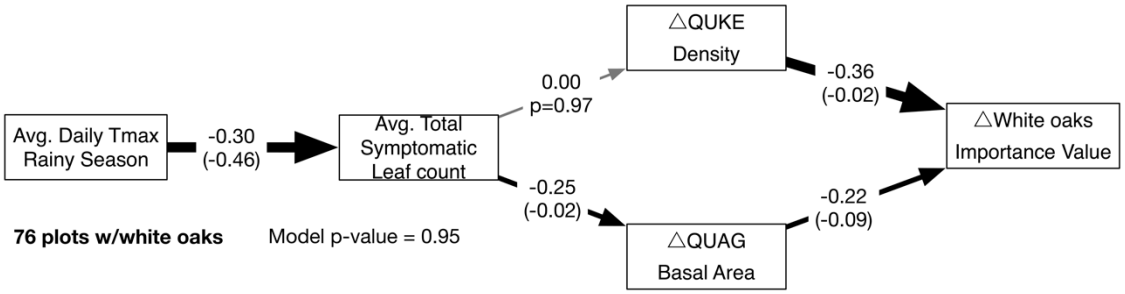

Figure 4.10. Apparent competition between susceptible oaks and white oak species.

APPENDICES

Appendix A. Chapter 3 Detailed Model Results

Table A1 Results from the d-sep test of conditional independence claims for the path model in Fig. 4.7.

Missing Path	Estimate	SE	df	Crit. Value	p-value
quag_BA_change ~ avg_tmax_rs	0.0159	0.0124	179	1.287	0.1997

Fisher's-*C*	df	p-value
3.22	2	0.2

Table A2 Standardized and unstandardized coefficient estimates for the path model in Fig. 4.7.

Response	Predictor	Std. Est.	Std. SE	Raw Est.	Raw SE	p-value
umca_BA_change	quag_BA_change	-0.2566	0.0718	-0.0745	0.0208	0.0005
umca_BA_change	avg_tmax_rs	-0.1549	0.0718	-0.0075	0.0035	0.0324
quag_BA_change	avg_total_slc.log	-0.2843	0.0715	-0.0298	0.0075	0.0001
avg_total_slc.log	avg_tmax_rs	-0.2884	0.0714	-0.4574	0.1132	0.0001
~~umca_BA_change	~~avg_total_slc.log	NA	NA	0.2692	NA	0.0001

Table A3 Results from the d-sep test of conditional independence claims for the path model in Fig. 4.8.

Missing Path	Estimate	SE	df	Crit. Value	p-value
umca_BA_change ~ avg_tmax_rs	-0.0059	0.0052	64	-1.1219	0.2661
quke_BA_change ~ avg_tmax_rs	0.0190	0.0169	64	1.1232	0.2655

Fisher's-*C*	df	p-value
5.3	4	0.258

Table A4 Results from the d-sep test of conditional independence claims for the path model in Fig. 4.9.

Missing Path	Estimate	SE	df	Crit. Value	p-value
quag_density_change ~ umca_BA_change	0.8114	7.8204	65	0.1038	0.9177
psme_IV_change ~ avg_tmax_rs	0.0210	0.0149	64	1.4114	0.1630
quag_density_change ~ avg_tmax_rs	-0.1432	0.2806	65	-0.5102	0.6116
psme_IV_change ~ avg_total_slc.log	0.0027	0.0083	63	0.3284	0.7437

Fisher's-*C*	df	p-value
5.38	8	0.717

Table A5 Results from the d-sep test of conditional independence claims for the path model in Fig. 4.10.

Missing Path	Estimate	SE	df	Crit. Value	p-value
white_oak_IV_change ~ avg_tmax_rs	-0.0009	0.0056	72	-0.1519	0.8797
quag_BA_change ~ avg_tmax_rs	-0.0061	0.0154	73	-0.3999	0.6904
quke_density_change ~ avg_tmax_rs	0.0398	0.0847	73	0.4693	0.6402
white_oak_IV_change ~ avg_total_slc.log	-0.0028	0.0040	71	-0.6983	0.4873
quke_density_change ~ quag_BA_change	0.2336	0.6449	73	0.3623	0.7182

Fisher's-*C*	df	p-value
3.99	10	0.948

Table A6. Standardized coefficients for the path model structure in Fig. 4.7.

Response	Predictor	Estimate	SE	p-value
umca_BA_change	quke_BA_change	-0.1137	0.0741	0.1263
white_oak_BA_change	quke_BA_change	-0.0149	0.0745	0.8414
psme_BA_change	quke_BA_change	0.0220	0.0745	0.7683
quke_BA_change	avg_total_slc.log	-0.1182	0.0740	0.1121
avg_total_slc.log	avg_tmax_rs	-0.2884	0.0714	0.0001
~~umca_BA_change	~~avg_total_slc.log	0.3452	NA	0.0000

Table A7. Standardized coefficients for the path model structure in Fig. 4.7.

Response	Predictor	Estimate	SE	p-value
umca_BA_change	quke_density_change	-0.0159	0.0745	0.8313
white_oak_BA_change	quke_density_change	-0.0588	0.0744	0.4306
psme_BA_change	quke_density_change	-0.0058	0.0745	0.9377
quke_density_change	avg_total_slc.log	-0.0043	0.0745	0.9541
avg_total_slc.log	avg_tmax_rs	-0.2884	0.0714	0.0001
~~umca_BA_change	~~avg_total_slc.log	0.3539	NA	0.0000

Appendix B. Chapter 2 Additional Model Results

Using data from plots with bay laurel resulted in a missing path between the average daily maximum temperature during the rainy season and the change in coast live oak bay laurel, and a statistically non-significant path between the symptomatic leaf count and the change in coast live oak basal area (Fig. B1). The data from plots with coast live oak indicated no missing paths (Fig. B2), otherwise showing similar relationships to the models using all 182 plots or the 161 plots with bay laurel. Consistently, cooler locations had higher pathogen loads, declines in coast live oak basal area, and increases in bay laurel basal area.

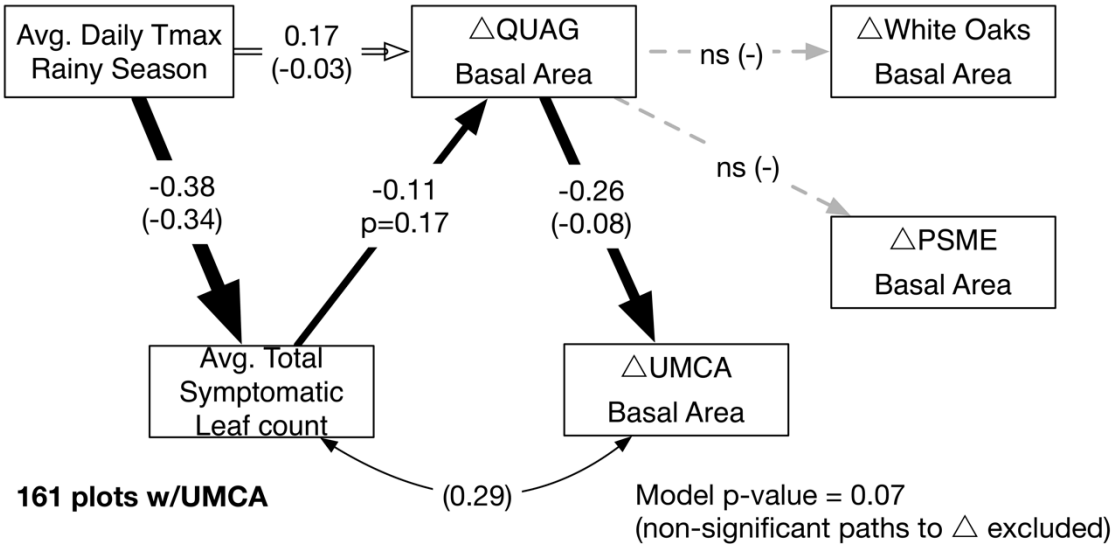

Figure B1. Path analysis results using the change in basal area of species from 161 plots with bay laurel.

Table B1 Unstandardized path coefficient estimates for the path model in Fig. B1.

Response	Predictor	Estimate	SE	p-value
umca_BA_change	quag_BA_change	-0.0834	0.0247	0.0009
quag_BA_change	avg_tmax_rs	0.0273	0.0132	0.0396
quag_BA_change	avg_total_slc.log	-0.0198	0.0144	0.1698
avg_total_slc.log	avg_tmax_rs	-0.3436	0.0672	0.0000
~~umca_BA_change	~~avg_total_slc.log	0.2882	NA	0.0001

Missing Path	Estimate	SE	df	Crit. Value	p-value
umca_BA_change ~ avg_tmax_rs	-0.0072	0.004	158	-1.8203	0.0706

Fisher's-*C*	df	p-value
5.3	2	0.071

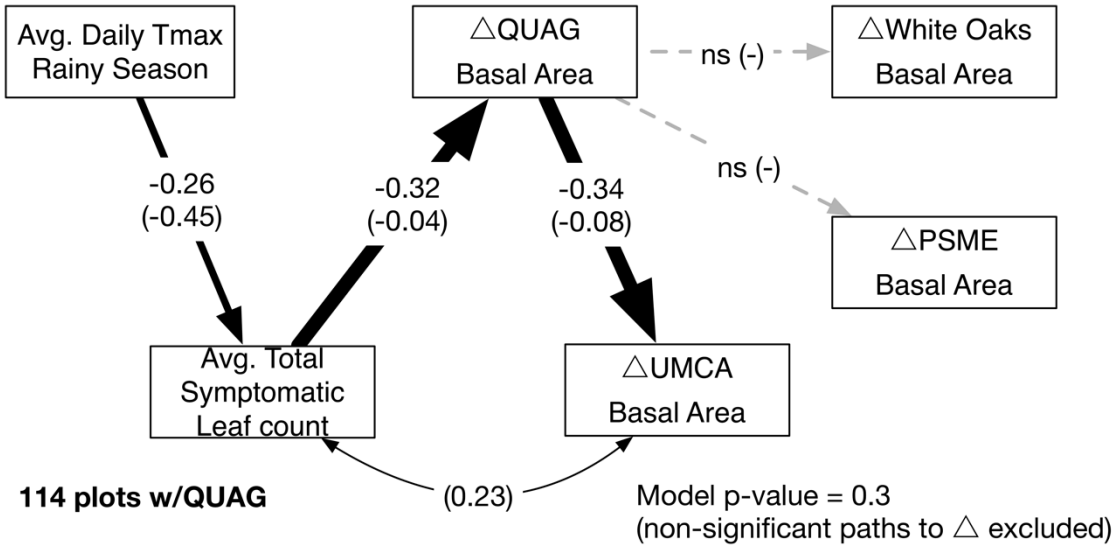

Figure B2. Path analysis results using the change in basal area of species from 114 plots where coast live oak was recorded.

Table B2 Unstandardized path coefficient estimates with standard error and results of the d-sep test for the path model in Fig. B2.

Response	Predictor	Estimate	SE	p-value
umca_BA_change	quag_BA_change	-0.0804	0.0209	0.0002
quag_BA_change	avg_total_slc.log	-0.0393	0.0109	0.0005
avg_total_slc.log	avg_tmax_rs	-0.4531	0.1605	0.0056
~~umca_BA_change	~~avg_total_slc.log	0.2280	NA	0.0073

Missing Path	Estimate	SE	df	Crit. Value	p-value
umca_BA_change ~ avg_tmax_rs	-0.0032	0.0046	111	-0.6864	0.4939
quag_BA_change ~ avg_tmax_rs	0.0271	0.0198	111	1.3666	0.1745

Fisher's-*C*	df	p-value
4.9	4	0.297

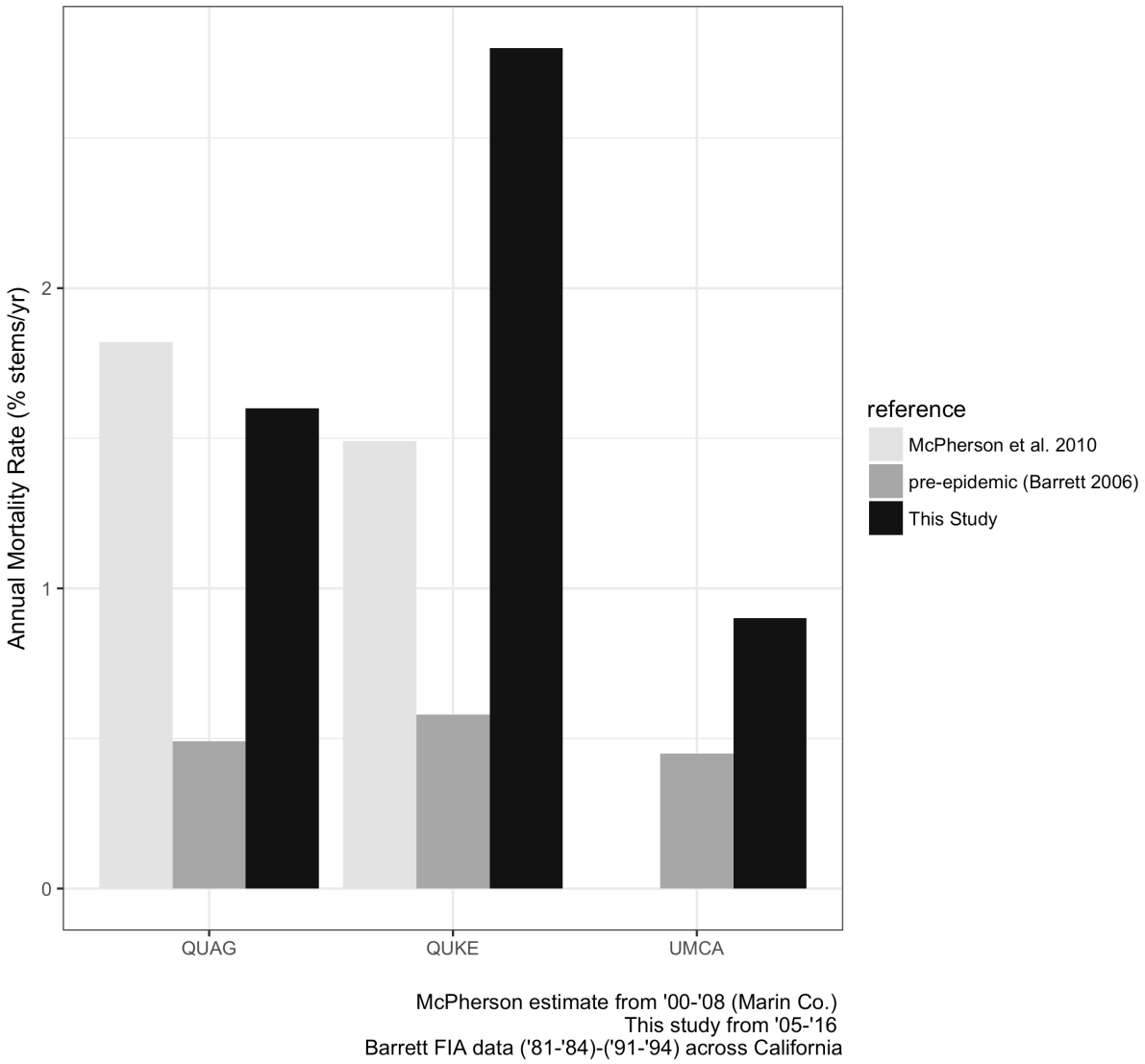

Figure B3. Comparisons of annual stem mortality rates of sudden oak death species.

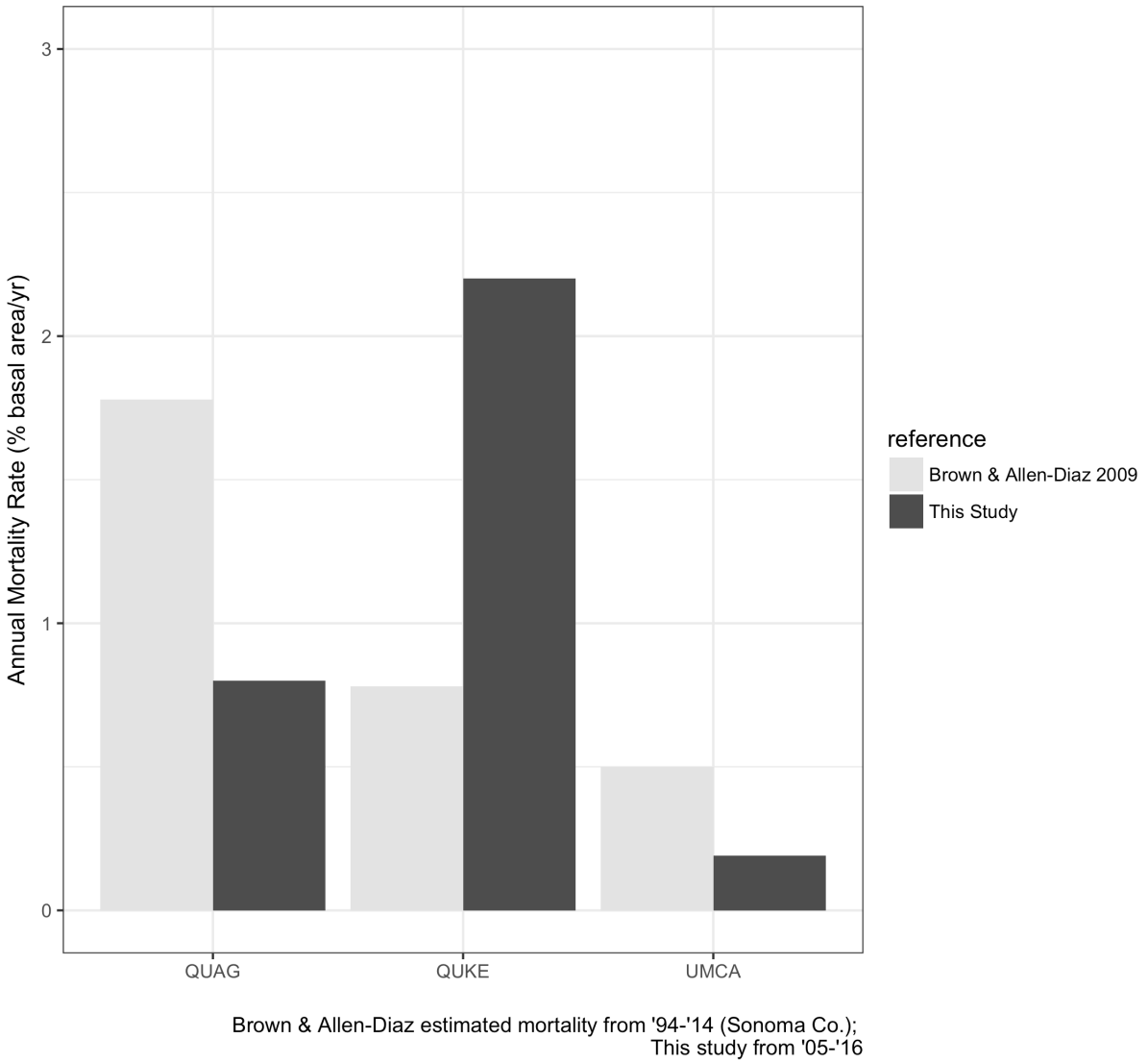

Figure B4. Contemporary comparison of annual basal area mortality rates of epidemiologically important sudden oak death species.

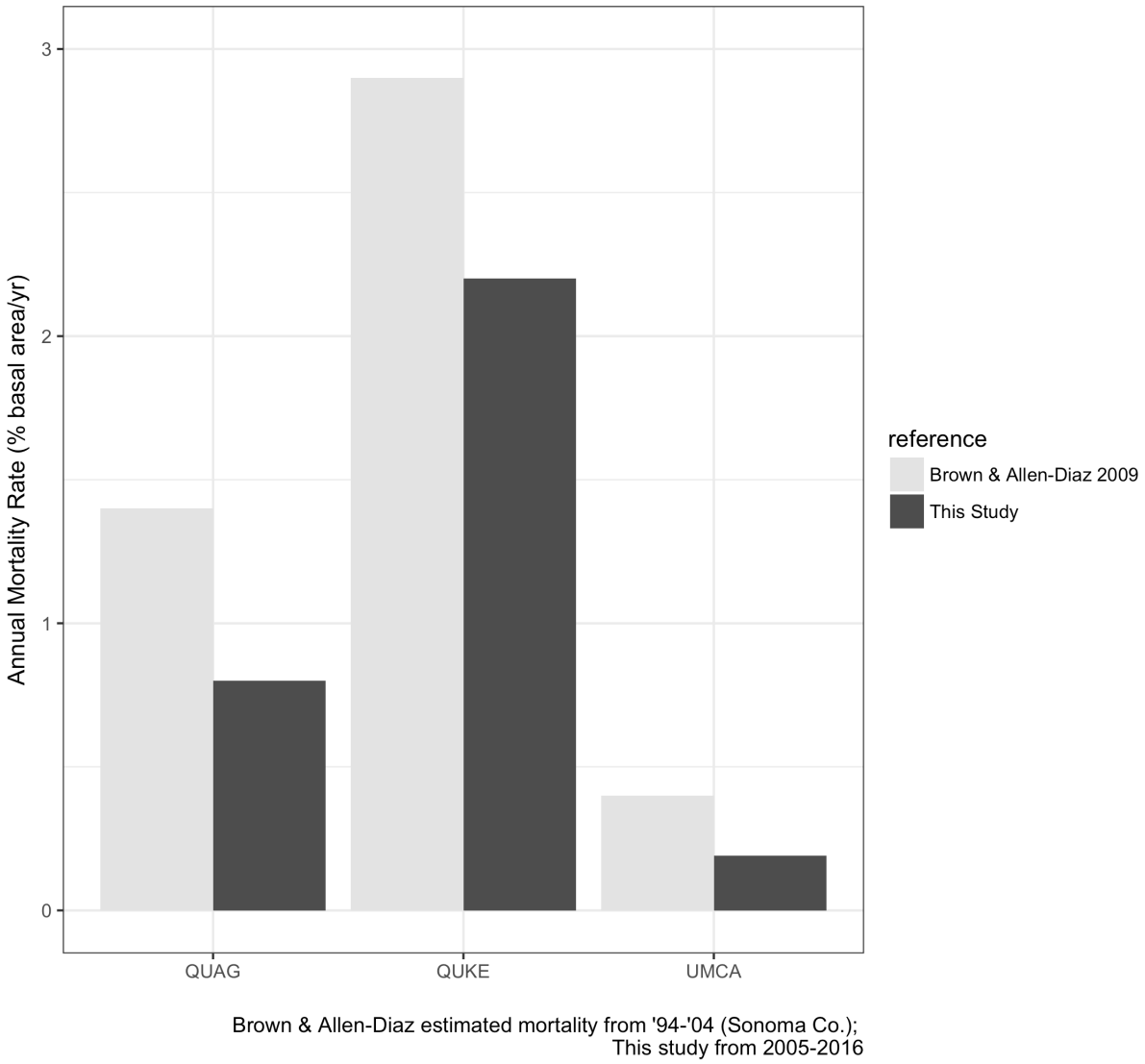

Figure B5. Comparisons of local annual basal area mortality rates to estimated mortality rates from 1994-2004.

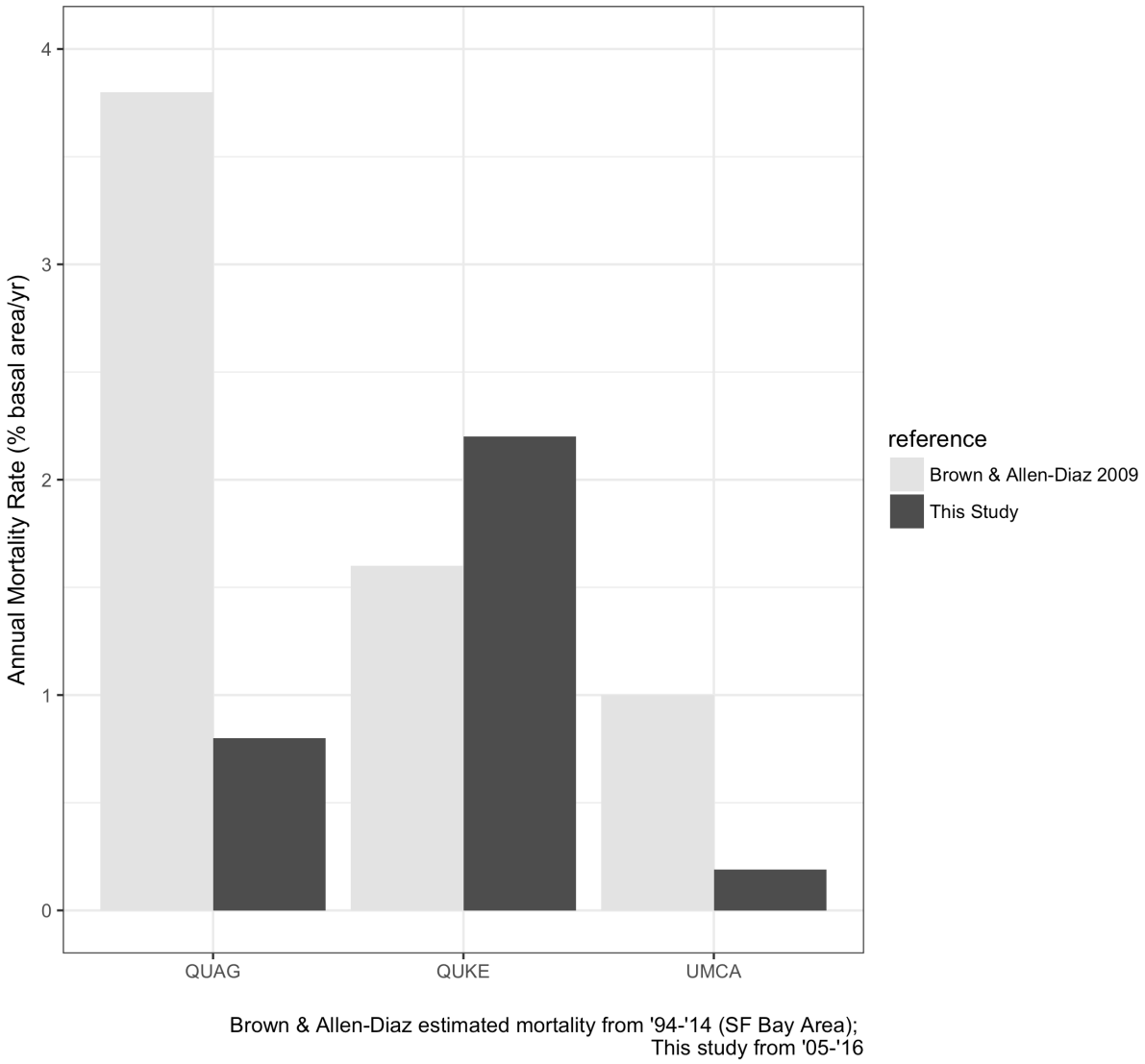

Figure B6. Comparisons of annual basal area mortality from this study to regional mortality rates predicted out to 2014.

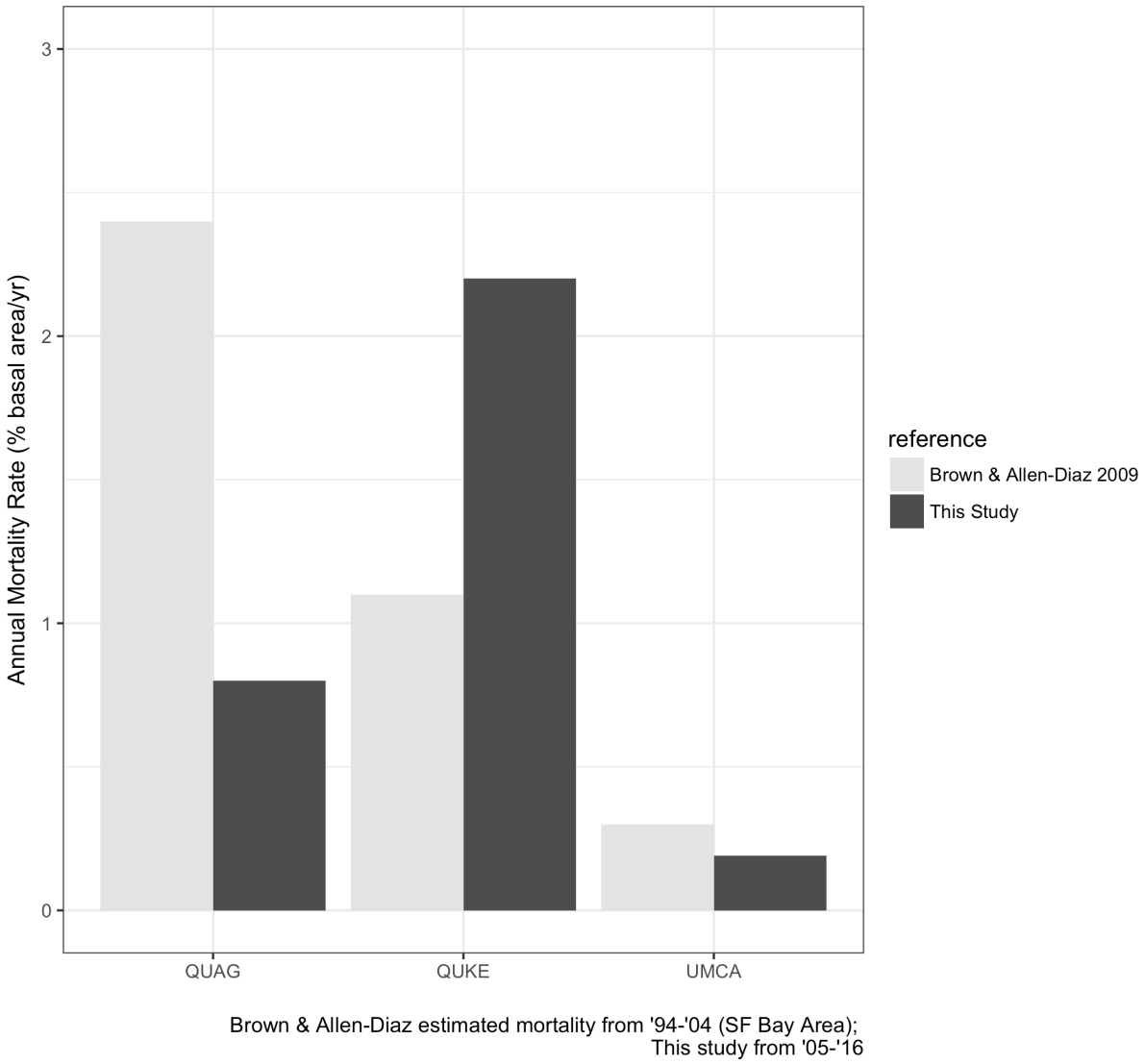

Figure B7. Comparisons of annual basal area mortality rates from this study to estimated regional mortality rates from 1994-2004.

Appendix C. Steps to Performing the d-sep Test

Steps for conducting the d-sep test (Shipley 2000, 2004, 2009)

1. Express the hypothesized causal relationships between the variables in the form of a directed acyclic graph.

2. List each of the k pairs of variables in the graph that do not have an arrow between them.

3. For each of the k pairs of variables (X_i,X_j), list the set of other variables, $\{Z\}$ that are direct causes of either X_i or X_j. The pair of variables, (X_i,X_j), along with its conditioning set, $\{Z\}$, define an independence claim, $(X_i,X_j) \mid \{Z\}$, and the full set of the k independence claims defines the basis set, B_u.

4. For each element in this basis set, obtain the probability, P_k that the pair (X_i,X_j) is statistically independent conditional on the variables Z. In other words, perform a regression model using an appropriate method. For example, in the model $X_i = X_j + Z$ the value for P_k of the independence claim is the p-value estimated for X_j. A p-value $\geq$ 0.2 will typically indicate independence, while a value $\leq$0.01 clearly suggests dependence, however, the values for assessing dependence or independence should be selected by the modeler *a priori* at the same time as the value in Step 6 as these are directly related. E.g., if your level for confirmation is going to be p$\geq$0.1, then your value for independence of any conditional independence claim should also be p$\geq$0.1.

5. Combine the k probabilities into the C-statistic: $C = -2\Sigma_{i=1}^{k} ln(P_i)$

6. Compare the value for C to a χ^2 (chi-square) distribution with $2k$ degrees of freedom. If the p-value is greater than the *a priori* selected value, e.g. 0.05, then the data provides sufficient support for the model structure.

7. If the data provide sufficient support for the model structure, then each component may be assessed and coefficients interpreted.